Associations between Oil Additives in Base Oils Probed by Pyrene Excimer Fluorescence

by

Kiarash Gholami Tazeh Shahri

A thesis

presented to the University of Waterloo

in fulfillment of the

thesis requirement for the degree of

Masters of Science

in

Chemistry

Waterloo, Ontario, Canada, 2017

Author's Declaration

I hereby declare that I am the sole author of this thesis. This is a true copy of the thesis, including any required final revisions, as accepted by my examiners.

I understand that my thesis may be made electronically available to the public.

Abstract

A recently developed method based on pyrene excimer fluorescence was used to probe the interactions of important polymeric oil additives. First, three ethylene-propylene (EP) copolymers representative of viscosity index improvers (VII) were maleated and fluorescently labeled with pyrene to yield three Py-EP samples. Each sample was dissolved in oil and toluene, an apolar substitute for oil. The fluorescence spectra of the Py-EP samples were acquired and analyzed to obtain a quantitative measure of the molar fraction (f_{inter}) of the pyrene labels that formed excimer intermolecularly for the Py-EP samples in oil and toluene as a function of solution temperature. The results demonstrated that f_{inter} remained more-or-less constant for the amorphous Py-EP sample in both solvents. However, the solutions of the semicrystalline Py-EP samples in oil and toluene showed an anomalous behavior for f_{inter} at intermediate temperatures, that was attributed to the formation of crystalline microdomains by the semicrystalline Py-EP samples and resulted in a sharp increase in the local pyrene concentration $[Py]_{loc}$ and thus f_{inter}. Moreover, f_{inter} and the molar fraction of aggregated pyrenes (f_{agg}) were found to be larger in oil than in toluene for a same Py-EP sample, suggesting that oil was a worse solvent than toluene to solubilize the Py-EP samples. These experiments were repeated to determine f_{inter} for solutions of the Py-EP samples in oil in the presence of two pour point depressants (PPDs). The results suggested that PPDs slightly increased f_{inter} for the Py-EP samples, indicating some level of interactions between the two polymers. However since the succinimide group used to link the pyrene labels to the EP backbone induced intermolecular interactions that might affect the conclusions drawn from the f_{inter} values, the focus of the study was changed to investigate the interactions between a pyrene-labeled poly(alkyl methacrylate) (Py-PAMA) used as a PPD mimic and EP copolymers in oil. In this case, the pyrene label was attached to the PAMA backbone via the same ester bond that connected the

alkyl chains to the polyester backbone. Consequently introduction of the pyrene label to PAMA did not induce any unwanted interactions between the Py-PAMA molecules.

The f_{inter}-vs-T profiles for two Py-PAMA samples in oil were determined. They also reflected a contraction of the polymer coils due to the crystallization of the alkyl side chains as the solution temperature was lowered. The temperature where the transition occurred was found to be dependent on the side chain length as would be the case for alkanes of different lengths. Based on these results, a poly(octadecyl methacrylate) sample labeled with 6.7 mol% pyrene Py(6.7)-$PC_{18}MA$ was selected and its f_{inter}-versus-T profiles were obtained in the presence of different oil additives in oil and octane. The addition of EP copolymers to the Py(6.7)-$PC_{18}MA$ solutions resulted in an increase in f_{inter} indicative of interactions between the EP copolymers and Py(6.7)-$PC_{18}MA$ molecules in oil. The increase in f_{inter} was found to be more pronounced at high temperatures for both amorphous (EP(AM)) and semicrystalline (EP(SM)) EP copolymers. At low temperatures, EP(AM) led to an increase in f_{inter} for Py(6.7)-$PC_{18}MA$ but not EP(SM) as it had crystallized and could no longer interact with Py(6.7)-$PC_{18}MA$.

Engine oils naturally contain a substantial amount of wax in their formulation which can promote interactions between different oil additives like VIIs and PPDs. Therefore, octane was employed as a wax-free engine oil substituent. An amount of wax similar to that present in engine oils was added to the Py(6.7)-$PC_{18}MA$ solution in octane to study its effect on the f_{inter}-versus-T profile. The presence of wax increased f_{inter} for Py(6.7)-$PC_{18}MA$ as would be expected from a PPD mimic that is believed to bind to wax crystals and control their growth. Naked EP copolymers were then added to the mixture of Py(6.7)-$PC_{18}MA$ and wax in octane. This led to another increase in f_{inter}. Such an effect was observed over the entire temperature range for the amorphous EP copolymer, while the crystallization of the semicrystalline EP copolymer at low temperatures

canceled the effect of this additive on f_{inter} for Py(6.7)-PC_{18}MA in a 10 g.L^{-1} wax solution in octane.

The experiments conducted in this thesis expanded the applicability of the procedure originally developed by S. Pirouz to determine the level of intermolecular interactions between EP copolymers in toluene to PAMAs in engine oil and octane. This study provided quantitative information about the level of interactions between Py(6.7)-PC_{18}MA and two EP copolymers that are representative of the interactions that would exist between PPDs and VIIs in engine oils.

Acknowledgements

I would like to express my deepest gratitude to my supervisor, Prof Jean Duhamel, for his great support, insightful comments, and considerable encouragements during this project. I would also like to extend my appreciation to my committee members, Profs. Juewen Liu and Mario Gauthier.

My sincere thanks also go to Afton Chemical Corporation and the Natural Sciences and Engineering Research Council of Canada (NSERC). I would also like to thank Dr. Solmaz Pirouz and Dr. Sheng Jiang for all their support toward this project.

I cannot forget the valuable help from all my lab colleagues, in particular Remi Casier, Damin Kim, Lu Li, Shiva Farhangi, and Janine Thoma.

Foremost, I would also like to extend my deepest gratitude to my family. Without their encouragement, I would not have had a chance to stand here.

Table of Contents

List of Figures

List of Tables

List of Schemes

List of Abbreviations

η	Viscosity
λ_{em}	Emission wavelength
λ_{ex}	Excitation wavelength
λ_{Py}	Pyrene content in µmol of pyrene per gram of polymer
τ_E	Fluorescence lifetime of pyrene excimer
τ_M	Fluorescence lifetime of excited pyrene monomer
a.u.	Arbitrary units
AIBN	Azobisisobutyronitrile
BUA	Butylamine
C	Concentration
^{13}C NMR	Carbon nuclear magnetic resonance
D_h	Hydrodynamic diameter
$E0$	Well-stacked pyrene dimers
EP	Ethylene propylene
f_{agg}	Molar fraction of aggregated pyrenes in solution
FBM	Fluorescence blob model
f_{diff}	Molar fraction of pyrenes forming excimer via diffusion in solution
f_{free}	Molar fraction of isolated pyrenes in solution
f_{inter}	Molar fraction of pyrenes forming excimer intermolecularly
FRET	Fluorescence resonance energy transfer
FTIR	Fourier transform infrared spectroscopy
GPC	Gel permeation chromatography
I_E/I_M	Ratio of excimer-to-monomer fluorescence intensities
k_1	Diffusion-controlled rate constant of pyrene excimer formation

k_{-1}	Dissociation rate constant of pyrene excimer
l	Path length of a UV cell
L	Chain length
M_n	Number-average molecular weight
MFA	Model free analysis
OCP	Olefin copolymers
P_A	Peak-to-valley ratio of the pyrene absorption
PAMA	Poly(alkyl methacrylate)
$PC_{12}MA$	Poly(dodecyl methacrylate)
$PC_{18}MA$	Poly(octadecyl methacrylate)
PPD	Pour point depressant
*P*y	Pyrene
Py_{agg}	Aggregated pyrenes
Py_{diff}	Pyrenes forming excimer via diffusion
Py-EP	Pyrene-labeled EP copolymer
Py_{free}	Isolated pyrenes
Py-MSI	1-Pyrenemethylsuccinimide
$PyNH_2$	1-pyrenemethylamine
SSF	Steady-state fluorescence
TCE	Trichloroethylene
TCB	Trichlorobenzene
THF	Tetrahydrofuran
TRF	Time-resolved fluorescence
V_{coil}	Volume of a polymer coil
V_h	Hydrodynamic volume
VII	Viscosity index improver

Chapter 1

Literature Review

The purpose of this thesis is to study the solution behavior of some of the components of engine oils, by fluorescently labeling polymers that are employed by the industry as engine oil additives and monitoring their fluorescence response under different conditions. Accordingly, the first part of this introduction provides background information about the various components of an engine oil, notably about viscosity index improvers (VIIs) and pour point depressants (PPDs) as well as a brief review of the techniques being employed to characterize their properties. The next part focusses on the principles and applications of fluorescence spectroscopy, some of the interesting features of the fluorescence spectra of macromolecules labeled with the chromophore pyrene, and a brief description of the methods and models used to analyze the florescence data. The third and last section of this chapter describes the research objectives and the organization of the different chapters of this thesis.

1.1 Oil Additives

The main function of an engine oil is to reduce wear on the moving parts of an engine, by providing a lubricating layer between them. For several decades the base oil, that usually contains comparatively heavy petroleum hydrocarbons of crude oil, has been the key component of many engine oils. However, the base oil on its own would not be able to meet all the requirements desired from an engine oil. Therefore, a number of chemicals must be added to the base oil to maintain the efficiency and durability of the engine oil. These additives include viscosity index improvers (VIIs), dispersants, detergents, pour point depressants (PPDs), antioxidants, and antiwears.[1] Each chemical must be added in the proper concentration range to ensure that the resulting engine oil exhibits the expected lubricating properties within the intended operation time and temperature range. The concentration of the chemicals typically found in engine oils is listed in Table 1.1.[1,2]

Table 1.1 Concentration of the additives in engine oil formulations.[1]

Component	Weight %	Component	Weight %
Base Oil	71.5-96.2	Viscosity Index Improver	0.1-3.0
Detergent	2-10	Antioxidant/Wear	0.1-2.0
Dispersant	1-9	Pour Point Depressant	0.1-1.5

From the list of chemicals presented in Table 1.1, VIIs and PPDs are the focus of this thesis and will be described in more detail hereafter.

1.1.1 Viscosity Index Improvers (VIIs)

VIIs, as their name suggests, can effectively improve the viscosity index of an engine oil by reducing the inherent decrease in oil viscosity that takes place upon increasing the operation temperature. These additives are polymers whose hydrodynamic volume in the oil increases with increasing temperature (Figure 1.1). This phenomenon increases the volume fraction of the solution that is occupied by the polymer coil, and thus the solution viscosity. Without VIIs, the oil would be too thin to form a protective film between the adjacent moving parts of the engine at high temperatures. However, a base oil with a higher viscosity at high temperature would likely damage the engine at low temperature since the viscosity would be too high, thus preventing oil flow and protection of the moving parts of the engine. This situation is encountered more frequently in countries with a cold climate, where the engine start-up temperature might be lower than −40 °C during the winter, while the temperature can reach +200 °C in some parts of an engine.[3,4] VIIs are polymers with a molecular weight ranging from 50,000 to 500,000 $g.mol^{-1}$.[2,5] Ethylene-propylene (EP) copolymers constitute an important family of VIIs. EP copolymers can be amorphous or semicrystalline depending on their ethylene content, an ethylene content of 60 mol% or lower resulting in amorphous EP copolymers while an ethylene content of 65 mol% or

higher results in semicrystalline EP copolymers.[6] In the case of amorphous polyolefins, the hydrodynamic volume of the polymer coil increases continuously with increasing oil temperature. In the case of semicrystalline polyolefins, however, the continuous change in polymer coil size with temperature is accompanied by a sharp transition at low temperatures where long oligoethylene sequences crystallize, in a process that reduces the hydrodynamic volume of the polymeric coils at the crystallization temperature. Since the 1940s synthetic polymers, such as olefin copolymers (OCP), alkyl methacrylate copolymers (AMCP), and hydrogenated styrene-diene copolymers have been used as VIIs.[2,7,8]

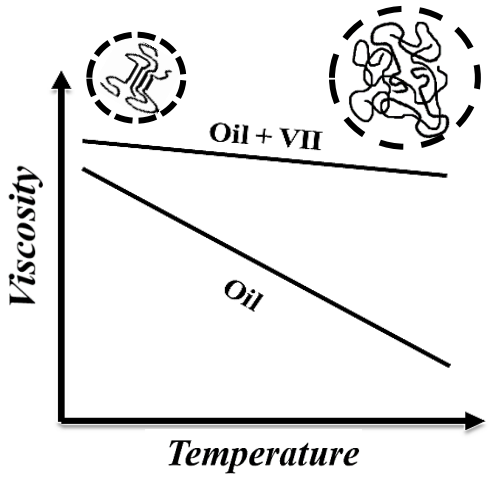

Figure 1.1. Comparison of the profile of oil viscosity versus temperature in the absence (bottom) and presence (top) of VII.

1.1.2 Pour Point Depressants (PPDs)

Beside the unwanted decrease of oil viscosity with temperature, another problem that is usually encountered with base oils, especially at very low temperatures, is the formation of networks made of crystallized wax. Waxes are long chain hydrocarbons that crystallize at low temperature.[9,10] Despite the removal of a substantial amount of wax during the refining of base oil, a small amount

of these long chain hydrocarbons must be left in the oil to bring the oil viscosity within a desired range. Networks of wax crystals prevent the oil flow and consequently the lubrication of the engine.[11,12] Usually the motion of the engine pistons provides sufficient shear stress to prevent the formation of wax crystal networks. However, the aggregation of wax at low temperatures remains an unavoidable problem for cold start-ups, and wax aggregates have a detrimental effect on the lifetime of internal combustion engines. The lowest temperature at which the oil stops flowing is called the pour point (PP). Therefore, additives used to lower the PP of engine oils are referred to as pour point depressants (PPDs). Alkylaromatic polymers and poly(alkyl methacrylate)s (PAMA) are the two general types of PPDs that are used by the lubricant industry.[3] The presence of a PPD has been shown to lower the PP of an engine oil by up to 20 °C[13] as schematically illustrated in Figure 1.2.

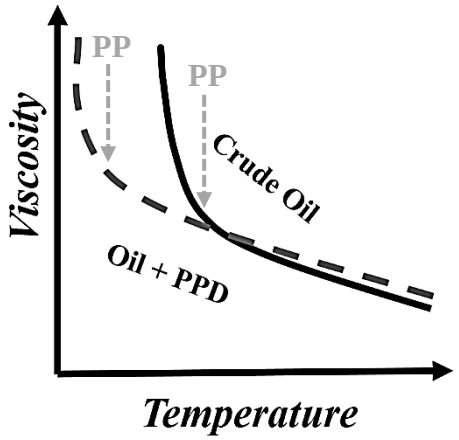

Figure 1.2. Change in oil pour point in the absence (—) and presence (- - -) of PPD.

1.2 Characterization of Polymeric Oil Additives

Since the 1940s, the oil industry has employed different types of polymers as engine oil additives to optimize the oil service life and enhance its performance all year round, under high and low temperature conditions. However, the extreme physical and chemical stresses encountered inside the engine by these polymers results in chain cleavage causing partial or total loss of their function

throughout their service life. The stability of these polymeric additives is directly related to the chemical structure and the molar ratio of each of their constituting co-monomers, as well as external factors such as the type and operation temperature of the engine. Longer polymeric additives generally yield more viscous solutions. However, higher molecular weight polymers are subject to chain cleavage and their solutions undergo shear thinning. Therefore, an optimal chain length must be determined for the polymers used as VII or PPD. This requires striking a balance between viscosity optimization, minimization of chain scission, and reduction in shear-thinning. For instance, the range of molecular weights used for VIIs is usually between 50K and 200K, with a polydispersity index between 2 and 2.8.[4]

During the past decades, several methods have been developed and applied to characterize EP copolymers and PAMAs and gauge their efficiency as VIIs and PPDs, respectively. These methods are based on the use of Fourier transform infrared (FTIR) and carbon nuclear magnetic resonance (^{13}C NMR) spectroscopy to determines the chemical composition of the polymers, differential scanning calorimetry (DSC) to determine their crystallinity, light scattering and intrinsic viscosity measurements to monitor the dimensions of the polymer coils in solution, rheology to probe changes in viscosity, and gel permeation chromatography (GPC) to characterize the molecular weight distribution of the polymers. More recently, fluorescence measurements have been introduced to characterize the interactions between polymers in solution. The following sections provide some background on the applications of fluorescence to characterize polymer interactions.

1.2.1 Fluorescence Study of Solutions of Pyrene-Labeled Macromolecules (PyLMs)

The emission of light from a chromophore can occur through fluorescence or phosphorescence.[14] While phosphorescence represents a transition from the triplet excited state to the ground state that

occurs between 10^{-3} and 1 s, fluorescence is a transition between the excited singlet state S_1 to the ground state that takes place on a comparatively shorter timescale, within around 10 ns (see Figure 1.3).[13] For fluorescence to happen, the dye must be excited to an upper electronic state upon absorption of a photon that happens over a few femtoseconds (10^{-15} s). The excited molecule then relaxes quickly, within a few picoseconds (10^{-12} s), from any vibrational levels of the upper excited states to the lowest vibrational level of S_1, in a process called internal conversion. Fluorescence occurs when the emission of a photon enables the molecule to relax back to any of the vibrational energy levels of the ground state (S_0). The absorption, internal conversion, and fluorescence steps can be illustrated by the Jablonski diagram shown in Figure 1.3.

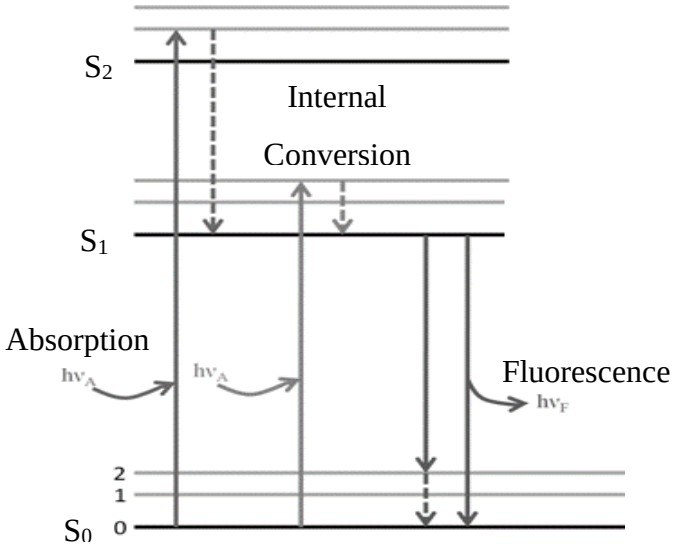

Figure 1.3. Jablonski diagram for absorption, internal conversion, and fluorescence.[14]

Polymers usually need to be fluorescently tagged with a dye, since most do not fluoresce naturally. Fluorescence is then used to provide structural and dynamic information on the labeled polymers. The fluorescent dye is covalently attached onto reactive groups that are either naturally present or chemically introduced on the macromolecule. In many cases, these reactive groups can be introduced either randomly along the backbone or at the chain ends. The labeled polymers can

be probed using a continuous or pulsed light source to acquire their steady-state fluorescence (SSF) spectra or their time-resolved fluorescence (TRF) decay, respectively. Pyrene, naphthalene, coumarin, and succinimide are some examples of fluorophores that have been widely used to study polymers.[15] Among these, pyrene is the most commonly used aromatic molecule for labeling purposes because of its interesting photophysical properties.[4,16-19] Its relatively large molar extinction coefficient, high quantum yield, and long fluorescence lifetime make pyrene an ideal dye to probe macromolecules even at very low polymer concentrations (~ 5 mg/L) in solution.[18] Thanks to its long (200-300 ns) natural monomer lifetime (τ_M), a pyrene monomer remains excited long enough to diffusionally encounter a ground-state pyrene and form an excimer, which decays with its own lifetime (τ_E) around 50 ns and at longer wavelengths (see Scheme 1.1 and Figure 1.4).[20]

Another interesting feature of pyrene is that since this molecule can act as both the excited dye and a ground-state quencher, double labeling of a polymer with a dye and a quencher to probe the intramolecular rate of quenching is unnecessary, and the rate of quenching of an excited pyrene monomer can be determined from the rate of pyrene excimer formation obtained with a pyrene-only labeled polymer. Pyrene excimer formation can be applied to describe the distribution of pyrene labels along the polymer, or to determine the level of interpolymeric interactions in solution. How this is accomplished is described hereafter.

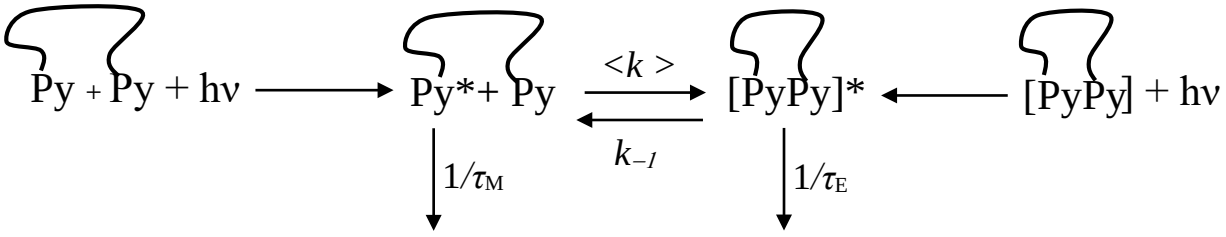

Scheme 1.1. Kinetic scheme for excimer formation between pyrene labels covalently attached onto a polymer.

Upon absorption of a photon, an excited pyrene monomer in Scheme 1.1 can either fluoresce with a lifetime τ_M or encounter a ground-state pyrene to form an excimer with an average rate constant $\langle k \rangle$. Pyrene dimers resulting from the incorporation of pyrene labels onto successive structural units of a macromolecule can also absorb a photon as a separate entity and form an excimer instantaneously upon direct excitation, as shown in the right side of Scheme 1.1. The brackets used for $\langle k \rangle$ indicate that the rate constant is averaged over all pyrene pairs generated along the polymer chain. In essence, $\langle k \rangle$ is equal to the product $k_{diff} \times [Py]_{loc}$, where k_{diff} is a biomolecular rate constant describing pyrene excimer formation by diffusion and $[Py]_{loc}$ is the local pyrene concentration. Once formed, the excimer can fluoresce with a lifetime τ_E or dissociate with a rate constant k_{-1}. Since k_{-1} is much smaller than $1/\tau_E$, the dissociation of the excimer is usually neglected.[16,19] The typical fluorescence spectrum of a pyrene-labeled ethylene propylene copolymer (Py-EP) sample in oil is shown in Figure 1.4.

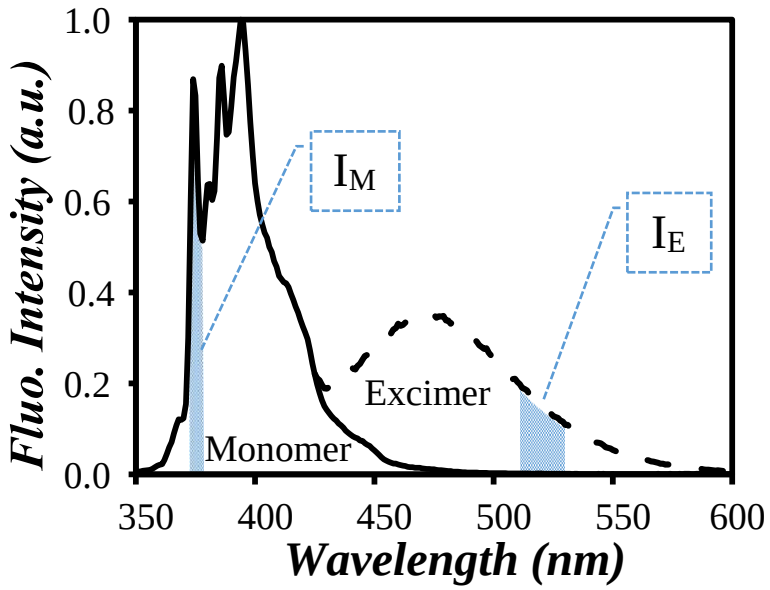

Figure 1.4. Steady-state fluorescence spectrum of a Py-EP sample in oil. λ_{ex} =344 nm, $[Py]$ = 2.5 × 10^{-6} mol.L^{-1}, pyrene content equals 116 μmol.g^{-1}.

The spectrum shown in Figure 1.4 can be used to determine the ratio of the intensity of the excimer (I_E) over that of the monomer (I_M) by integrating the fluorescence spectrum from 500 to 530 nm and from 372 to 379 nm, respectively. In turn, the I_E/I_M ratio depends on the local concentration of pyrene ($[Py]_{loc}$) in the solution, according to Equation 1.1 where K is a proportionality constant. The I_E/I_M ratio can be determined at high and low Py-EP concentrations to yield the I_E/I_M(high) and I_E/I_M(low) ratios, which provide a measure of $[Py]_{loc}$ under conditions where pyrene excimer formation occurs both intra- and intermolecularly and solely intramoleculary, respectively.[4] In turn, $[Py]_{loc}$(intra & inter) and $[Py]_{loc}$(intra) can be rearranged to yield the molar fraction of pyrenes that form excimer intermolecularly (f_{inter}) as shown in Equation 1.2.

$$I_E / I_M = K \frac{[E^*]}{[M^*]} = \frac{k_{diff}\,[Py]_{loc}}{\frac{1}{\tau_E} + k_{-1}} \qquad (1.1)$$

$$f_{inter} = \frac{[Py]_{loc}\left(\begin{smallmatrix}\text{inter \&}\\ \text{intra}\end{smallmatrix}\right) - [Py]_{loc}\,(\text{intra})}{[Py]_{loc}\left(\begin{smallmatrix}\text{inter \&}\\ \text{intra}\end{smallmatrix}\right)} = \frac{I_E / I_M\left(\begin{smallmatrix}\text{inter \&}\\ \text{intra}\end{smallmatrix}\right) - I_E / I_M\,(\text{intra})}{I_E / I_M\left(\begin{smallmatrix}\text{inter \&}\\ \text{intra}\end{smallmatrix}\right)} \qquad (1.2)$$

The molar fraction f_{inter} is a measure of the level of intermolecular interactions that exist between pyrene-labeled macromolecules (PyLMs) such as the Py-EP sample whose spectrum was shown in Figure 1.4. The procedure developed to calculate f_{inter} will be illustrated later to determine the level of intermolecular interactions taking place in engine oil as a function of temperature for amorphous (EP(AM)) and semicrystalline (EP(SM)) EP copolymers.

1.2.2 Distribution of Pyrene Labels for a PyLM from the Model Free Analysis (MFA)

When dealing with excimer formation between pyrene labels covalently attached onto a polymer, it becomes important to determine how excimer formation proceeds, either through diffusive

encounters between two pyrene labels or direct excitation of a pre-formed pyrene dimer. The paths toward excimer formation through diffusive encounters or direct excitation were described in Scheme 1.1. They are a consequence of the existence of four different pyrene species in solution, namely those pyrenes that are isolated along the chain and emit as if they were free in solution (Py^*_{free}), those that form excimer by diffusive encounters with another pyrene (Py^*_{diff}), or those that are aggregated and form excimer instantaneously upon direct excitation. There are usually two types of excimer encountered in PyLMs, depending on whether they are the result of an encounter that yields two well-stacked or two poorly stacked pyrene moieties that generate two excimers, referred to as (*E0**) or (*D**) excimer, respectively. The model free analysis (MFA) of the monomer and excimer fluorescence decays was introduced ten years ago to determine the molar fractions f_{diff}, f_{free}, f_{E0}, and f_D of the pyrene species Py^*_{diff}, Py^*_{free}, *E0**, and *D**, respectively.[21] The species *E0** and *D** usually represent aggregated pyrenes, so that the molar fraction f_{agg} is often employed to represent the sum $f_{E0} + f_D$ of aggregated pyrene labels. Comparison of f_{diff} and f_{agg} provides a means to assess the importance of excimer formation by diffusive encounters over direct excitation of aggregated pyrenes. Scheme 1.2 illustrates the different pyrene species encountered along a backbone randomly labeled with pyrene.

The parameters retrieved from the MFA of the fluorescence decays acquired with PyLMs also include the lifetimes τ_{E0} and τ_D of the excimer *E0** and *D**, respectively, as well as the average rate constant of pyrene excimer formation $\langle k \rangle$ (see Scheme 1.4). One interesting feature of the MFA is that the parameters that it retrieves can be combined into Equation 1.3 to yield the absolute $(I_E/I_M)^{TRF}$ ratio obtained by time-resolved fluorescence (TRF). $(I_E/I_M)^{TRF}$ can be compared to the $(I_E/I_M)^{SSF}$ ratio obtained by steady-state fluorescence (SSF).

$$(I_E / I_M)^{TRF} = \frac{(f_{diff}^{E0}\tau_{E0} + f_{diff}^{D}\tau_D) < k > < \tau > + f_{E0}\tau_{E0} + f_D\tau_D}{(f_{diff}^{E0} + f_{diff}^{D}) < \tau > + f_{free}\tau_M} \qquad (1.3)$$

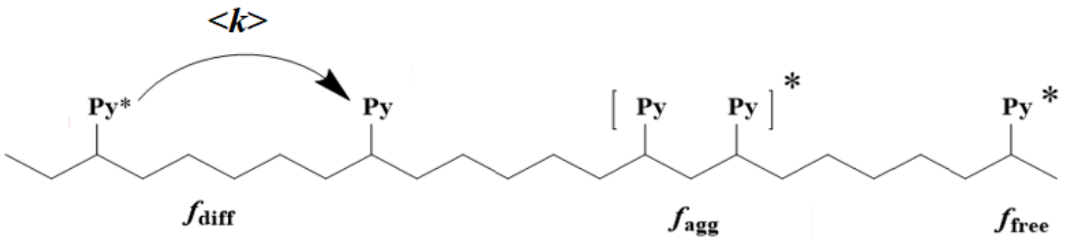

Scheme 1.2. Illustration of the pyrene species formed on a polymer randomly labeled with pyrene.

1.2.3 Applications

So far, the procedure used to determine f_{inter} has only been applied to estimate the level of intermolecular interactions that take place between polyolefins in toluene. In these experiments, semicrystalline and amorphous EP copolymers were maleated and labeled with 1-pyrenemethylamine to yield EP copolymers randomly labeled with pyrene (Py-EP).

As reported previously, a solution of 0.01 g.L^{-1} Py-EP sample and 10 g.L^{-1} unlabeled EP in toluene could be used to measure I_E/I_M(intra).[4,21] Having a low amount of Py-EP with a large excess of unlabeled EP copolymer ensured that pyrene excimer formation would occur intramolecularly within isolated pyrene-labeled macromolecules. The ratio I_E/I_M(inter & intra) could be simply obtained from a solution of 10 g.L^{-1} solution of Py-EP sample in toluene. The I_E/I_M ratios obtained at low and high Py-EP concentrations were then determined as a function of temperature and plotted in Figure 1.5 for an amorphous (EP(AM)) and a semicrystalline (EP(SM)) EP copolymer.

The I_E/I_M ratios of Py-EP(AM) at high and low concentrations and the I_E/I_M ratio of Py-EP(SM) at low concentration increased linearly with increasing temperature from –30 to +25 ^{o}C. This behavior suggested that under these conditions, excimer formation was diffusion controlled and

thus solely depended upon the solution viscosity, that decreased with increasing temperature. A lower solution viscosity favored diffusive encounters, resulting in a large I_E/I_M ratio. In contrast, the 10 g.L^{-1} Py-EP(SM) solution showed a much more complex behavior. I_E/I_M increased first from –30 to –15 °C, decreased from –15 to 0 °C, and increased again from 0 to +25 °C. Intrinsic viscosity measurements as a function of temperature indicated that EP(SM) undergoes a collapse in the same temperature range where the unusual I_E/I_M behavior was observed. As confirmed by Pirouz et al,[4,22] this behavior was due the formation of crystalline microdomains by the semicrystalline EP copolymer in toluene, that resulted in an increase in $[Py]_{loc}$ as the temperature decreased from 0 to –10 °C in Figure 1.5A, and thus of the I_E/I_M ratio according to Equation 1.1. The complex behavior observed for I_E/I_M in Figure 1.5A for Py-EP(SM) is a common feature of semicrystalline EP copolymers.[17]

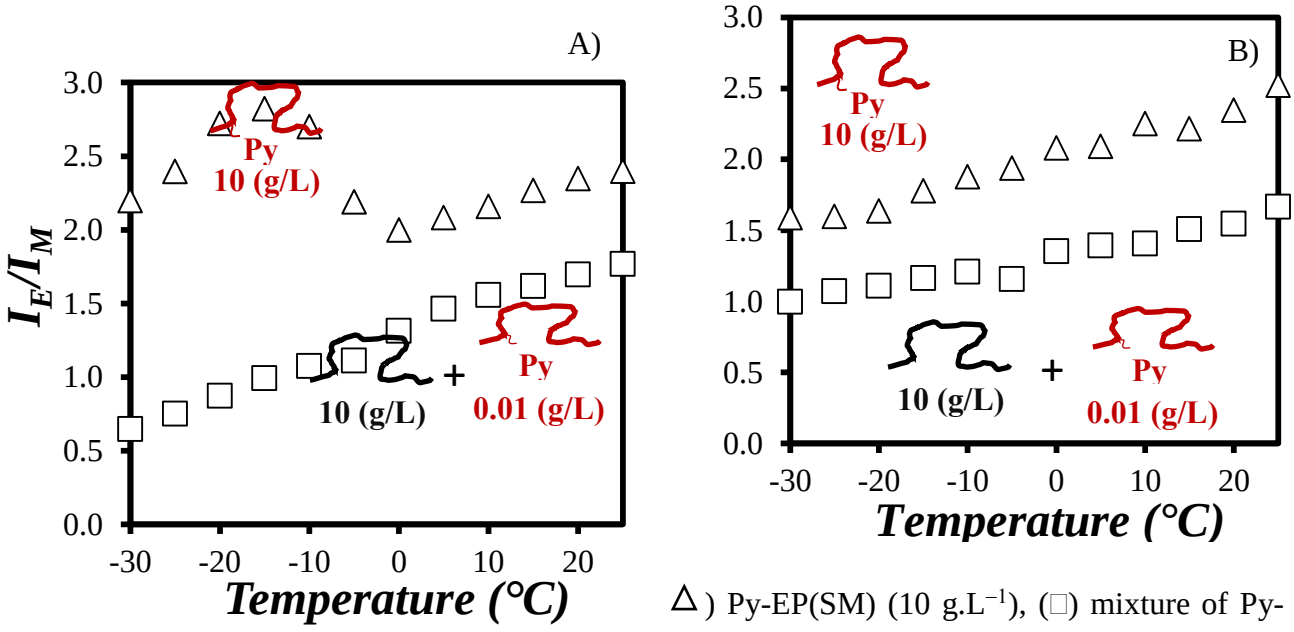

△) Py-EP(SM) (10 g.L^{-1}), (□) mixture of Py-EP(SM) (0.01 g.L^{-1}) and EP(SM) (10 g.L^{-1}), B) (△) Py-EP(AM) (10 g.L^{-1}), (□) mixture of Py-EP(AM) (0.01 g.L^{-1}) and EP(AM) (10 g.L^{-1}).

The I_E/I_M-vs-T profiles in Figure 1.5 could be combined according to Eq. 1.2 to yield f_{inter} between pyrene pendants, and consequently between EP copolymers in the solution. The molar fraction was plotted as a function of temperature in Figure 1.6 for both polymers. The molar fraction f_{inter} did not exhibit much change with temperature for Py-EP(AM), while the f_{inter} plot showed two clear-cut temperature regimes for the semicrystalline samples. In the case of Py-EP(SM), f_{inter} equaled 0.64 ± 0.05 for temperatures lower than −10 °C, and decreased to 0.30 ± 0.03 at temperatures greater than +5 °C. The decrease in f_{inter} at higher temperature for the semicrystalline EP copolymer was due to the melting of microcrystals present at low temperatures, which released EP(SM) chains into the solution, leading to a sharp decrease in the local pyrene concentration of the Py-EP(SM) sample. On the other hand, the amorphous sample did not undergo any conformation change in solution as a function of temperature, so that the level of intermolecular interactions remained unchanged with temperature.

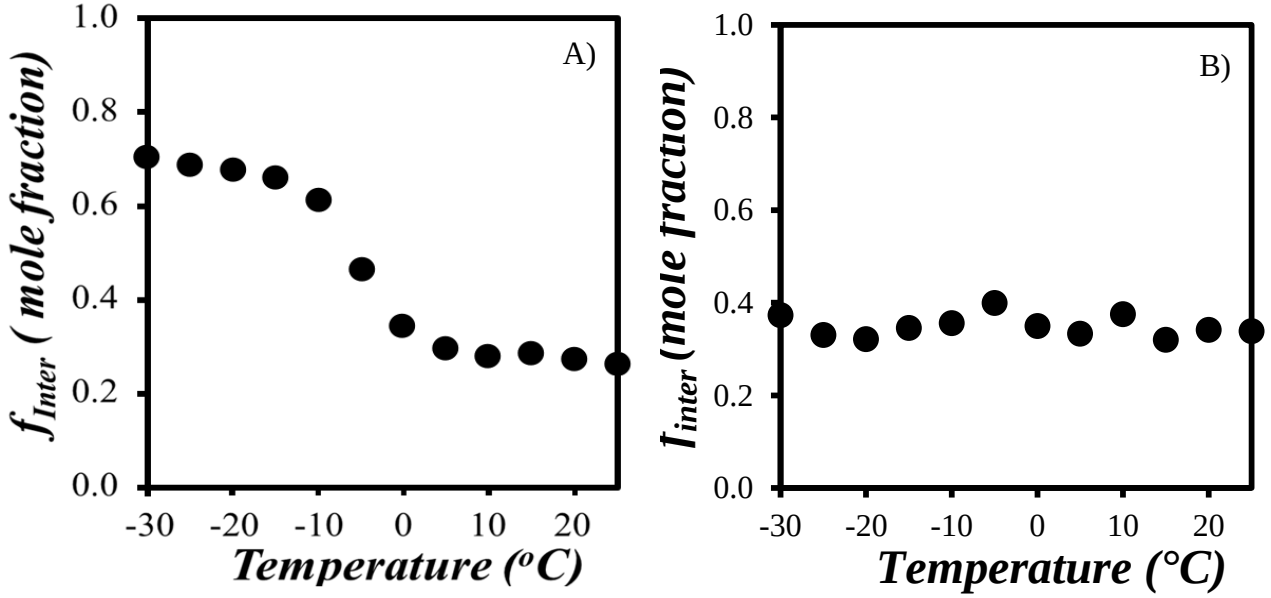

Figure 1.6. Molar fraction f_{inter} of pyrene labeled EP copolymers forming excimer intermolecularly in toluene for A) Py-EP(SM) and B) Py-EP(AM) at a polymer concentration of 10 g.L^{-1}.

The procedure described with Figures 1.5 and 1.6 enables one to characterize the level of intermolecular interactions for a selected macromolecule that has been specifically pyrene-labeled. It has been applied to probe how the presence of wax in a solution affects the level of intermolecular interactions between amorphous and semicrystalline EP copolymers.[4,21] Of course, this procedure could also be extended to other macromolecular oil additives, such as PPDs.

1.2.4 Conclusions

This chapter reviewed briefly the various chemicals found in engine oils, as well as the fluorescence principles that will be applied in this thesis. This chapter also highlighted some of the interesting features of the fluorescence spectra and decays obtained for macromolecules labeled with the chromophore pyrene, and some of the methods and models used to analyze the results obtained by these different florescence techniques. As illustrated in this chapter, both SSF and TRF can be used to obtain the I_E/I_M ratio of the pyrene-labeled samples in solution. In particular, the direct dependency that exists between the I_E/I_M ratio and $[Py]_{loc}$ enables one to determine quantitatively the level of intermolecular interactions between oil additives in solution by measuring the molar fraction f_{inter}.

The generality of the method described in this chapter explains how pyrene excimer fluorescence can be applied to probe the extent of intermolecular interactions of different macromolecules in solution. Pyrene excimer fluorescence provides the experimentalist with a powerful analytical means to investigate both quantitatively and qualitatively polymer-polymer interactions in solution, and seems to be particularly well-suited to study the solution behavior of EP copolymers and PAMAs used, respectively, as VIIs and PPDs by the oil additive industry.

1.2.5 Thesis Outline and Objectives

The objective of this thesis was to apply pyrene excimer fluorescence (PEF) to characterize the level of intermolecular associations between EP copolymers used as VII in engine oil and other apolar solvents, as a function of temperature, in the presence and absence of a PPD. Consequently, the properties of VIIs and PPDs were presented and the application of fluorescence to study interpolymeric interactions between VII mimics in toluene was described in Chapter 1. To this end, two EP copolymers were pyrene-labeled and a number of experimental techniques, notably FTIR, GPC, SSF, and TRF, were applied to determine the chemical composition, the molecular weight distribution, and the level of intermolecular associations (f_{inter}) for different types of Py-EP copolymers used as VIIs in toluene and oil and in the presence or absence of a PPD. The results of this study are presented in Chapter 2. However interactions between the succinimide groups linking pyrene to the EP backbone of the EP copolymers led to unwanted interactions between Py-EP molecules in oil that might compromise the conclusions drawn from the analysis of the f_{inter} values.

Consequently the same types of experiments were conducted on a pyrene-labeled poly(alkyl methacrylate) (Py-PAMA) used as a PPD mimic, to determine its level of intermolecular interactions in octane and oil and in the presence or absence of a VII. The use of octane also enabled the study of the effect that wax had on the level of intermolecular interactions of the Py-PAMA sample in the presence or absence of a VII. The studies on the behavior of Py-PAMA in oil and octane are described in Chapters 3 and 4, respectively. Chapter 5 reviews all the conclusions that are reached in this thesis and provides suggestions for future work.

Chapter 2

Probing the Interactions between Viscosity Index Improvers (VIIs), Pour Point Depressants (PPDs), and Waxes Present in engine Oil Using Pyrene-Labeled EP Copolymers

2.1 Outline

Fluorescence was applied to characterize the level of interpolymeric interactions that take place between ethylene-propylene (EP) copolymers representative of viscosity index improvers used by the oil additive industry, that were labeled with the dye pyrene to yield Py-EP samples. Two semicrystalline (EP(SM)) and one amorphous (EP(AM)) copolymer were maleated and fluorescently labeled with 1-pyrenemethylamine to yield three Py-EP samples. The fluorescence signal of the Py-EP samples was analyzed to yield f_{inter}, the molar fraction of pyrene labels that formed excimer intermolecularly upon encounter between an excited and a ground-state pyrene. The fraction f_{inter} is a measure of the level of intermolecular interactions that take place between the Py-EP samples. It was determined by acquiring the fluorescence spectra of Py-EP solutions at low and high Py-EP concentrations. Since the ratio of the intensity of the pyrene excimer over that of the pyrene monomer obtained from the fluorescence spectra of the Py-EP solutions is proportional to the local pyrene concentration ($[Py]_{loc}$), the fluorescence measurements conducted at low and high Py-EP concentration provided a measure of $[Py]_{loc}$ when pyrene excimer was formed intra and/or intermolecularly. The quantities used to represent $[Py]_{loc}$ were then employed to calculate f_{inter}. The parameter f_{inter} was determined as a function of temperature for the three EP copolymers in engine oil according to a procedure that was first developed for Py-EP samples in toluene. It remained constant as a function of temperature for EP(AM), but showed a clear break point at 0 °C and 10 °C for the EP(SM1) and EP(SM2) copolymers, respectively, reflecting their crystallization. Finally, two types of pour point depressants were added to the solution of Py-EP samples in engine oil and the f_{inter} –vs–T plots were generated. They showed little difference, whether PPD was present or not in the solution. The absence of effect was attributed to strong pyrene aggregation observed for the Py-EP samples in oil.

2.2 Introduction

An engine oil is mainly used as a lubricant in internal combustion engines, to generate a protective film between the adjacent surfaces of moving parts of the engine, and subsequently minimize contacts between them. A suitable oil must reduce friction effectively between the engine components as the temperature ramps up from the time when the engine is first ignited to normal operating conditions, a temperature range that might spread from –30 to 200 °C.[1] The lower temperature boundary depends on the season and location of the engine. Many additives such as viscosity index improvers (VIIs), pour point depressant (PPDs), detergents, antioxidants, dispersants, or anti-foam and anti-wear agents are incorporated into oils to improve the engine performance.[2] Among these chemicals, polymeric VIIs play a key role in reducing the inherent decrease in oil viscosity that occurs with increasing temperature. Oils lacking VIIs have insufficient film-forming ability, resulting in unwanted abrasion of the engine parts.[1,3]

Since the viscosity of a polymer solution prepared with a same massic polymer concentration increases with increasing molecular weight of the polymer, high molecular weight polymers could be thought of as good candidates for VIIs, as they would substantially increase the oil viscosity at high temperatures, where the oil would otherwise become too thin to act as a lubricant. However, long chain polymers are more prone to chain scission under high mechanical shear.[4] Lower molecular weight polymers are more shear resistant, but do not increase the solution viscosity to the same extent at higher temperatures. Therefore, the selection of an optimal VII requires a balance between the thickening efficiency and shear stability of the polymer.[5]

The best known polymer additives used as VIIs are poly(alkyl methacrylate)s (PAMAs), ethylene propylene (EP) copolymers, and hydrogenated styrene-diene copolymers.[6-8] Among these, EP copolymers, produced by solution polymerization of ethylene and propylene, have been

used for many years as VIIs.[1-5] The ethylene-to-propylene ratio defines whether an EP copolymer can be used as a VII, depending on its effect on the oil viscosity and its low temperature solubility. The ethylene contents of EP copolymers used as VIIs is normally in the 40–60 wt% or 50–70 mol% range.[10,11] In order to determine the optimal ratio, several parameters need to be taken into account. An EP copolymer with a higher ethylene content will thicken the solution better as well as have higher oxidative stability. However, a high ethylene content will lower the solubility of the EP copolymer due to polymer crystallization resulting in polymer insolubility at low temperatures. Moreover, microcrystals generated by EP copolymers with a high ethylene content might interact with the wax present in oils. In the case of semi-crystalline polyolefins, crystalline microdomains formed at low temperature reduce the hydrodynamic volume of the polymer coils, which results in an overall viscosity decrease of the solution, since the viscosity of the solution is related to the volume fraction of the solution occupied by the polymer coils (see Figure 1.2). Simultaneously, expansion of the polymeric coils at higher temperatures increases the solution viscosity. This phenomenon helps maintain the oil viscosity within a specific range during the operation of the engine.[10]

The durability of a polymeric VII must also be taken into account. This property depends on a number of factors such as the chemical composition and structure of the VII, as well as the engine type. The range of molecular weights used for VIIs is usually between 50K and 200K, with a polydispersity index between 2 and 2.8.[1] During the past decades, several methods have been developed and applied to characterize EP copolymers and gauge their efficiency as VIIs.[10,12] These methods are based on the use of Fourier transform infrared (FTIR) and carbon nuclear magnetic resonance (^{13}C NMR) spectroscopy to determine the chemical composition of an EP copolymer, differential scanning calorimetry (DSC) to determine its crystallinity, light scattering and intrinsic

viscosity measurements to monitor the dimensions of the polymer coils in solution, gel permeation chromatography (GPC) to characterize the molecular weight distribution of the polymer, and fluorescence measurements to monitor the polymeric interactions in solution.[1,12]

The use of excimer fluorescence generated by pyrene labels covalently attached onto EP copolymers, referred to as Py-EP samples, has been shown to be a particularly effective means to quantitatively measure the actual level of interpolymeric association between different types of EP copolymers used as VIIs in toluene.[1,3,11,12] It has been demonstrated earlier that the molar fraction f_{inter} of Py-EP copolymers forming excimer intermolecularly in solution can be easily determined from the fluorescence intensity ratio I_E/I_M of excimer-to-monomer using the fluorescence spectrum of Py-EP copolymers.[1,3] Taking advantage of the fact that the I_E/I_M ratio of a Py-EP sample in solution is directly proportional to the local pyrene concentration inside the polymer coils $[Py]_{loc}$, comparison of the I_E/I_M(inter & intra) and I_E/I_M(intra) that were obtained at, respectively, high and low Py-EP concentrations, yielded f_{inter}. This molar fraction can be effectively used to probe the level of intermolecular interactions taking place between the Py-EP molecules as described hereafter.

2.3 Experimental

Chemicals. Acetone (HPLC grade), toluene (HPLC grade, 99.9%), biphenyl (99%), maleic anhydride (98%), succinic anhydride (99%), dodecane (anhydrous, 99%), 1−pyrenemethylamine hydrochloride ($PyCH_2NH_2$ HCL, 95%), and *tert*-butyl peroxide (98%) were purchased from Sigma-Aldrich and were employed without further purification. Three ethylene-propylene copolymers, two semicrystalline (EP(SM1) and EP(SM2)) and one amorphous (EP(AM)), as well as a Group II oil and two PPDs (PPD1 and PPD2) were supplied by Afton.

***Gel Permeation Chromatography* (*GPC*).** A polymer Char high-temperature gel permeation chromatograph (GPC) was used to calculate the weight-average (M_w) and number-average (M_n) molecular weights and polydispersity index (PDI) at 145 °C and with a flow rate of 1 mL/min of 1,2,4-trichlorobenzene (TCB). The GPC instrument was equipped with three detectors, namely 15^o angle light scattering, differential refractive index, and differential viscosity detectors.

***Fourier Transform Infrared* (*FTIR*).** A Bruker Tensor 27 FTIR spectrometer was used to confirm the chemical composition of the naked, maleated, and pyrene-labeled EP copolymers. The samples dissolved in toluene were deposited drop wisely onto an NaCl FTIR cell. Application of a stream of nitrogen on the FTIR cells evaporated the toluene, leaving behind a thin layer of polymer which was placed in the spectrophotometer to acquire its FTIR spectrum.

***UV-Visible Spectrophotometer* (*UV-Vis*).** The absorbance/transmittance of all the solutions were measured in the 200–600 nm range with a Cary 100 UV-Vis and a Cary 5000 UV-Vis spectrophotometer using quartz cells with 0.1 and 10 mm path length.

Steady-State Fluorometer. A Photon Technology International (PTI) LS-100 fluorometer was employed to acquire the SSF spectra of the Py-EP solutions. The fluorometer included a PTI 814 photomultiplier detection system and an Ushio UXL-75Xe xenon arc lamp. Solutions with concentrations of the Py-EP samples between 0.01 and 0.1 $g.L^{-1}$ were low enough to avoid the inner filter effect, and a square cell with a circular neck was used to acquire the fluorescence spectra with the right-angle geometry. The inner filter effect was a problem for the higher 10 $g.L^{-1}$ Py-EP concentrations and a triangular cell was used with the front-face geometry for spectra acquisition. The solutions in toluene and oil needed to be degassed for 40-50 minutes under a gentle flow of N_2 to remove oxygen, a powerful fluorescence quencher. The cells were then sealed quickly with a Teflon stopper. The fluorescence spectra were acquired by exciting the solutions at

344 nm and monitoring their emission between 350 and 600 nm. The spectra were background-corrected by subtracting the light scattering envelope of the solutions without Py-EP samples.

Cryostat (Optistat DN). The fluorescence spectra for the Py-EP solutions were acquired at temperatures between –30 (± 0.2) °C and +25 (± 0.2) °C with a cryostat from Oxford Instruments (Optistat DN). The fluorescence cells containing the degassed Py-EP solutions were introduced inside the cryostat which was placed in the steady-state fluorometer. A set of fluorescence experiments began by cooling the solution to the lowest temperature. The temperature of the solution was then increased in 5°C increments until the maximum temperature (+25°C) was reached. To ensure accurate measurements and that the Py-EP solution had reached a stable temperature, the solution was left in the cryostat for 5 min after reaching its set temperature and a fluorescence spectrum was acquired.

Time-Resolved Fluorescence. Fluorescence decay measurements were carried out with an IBH time-resolved fluorometer by exciting the Py-EP solutions at 340 nm with a nano-LED light source. Background and light scattering corrections were applied when fitting the fluorescence decays of the pyrene monomer and excimer globally with the model free analysis (MFA). The global analysis of the fluorescence decays of a Py-EP solution was considered acceptable if the χ^2 was lower than 1.30, and the residuals and the autocorrelation of the residuals were randomly distributed around zero. Details on the MFA can be found in published reviews.[18,19]

***Carbon Nuclear Magnetic Resonance* (^{13}*C NMR*).** The EP samples (20 g.L^{-1}) were dissolved in TCE-d_2, placed in an NMR tube, and kept in a heating block overnight at 120 ^{o}C to homogenize the solutions.[11] The ^{13}C NMR spectra for the samples were acquired at 125 ^{o}C on a Bruker 500 MHz NMR spectrometer. The ^{13}C NMR spectra for EP(AM), EP(SM1), and EP(SM2) are shown in Figure S2.1.

Pyrene Labeling. The synthesis of the Py-EP samples was carried out in two steps as outlined in a published procedure.[11,12] EP copolymer (2 g) and biphenyl (60 g) were heated in a three-neck round-bottom flask equipped with a condenser. To ensure the dissolution of the EP copolymer, the mixture was heated for 12 hrs at 155-160 °C. Maleation of the EP copolymer was carried out under a stream of nitrogen with the addition of maleic anhydride (MA) (61 mg, 0.8 mmol) and *tert*-butyl peroxide (202 mg, 1.4 mmol) to generate radicals. Successful maleation required that the reaction temperature be maintained at 180-185 °C for only 30 min (Scheme 2.1). After completion of the reaction, successive aliquots of the hot solution of the maleated EP copolymer solution in biphenyl were dropped immediately into acetone, where the maleated EP copolymer precipitated. The precipitated polymer was then re-dissolved in the smallest possible amount of toluene. To ensure the removal of unreacted MA from the solution, the precipitation into acetone of the polymer solution in toluene was repeated four times and the purified polymer was then stored in toluene to avoid hydrolysis of the succinic anhydride ring.

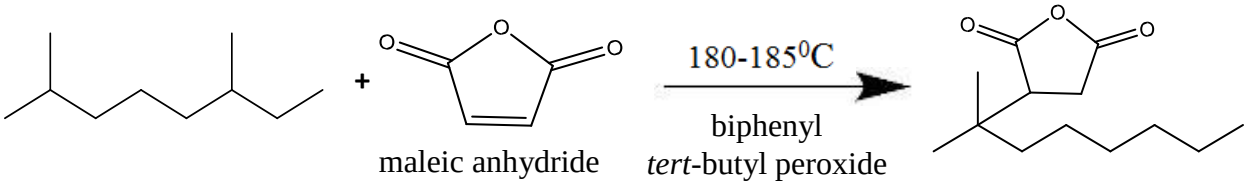

Scheme 2.1. Reaction scheme for the maleation of the EP copolymer

Before the labeling reaction, a solution of the maleated EP copolymer in toluene was precipitated into acetone one last time. The polymer (1 g) was then partially dried under a stream of nitrogen to minimize crosslinking before adding $PyCH_2NH_2$ (185 mg, 0.8 mmol) in a three-neck round-bottom flask containing dodecane (60 mL) at 180-185 ^oC. The reaction vessel was equipped with a condenser and kept under nitrogen atmosphere for 12 hours (Scheme 2.2). The

required amount of $PyCH_2NH_2$ was prepared from $PyCH_2NH_2$,HCl through a liquid-liquid extraction as discussed in the literature.[13,14] To this end, $PyCH_2NH_2$,HCl (214 mg, 0.8 mmol) was dissolved in water (160 mL) and then added to a separatory funnel along with two NaOH pellets. After the addition of hexane (140 mL) and vigorous shaking, the organic phase was isolated and hexane was evaporated to get $PyCH_2NH_2$.

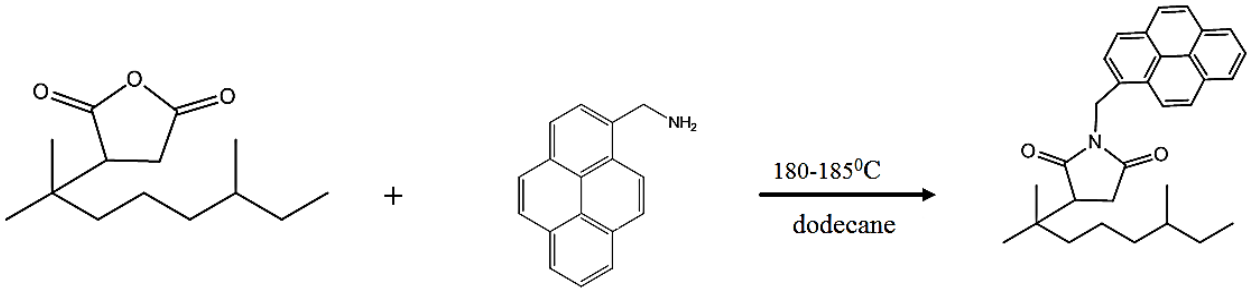

1-pyrenemethylamine

Scheme 2.2. Pyrene labeling of the maleated EP copolymer.

Following completion of the reaction, the labeled EP copolymers were dissolved in dodecane and precipitated into acetone. The precipitated polymers were then redissolved in toluene and precipitated into acetone. The procedure was repeated four times. The Py-EP samples were kept in toluene to minimize crosslinking which had been found to occur when the Py-EP samples were stored in the dry form. To prepare a concentrated Py-EP solution in oil, the Py-EP solution in toluene was precipitated into the acetone and the precipitate was redissolved in the oil at 140-150 °C for two hours to ensure that the toluene and acetone had fully evaporated.

2.4 Chemical Composition. After the synthesis of the Py-EP(AM), Py-EP(SM1), and Py-EP(SM2) copolymers,[9] FTIR spectroscopy was employed to verify the chemical composition of the samples after each reaction (Figure 2.1). The absorption peaks at 1379 cm^{-1} and 1462 cm^{-1} correspond to the methyl and methylene groups, whereas the absorption at 1866 cm^{-1} and 1785 cm^{-1} represent the carbonyl groups of succinic anhydride. Upon reaction with 1-pyrenemethylamine, the major peak at 1785 cm^{-1} for the carbonyl of succinic anhydride shifted to 1710 cm^{-1} which is characteristic of the succinimide carbonyls.

Following the assignment of the FTIR absorption peaks at 1379 and 1462 cm^{-1}, the Abs(1379 cm^{-1})/Abs(1462 cm^{-1}) ratio could be used as a measure of the propylene content of the EP copolymers.[1] The ratio Abs(1379 cm^{-1})/Abs(1462 cm^{-1}) took an average value of 0.80 ± 0.02, 0.56 ± 0.01, and 0.60 ± 0.01 for the EP(AM), EP(SM1), and EP(SM2) samples, respectively. The higher ratio value of EP(AM) was characteristic of a larger propylene content consistent with the amorphous character of this EP copolymer. The higher ethylene content reflected by the lower Abs(1379 cm^{-1})/Abs(1462 cm^{-1}) ratio of EP(SM1) and EP(SM2) suggested that these samples might exhibit longer oligoethylene sequences that would crystallize at low solution temperatures. This ratio did not change markedly after maleation and pyrene labeling of the EP copolymers, which suggested that these reactions did not affect the chemical composition of the EP copolymers, as would be expected.

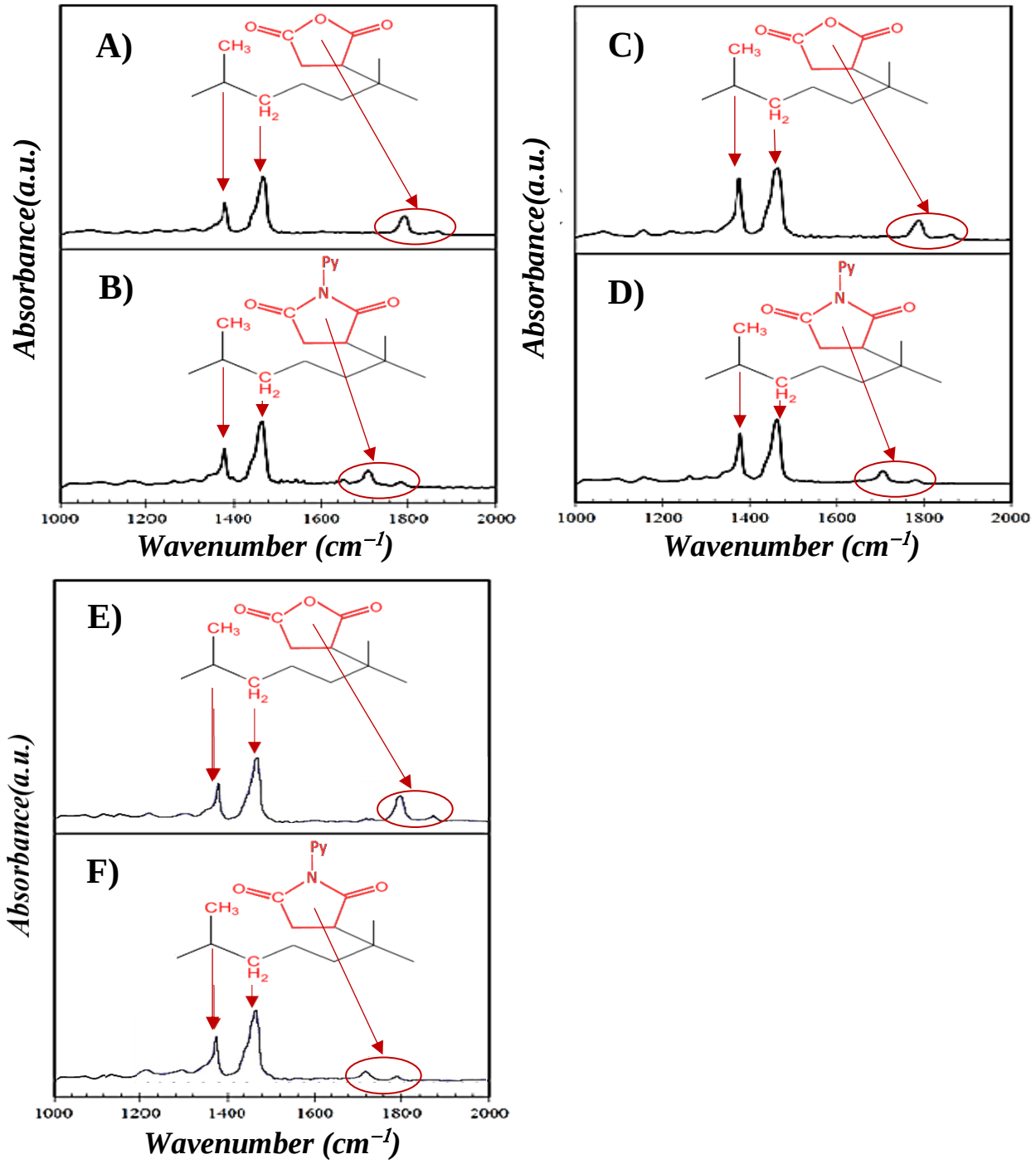

Figure 2.1. FTIR spectra for A) EP(SM1)-MA, B) Py(116)-EP(SM1), C) EP(AM)-MA, D) Py(108)-EP(AM), E) EP(SM2)-MA, F) Py(100)-EP(SM2).

^{13}C NMR was used to determine the mole fractions of ethylene and propylene of the EP copolymers by applying a well-documented procedure.[11] This procedure was used earlier to show that the samples EP(AM) and EP(SM1) contained 60 and 78 mol% ethylene,[1] and in this study to determine that EP(SM2) had 68 mol% ethylene content. These ethylene contents are in agreement with the Abs(1379 cm^{-1})/Abs(1462 cm^{-1}) ratios showing that EP(SM2) was expected to have an ethylene content lower than EP(SM1) but higher than EP(AM).

Table 2.1. Summary of the FTIR and GPC results for the naked, maleated, and pyrene-labeled EP copolymers.

Batch	Polymer Type	$\frac{Abs(1379\,cm^{-1})}{Abs(1462\,cm^{-1})}$	$\frac{Abs(1790\,cm^{-1})}{Abs(1462\,cm^{-1})}$	$\frac{Abs(1710\,cm^{-1})}{Abs(1462\,cm^{-1})}$	M_n (g/mol)	M_w (g/mol)	PDI (M_W/M_n)
1	EP(AM)	0.80	-	-	59,000	125,000	2.11 a)
	EP(AM)-MA	0.82	0.34	-	-	-	-
	Py(108)-EP(AM)	0.79	-	0.20	25,000	61,000	2.42 a)
2	EP(SM1)	0.56	-	-	55,000	145,000	2.63 a)
	EP(SM1)-MA	0.57	0.28	-	-	-	-
	Py(116)-EP(SM1)	0.56	-	0.24	33,000	92,000	2.77 a)
3	EP(SM2)	0.60	-	-	22,800	145,900	6.40 b)
	EP(SM2)-MA	0.60	0.40	-	-	-	-
	Py(100)-EP(SM2)	0.59	-	0.16	-	-	-

a) Pirouz et al.[1]; b) this study.

2.5 Pyrene Content (λ_{Py}) and P_A Value

After the synthesis, purification, and characterization of the chemical composition of the Py-EP copolymers by FTIR spectroscopy, UV-Vis absorption was applied to determine the pyrene

content (λ_{Py}) and also the peak-to-valley ratio (P_A) of the Py-EP samples (Figure 2.2). The P_A value was determined from the ratio of the absorbance (Abs) of the peak at 345 nm to that of the trough at 336 nm as described in Equation 2.1.

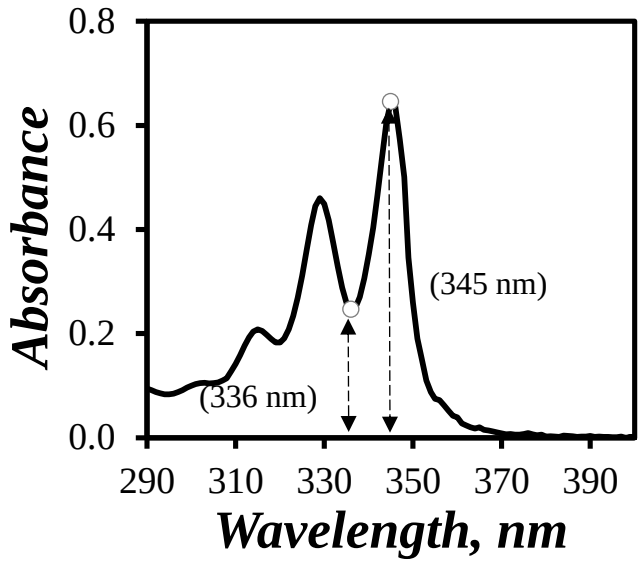

Figure 2.2. UV-Vis absorption spectrum of Py-EP(AM) in toluene

$$P_A = \frac{Abs(345nm)}{Abs(336nm)} \qquad (2.1)$$

A P_A value lower than 3.0 reflects the presence of pyrene aggregates, whereas a P_A value equal to or greater than 3.0 indicates that no significant pyrene-pyrene interactions exist (Scheme 2.3).[1]

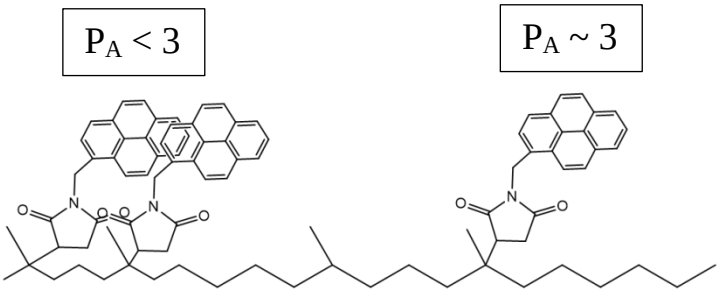

Scheme 2.3. Illustration of the effect of pyrene aggregation on the P_A value.

The absorbance at 345 nm can also be used to determine the pyrene concentration by application of the Beer-Lambert law, and subsequently the pyrene content (λ_{Py}) of a Py-EP sample, through Equations 2.2 and 2.3.

$$Abs = \varepsilon_{Py}[Py]\,l \qquad \varepsilon_{Py} = 44{,}800 \pm 300\ (M^{-1}.cm^{-1}) \tag{2.2}$$

$$\lambda_{Py} = \frac{[Py]}{(m/V)} \tag{2.3}$$

In Equation 2.2, ε_{Py} is the molar extinction coefficient of 1-pyrenemethylsuccinimide in toluene at 345 nm, l is the path length of the UV cell, and the ratio (m/V) in Equation 2.3 represents the massic concentration of the Py-EP solution.

The P_A values were determined and are listed in Table 2.2. The P_A value always decreased when going from toluene to oil, probably because toluene is a better solvent for the succinimide pendants than an aliphatic oil.[16]

Table 2.2. Pyrene content (λ_{py}) of the Py-EP samples, molar fraction of the different pyrene species in solution, and P_A value.

Sample Description	λ_{Py} ($\mu mol.g^{-1}$)	Solvent	τ_M (ns)	f_{diff}	f_{free}	f_{agg}	f_D	f_{E0}	<k> ($10^6\ s^{-1}$)	P_A
Py(108)-EP(AM)	108	toluene	243	0.580	0.185	0.235	0.073	0.162	18.7	2.76
Py(116)-EP(SM1)	116			0.481	0.168	0.351	0.065	0.286	16.6	2.61
Py(100)-EP(SM2)	100			0.582	0.055	0.364	0.281	0.083	12.6	2.57
Py(108)-EP(AM)	108	oil	315	0.435	0.072	0.493	0.071	0.423	5.2	2.50
Py(116)-EP(SM1)	116			0.358	0.087	0.555	0.116	0.439	6.9	2.47
Py(100)-EP(SM2)	100			0.335	0.027	0.639	0.544	0.094	4.1	2.35

The MFA of the fluorescence decays acquired for the Py-EP sample in oil and toluene yielded the molar fraction of the different pyrene species in solution as described in Section 1.2.2

in the Introduction. The analysis indicates that an increase in the molar fraction of aggregated pyrenes (f_{agg}) reflects increased aggregation of the succinimide pendants in the oil, because an aliphatic oil is a poorer solvent than toluene for the succinimide groups.[14] The f_{agg} values listed in Table 2.2 indicate that more than 50 mol% of the pyrene labels were aggregated in oil. The increase of pyrene aggregation in oil obtained from the TRF experiments matches what was also found by UV-Vis absorption measurements that yielded lower P_A values, indicative of enhanced pyrene association in oil. Nevertheless, the fluorescence spectra acquired for the Py-EP(SM1), Py-EP(SM2), and Py-EP(AM) samples showed that enough excimer formation was produced to determine f_{inter} despite the higher viscosity of the oil as compared to toluene, which reduces excimer formation by diffusion. Aggregation of the pyrene labels in oil might complicate the analysis of the fluorescence data, however, since it may induce unwanted interactions between Py-EP copolymers via the succinimide groups.

2.6 Turbidity measurements

Turbidity measurements were conducted on EP(AM) and EP(SM1) solutions in oil, where the polymers were fully dissolved. Since a decrease in solution temperature can lead to a worsening of the solvent quality toward the polymer, turbidity measurements were carried out as a function of solution temperature and polymer concentration by monitoring the absorption of the polymer solution at 500 nm, where the oil does not absorb. A low absorption indicated a homogeneous polymer solution and that no microcrystals had formed. Based on the plots shown in Figures 2.3 and 2.4, it could be concluded that negligible formation of microcrystals took place at temperatures greater than −5 °C, as long as the EP copolymer concentration was kept below 10 g/L. The absorbance at low temperature was always much lower for EP(AM) than for EP(SM1). EP(AM)

formed fewer microcrystals in solution at low temperature, as would be expected from this amorphous polymer.

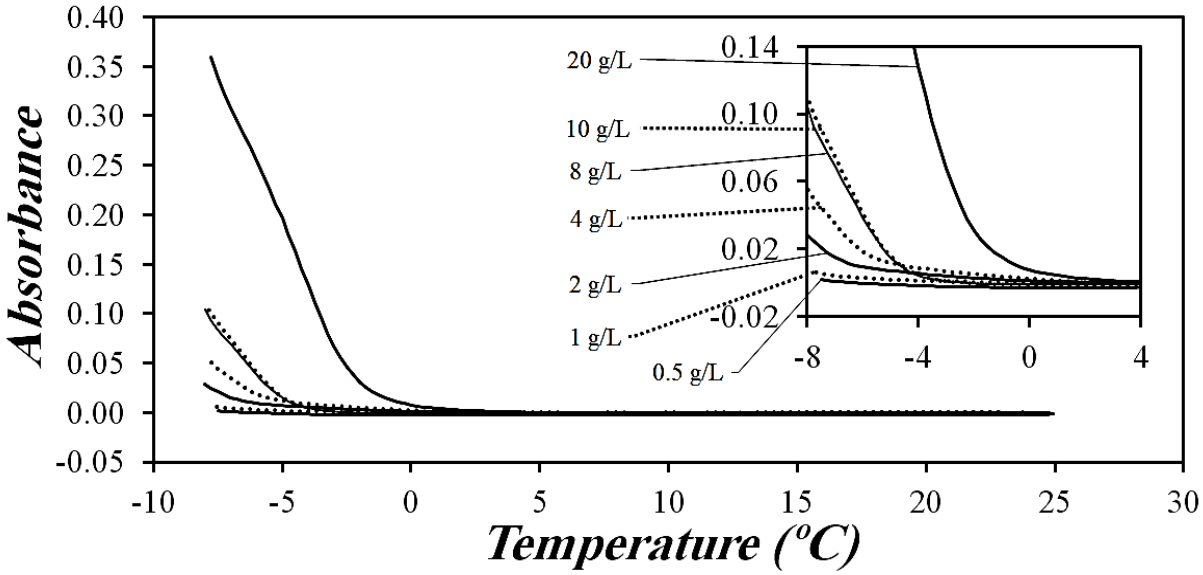

Figure 2.3. Plot of absorbance versus temperature for different concentrations of the EP(SM1) sample in oil at 500 nm.

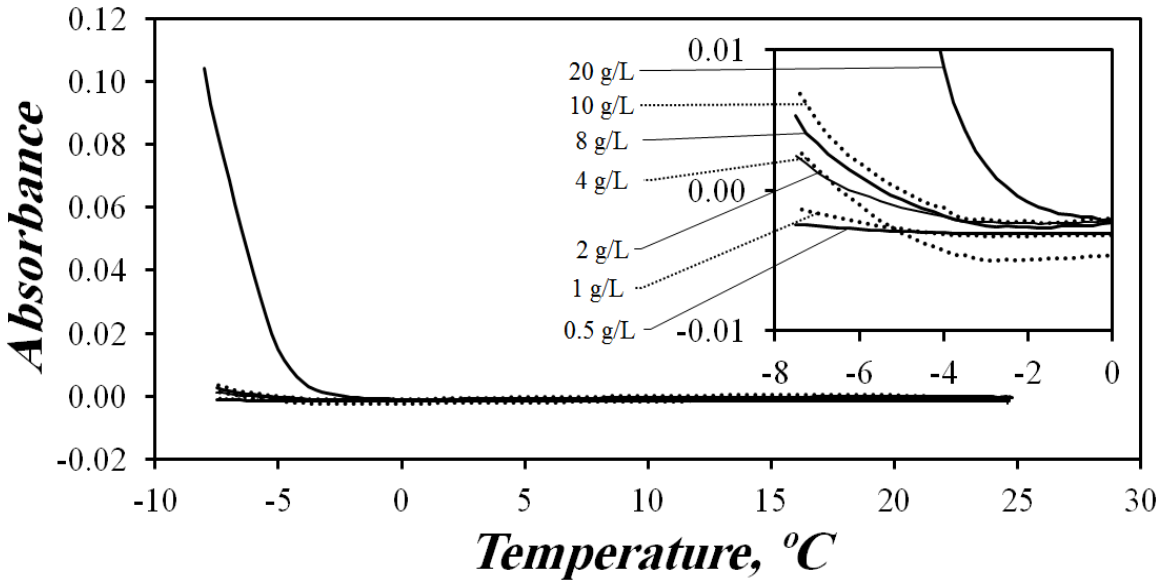

Figure 2.4. Plot of absorbance versus temperature for different concentrations of the EP(AM) sample in oil at 500 nm.

2.7 Intrinsic Viscosity Measurements

The behavior of the hydrodynamic volume (V_h) of the EP copolymers was monitored as a function of temperature, by measuring the intrinsic viscosity [η] of the solution of the EP copolymers in toluene and oil, as shown in Figure 2.5. As the solution temperature decreased, [η] remained constant for EP(AM) in toluene and oil but decreased abruptly at T = 0 °C for EP(SM1) and T = 10 °C for EP(SM2), in both solvents. The temperature where the sudden decrease in [η] was observed for the semicrystalline EP copolymers was assigned to the onset of microcrystal formation. The plots of intrinsic viscosity as a function of temperature for the semicrystalline sample showed a more pronounced drop in oil as compared to toluene, probably because oil was a worse solvent for the polymer. The decrease in intrinsic viscosity observed solely for the semicrystalline EP copolymers at low temperature is well documented and has been attributed to the formation of microcrystals that reduce V_h.[17]

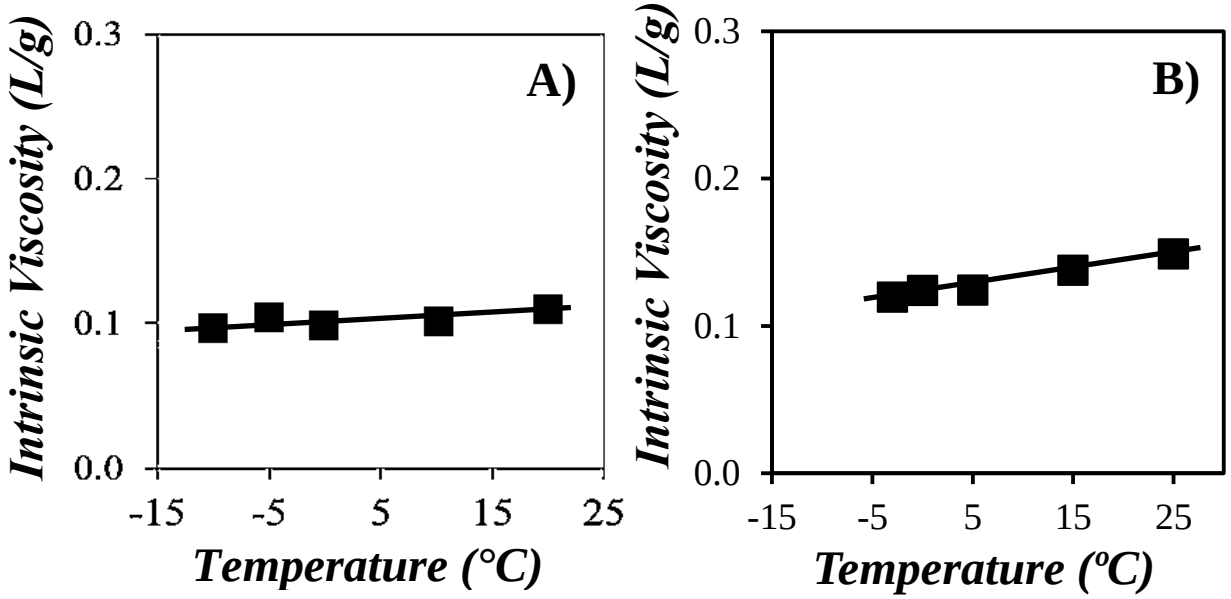

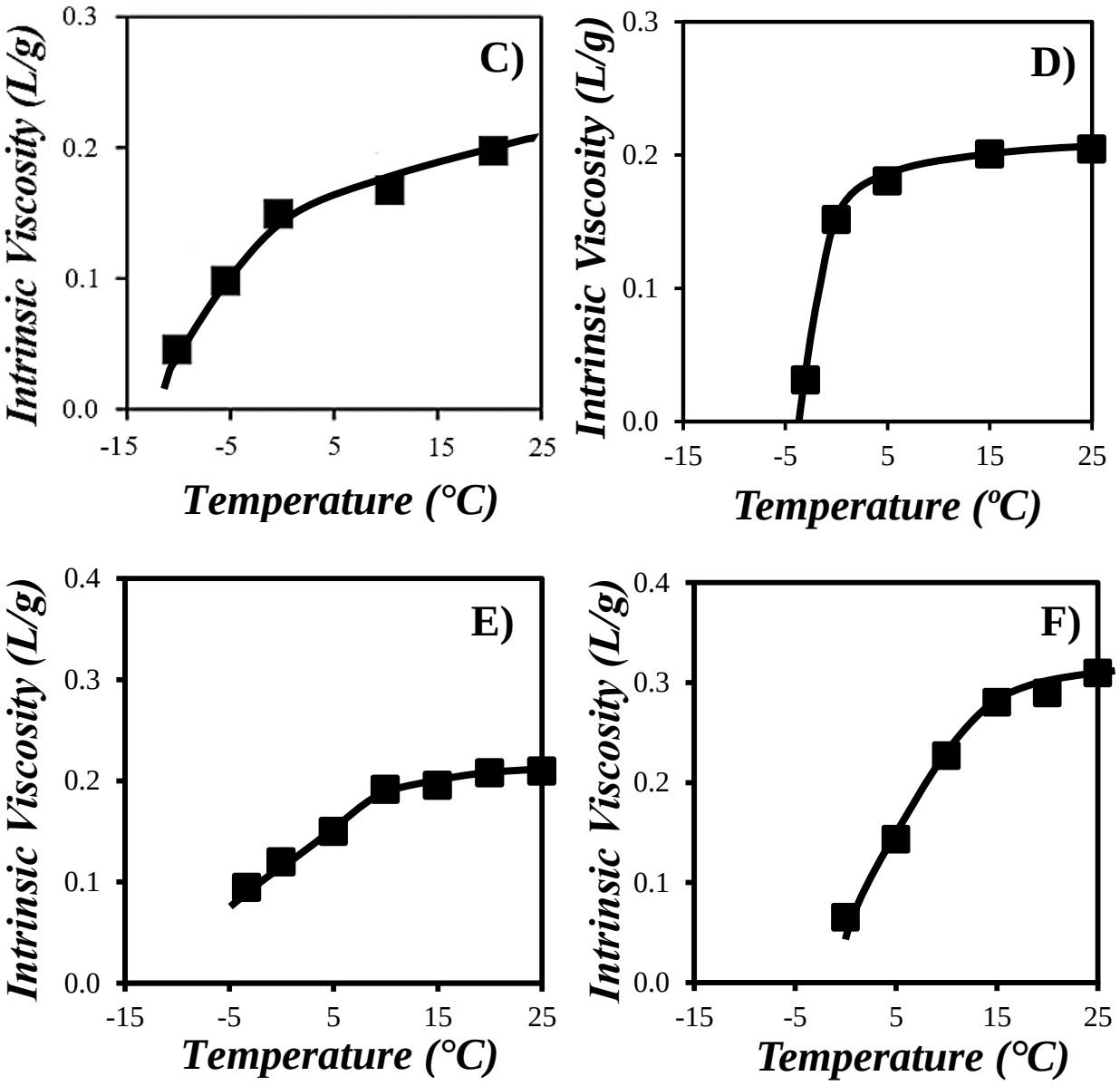

Figure 2.5 Plots of intrinsic viscosity as a function of temperature for A and B) EP(AM), C and D) EP(SM1), E and F) EP(SM2). A, C, E: toluene. B, D, F: oil. Plots A and C were already published.[1]

2.8 Level of Interpolymeric Interactions (f_{inter}) in Toluene

As discussed briefly in Chapter 1, the emission of an excited pyrene monomer can be identified by several sharp peaks between 360 and 425 nm in the fluorescence spectrum of a Py-EP solution

(see Figure 1.4). Pyrene excimer, in contrast, exhibits a structureless and broad emission centered around 480 nm.[18] Based on this behavior, the fluorescence intensity of the pyrene excimer (I_E) and monomer (I_M) of a Py-EP sample in solution were calculated by integrating its fluorescence spectrum over the wavelength ranges between 372 and 379 nm and between 500 and 530 nm, respectively. Integrating the monomer emission peak at the most blue-shifted peak at 375 nm ensured that the broad excimer emission centered at 480 nm would have a negligible effect on the fluorescence intensity of the pyrene monomer. Similarly, integrating the excimer fluorescence signal from 500 to 530 nm meant that it was sufficiently separated from the monomer emission, so that emission from the latter species would not interfere with that of the former. As demonstrated in earlier studies, the I_E/I_M ratio is directly proportional to the local pyrene concentration $[Py]_{loc}$ experienced by an excited pyrene, as reflected by Eq. 2.4.[1,20]

$$I_E/I_M = K(T) \times [Py]_{loc} \tag{2.4}$$

The multiplication factor *K(T)* is only affected by temperature and is independent of the local pyrene concentration.[9,20] Therefore, an increase in I_E/I_M observed at a certain temperature is indicative of an increase in $[Py]_{loc}$. If the increase in $[Py]_{loc}$ can be correlated back to an increase in the concentration of the pyrene-labeled macromolecule (PyLM) of interest, it represents a strong indication that the PyLMs interact with each other. Depending on the PyLM concentration, these interactions can occur intra- and intermolecularly. At high PyLM concentrations where the PyLMs undergo both intra- and intermolecular interactions, $[Py]_{loc}$(inter & intra) is reflected by the ratio I_E/I_M(inter & intra).

At low PyLM concentrations where the PyLMs undergo solely intramolecular interactions, the fluorescence spectrum yields the ratio I_E/I_M(intra) that is representative of $[Py]_{loc}$(intra).

According to Eq. 2.4, the ratios I_E/I_M(inter & intra) and I_E/I_M(intra) would be equal to $K(T)\times[Py]_{loc}$(inter & intra) and $K(T)\times[Py]_{loc}$(intra), respectively. Taking advantage of this relationship, the molar fraction of Py-EPs forming excimer intermolecularly (f_{inter}) can be rearranged as shown in Eq. 2.5.[1]

$$f_{\text{inter}} = \frac{[Py]_{loc}\left(\begin{smallmatrix}\text{inter \&}\\ \text{intra}\end{smallmatrix}\right) - [Py]_{loc}\,(\text{intra})}{[Py]_{loc}\left(\begin{smallmatrix}\text{inter \&}\\ \text{intra}\end{smallmatrix}\right)} = \frac{I_E / I_M\left(\begin{smallmatrix}\text{inter \&}\\ \text{intra}\end{smallmatrix}\right) - I_E / I_M\,(\text{intra})}{I_E / I_M\left(\begin{smallmatrix}\text{inter \&}\\ \text{intra}\end{smallmatrix}\right)} \tag{2.5}$$

Most interestingly, the multiplication factor $K(T)$ in Eq. 2.4 cancels out in Eq. 2.5 used to calculate f_{inter} for the Py-EP samples.

Experimentally, the ratio I_E/I_M(inter & intra) can be simply obtained from a solution prepared with a high concentration of Py-EPs. The earlier studies conducted by S. Pirouz et al.[1,3] confirmed that both intra- and intermolecular interactions were observed between Py-EP samples in a 10 $g.L^{-1}$ solution. On the other hand, the calculation of I_E/I_M(intra) was more challenging. The crystallization of the Py-EP(SM)s induced strong intermolecular interactions between the Py-EP coils even at low (0.01 $g.L^{-1}$) Py-EP concentration in toluene. Therefore, to ensure that the crystallization of the Py-EP samples in dilute solutions would not affect intramolecular excimer formation used for the determination of I_E/I_M(intra), the fluorescence spectrum of dilute (0.01 $g.L^{-1}$) solutions of the Py-EP samples was acquired in the presence of a 10 $g.L^{-1}$ excess concentration of the unlabeled EPs.[1,3] Under these conditions, the fluorescence spectrum of the mixture solely reflected the behavior of pyrene excimer formed intramolecularly from isolated Py-EP macromolecules in large aggregates of the naked EP copolymers.

Since an engine oil usually contains a few wt% of EP copolymer used as VII, the fluorescence spectra of 10 $g.L^{-1}$ Py(108)-EP(AM), 10 $g.L^{-1}$ Py(116)-EP(SM1), and 10 $g.L^{-1}$ Py(100)-EP(SM2)

solutions in toluene were initially acquired as a function of temperature. The fluorescence spectra of Py(108)-EP(AM) were normalized at 375 nm and are shown in Figure 2.6. The intensity of the excimer (I_E) relative to the normalized intensity of the monomer (I_M) increased continuously with increasing temperature. This increase in I_E reflected an increase in excimer formation by diffusive encounters due the lowering in solution viscosity that occurs upon increasing the solution temperature. The normalized florescence spectra for Py(116)-EP(SM1) in toluene, however, exhibited a different behavior in Figure 2.7A-C. This sample behaved similarly to Py(108)-EP(AM) at temperatures lower than −20 °C and above +5 °C. Upon increasing the temperature from −15 to 0 °C, I_E decreased relative to I_M. Interestingly, −10 °C corresponds to the crystallization temperature of Py(116)-EP(SM1) in toluene. A similar behavior was also observed for Py(100)-EP(SM2), whose fluorescence spectra showed features similar to those of the amorphous Py(108)-EP(AM) sample at temperatures lower than −10 °C and higher than +20 °C, but displayed an increase in I_E relatively to I_M with decreasing temperature around its crystallization temperature at +5 °C in Figure 2.7E.

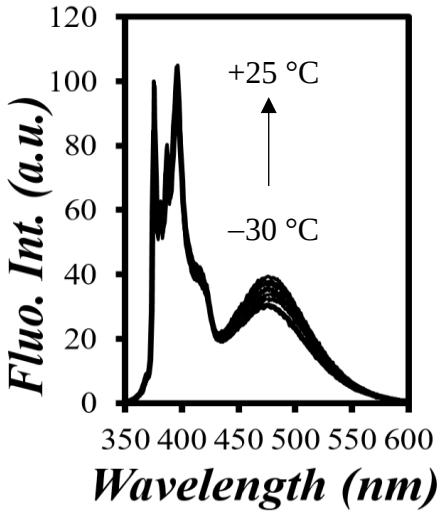

Figure 2.6. Fluorescence spectra normalized at 375 nm of 10 g.L^{-1} Py(108)-EP(AM) in toluene from −30 to 25 °C.

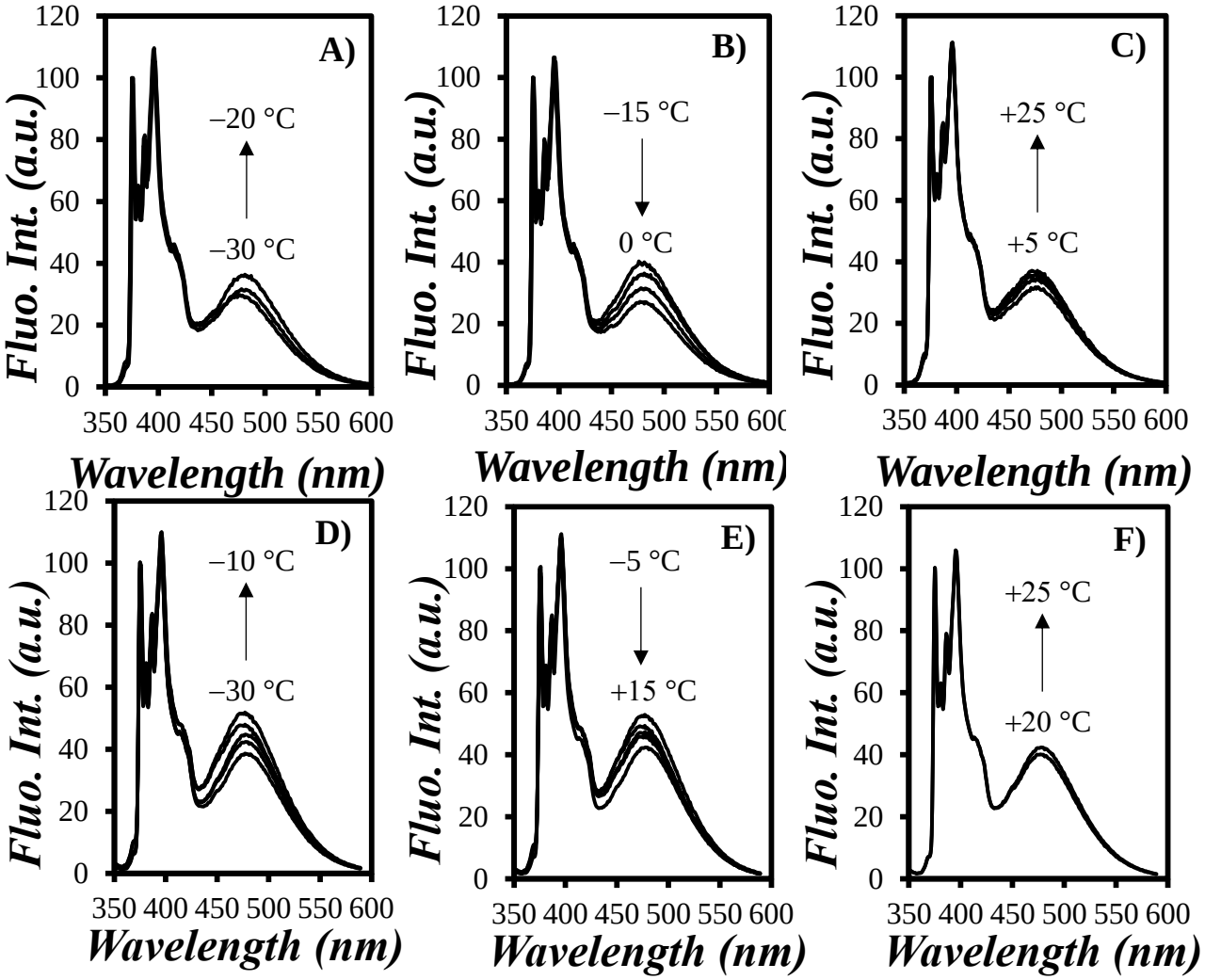

Figure 2.7. Fluorescence spectra of solutions in toluene of 10 g.L^{-1} Py(116)-EP(SM1) from A) −30 to −20 °C, B) −15 to 0 °C, and C) +5 to +25 °C, and 10 g.L^{-1} Py(100)-EP(SM2) from D) −30 to −10 °C, E) −5 to +15 °C, and F) +20 to +25 °C.

As discussed earlier, the molar fraction (f_{inter}) could be calculated as a function of temperature according to Eq. 2.5. As reported previously,[1,3] a solution of 10 g.L^{-1} Py-EP sample, along with a solution of 0.01 g.L^{-1} Py-EP sample and 10 g.L^{-1} unlabeled EP copolymer in toluene, were used to determine I_E/I_M(inter & intra) and I_E/I_M(intra), respectively. The ratios I_E/I_M(inter &

intra) and I_E/I_M(intra) were plotted as a function of temperature for each of the fluorescence spectra shown in Figures 2.6 and 2.7.

In the case of Py(108)-EP(AM) solutions, the I_E/I_M ratio increased continuously with increasing temperature at both high and low polymer concentrations since it represented excimer formation by diffusion that increased at higher temperatures. The 10 $g.L^{-1}$ EP(SM1) and EP(SM2) solutions yielded a different trend for I_E/I_M over the same temperature range (Figure 2.8B-C). Starting at −25 °C, the I_E/I_M ratio for a 10 $g.L^{-1}$ solution of Py(116)-EP(SM1) and Py(100)-EP(SM2) increased with increasing temperature, similarly to what was observed for the amorphous sample. The increase in I_E/I_M was then followed by a decrease from −15 °C to 0 °C and −5 °C to +20 °C for the Py(116)-EP(SM1) and Py(100)-EP(SM2) solutions, respectively. Upon increasing the solution temperature further, the I_E/I_M ratio increased for both semicrystalline samples. The anomalous behavior of the Py(116)-EP(SM1) and Py(100)-EP(SM2) solutions at intermediate temperatures was indicative of a change in the process of excimer formation that had two origins. The decrease in I_E/I_M observed at intermediate temperature upon increasing the solution temperature could be due to a hydrodynamic volume expansion of the polymeric coils that happened upon melting the compact crystalline microdomains of the semicrystalline EP copolymers, thus decreasing $[Py]_{loc}$, or the dissociation of Py-EP(SM) aggregates resulting also in a decrease in $[Py]_{loc}$. Both effects would be responsible for the break point observed in the I_E/I_M profiles of Py(116)-EP(SM1) and Py(100)-EP(SM2) and would be a consequence of the intermolecular formation of microcrystals in the solution. Interestingly, in the case of a mixture of 0.01 $g.L^{-1}$ Py-EP(SM)s with 10 $g.L^{-1}$ of unlabeled EP(SM), the break point was not observed around the crystallization temperature of the samples. Such an observation confirmed that the Py-EP(SM) polymers were isolated by the large excess of unlabeled EP(SM) present in the solution

and thus, that no intermolecular interaction took place between the Py-EP(SM) chains under such dilute conditions.

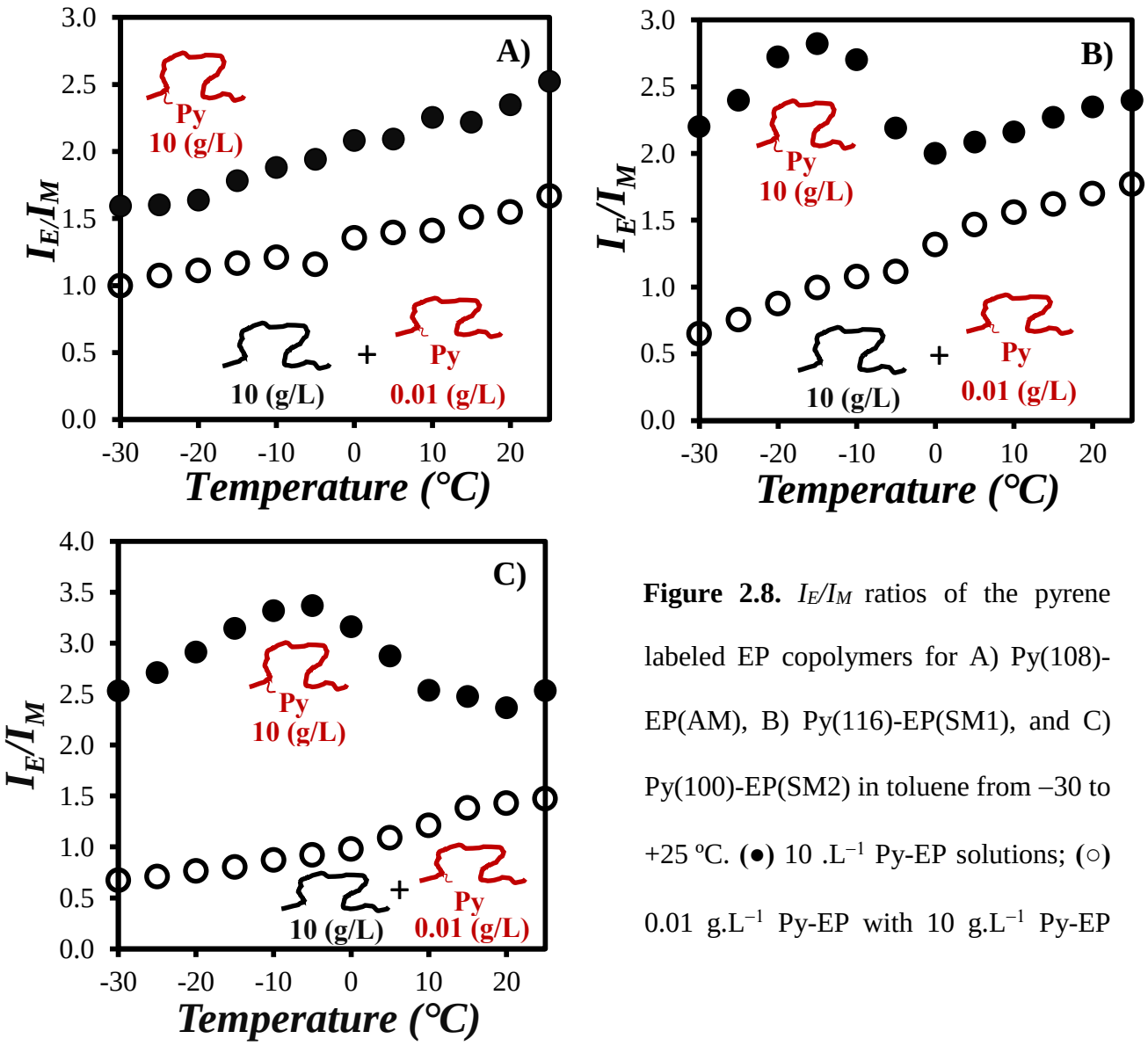

Figure 2.8. I_E/I_M ratios of the pyrene labeled EP copolymers for A) Py(108)-EP(AM), B) Py(116)-EP(SM1), and C) Py(100)-EP(SM2) in toluene from –30 to +25 ºC. **(●)** 10 .L^{-1} Py-EP solutions; **(○)** 0.01 g.L^{-1} Py-EP with 10 g.L^{-1} Py-EP

The I_E/I_M ratios were combined according to Equation 2.5 to yield f_{inter}, which was plotted as a function of temperature in Figure 2.9. Consistent with earlier studies for the EP(AM) sample in toluene,[1,3] f_{inter} remained constant around 0.36 ± 0.03 with temperature for the 10 g.L^{-1} EP(AM) solution in toluene as expected for an amorphous polymer (Figure 2.9A). In the case of the 10

g.L^{-1} Py(116)-EP(SM1) and Py(100)-EP(SM2) solutions in toluene, the transition caused by the formation of crystalline microdomains at intermediate temperatures was clearly observed in the f_{inter} plots. For the 10 g.L^{-1} Py(116)-EP(SM1) solution, f_{inter} decreased from 0.67 ± 0.03 at low temperature to 0.29 ± 0.02 at high temperature. The inflexion point of the transition in f_{inter} of this sample could be observed at T = –5 ± 5 °C. f_{inter} for Py(116)-EP(SM1) in toluene showed a similar profile to that obtained earlier by Pirouz et al. for the same copolymer and solvent.[1,3] In a similar manner, f_{inter} of Py(100)-EP(SM2) decreased from 0.73 ± 0.02 at low temperature to 0.42 ± 0.03 at high temperature with an inflexion point at T = +5 ± 5 °C.

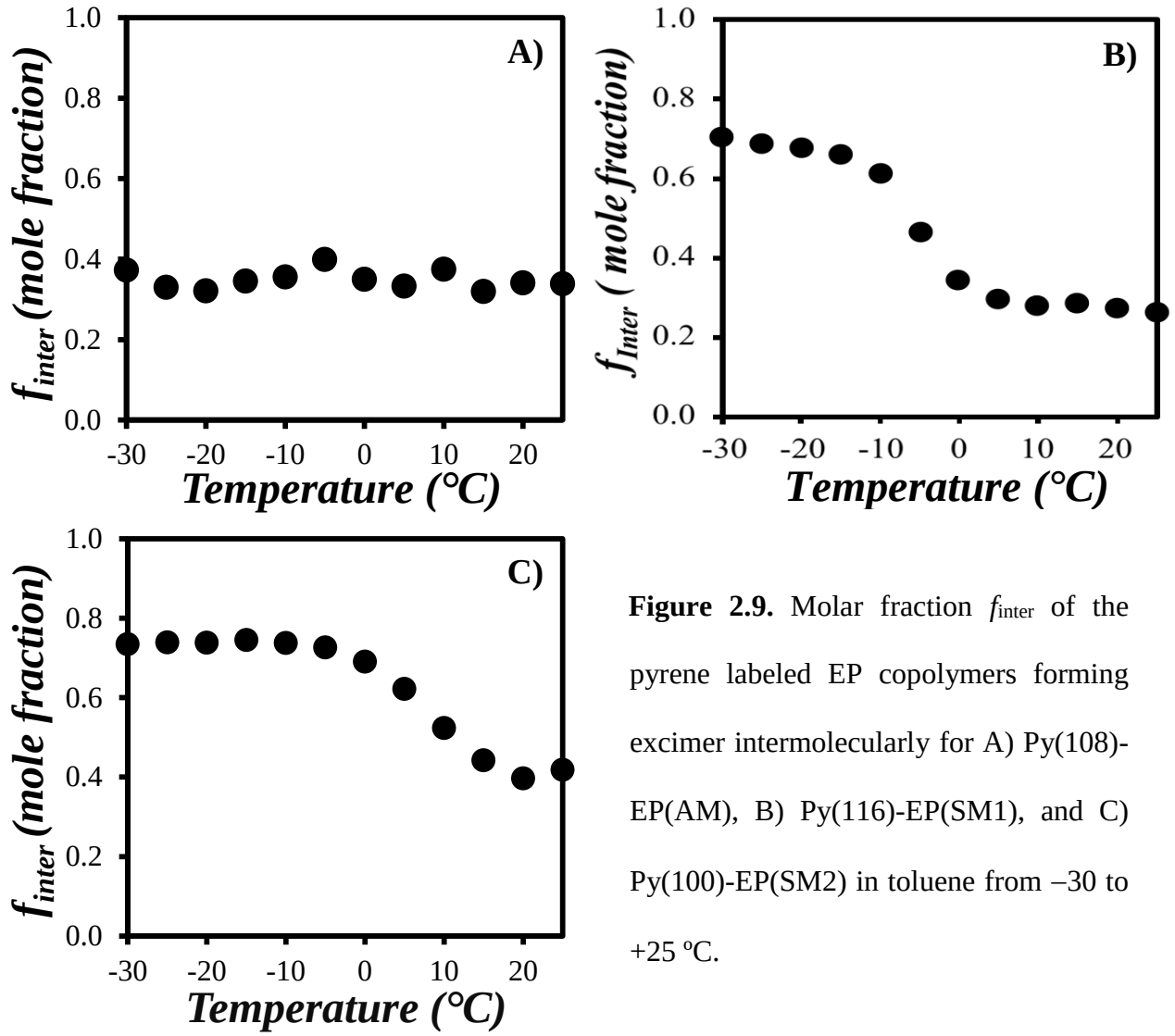

Figure 2.9. Molar fraction f_{inter} of the pyrene labeled EP copolymers forming excimer intermolecularly for A) Py(108)-EP(AM), B) Py(116)-EP(SM1), and C) Py(100)-EP(SM2) in toluene from –30 to +25 °C.

The temperature and f_{inter} values corresponding to each temperature regime were listed in Table 2.3. Both Py-EP(SM) samples exhibited three distinct regimes whereas Py-EP(AM) showed a constant f_{inter} value over the entire temperature range.

Table 2.3. Summary of the molar fraction (f_{inter}) obtained for a solution of the 10 g.L^{-1} Py–EP samples in toluene.

Sample	λ_{py}	T_C (°C)	Temp (°C)			
			–30 to –10	–10 to 0	0 to +10	+10 to +25
Py-EP(SM1)	116	–5	0.67 ± 0.03	-	0.29 ± 0.02	
Py-EP(SM2)	100	+5	0.73 ± 0.02		-	0.42 ± 0.03
Py-EP(AM)	108	-	0.36 ± 0.03			

2.9 Level of Interpolymeric Interactions (f_{inter}) in Oil

A similar method was applied to measure the level of intermolecular interactions of the EP copolymers in engine oil. To this end, a 10 g.L^{-1} solution of Py(116)-EP(SM1), Py(100)-EP(SM2), and Py(108)-EP(AM) in oil was used to acquire the SSF spectra of each of the samples (Figure 2.10). According to the fluorescence spectra of Py(108)-EP(AM) normalized at 375 nm and shown in Figure 2.10A, the intensity of the excimer (I_E) relatively to the normalized intensity of the monomer (I_M) increased continuously upon increasing the temperature of the oil. This phenomenon reflected a decrease in viscosity with increasing temperature associated with a decrease in pyrene-pyrene diffusive encounters. Py(116)-EP(SM1) however exhibited a different behavior upon decreasing the temperature of the solution in oil, consistent with what had been observed in toluene.

Two distinct regimes were identified depending on whether the solution temperature was above or below the crystallization temperature of the Py-EP(SM) samples. In the case of Py(116)-

EP(SM1) and Py(100)-EP(SM2), as the temperature increased from –30 to +25 °C, I_E increased continuously with respect to I_M but showed a decrease around their crystallization temperatures at 0 and +10 °C, respectively. As explained earlier, the continuous decrease in I_E observed with decreasing temperature was a consequence of the increase in viscosity that reduced pyrene diffusive encounters, whereas the decrease in I_E observed at 0 and +10 °C upon increasing the solution temperature was the result of the melting of the microcrystals of the EP(SM) samples that resulted in a lower $[Py]_{loc}$ leading to a decrease in excimer formation.

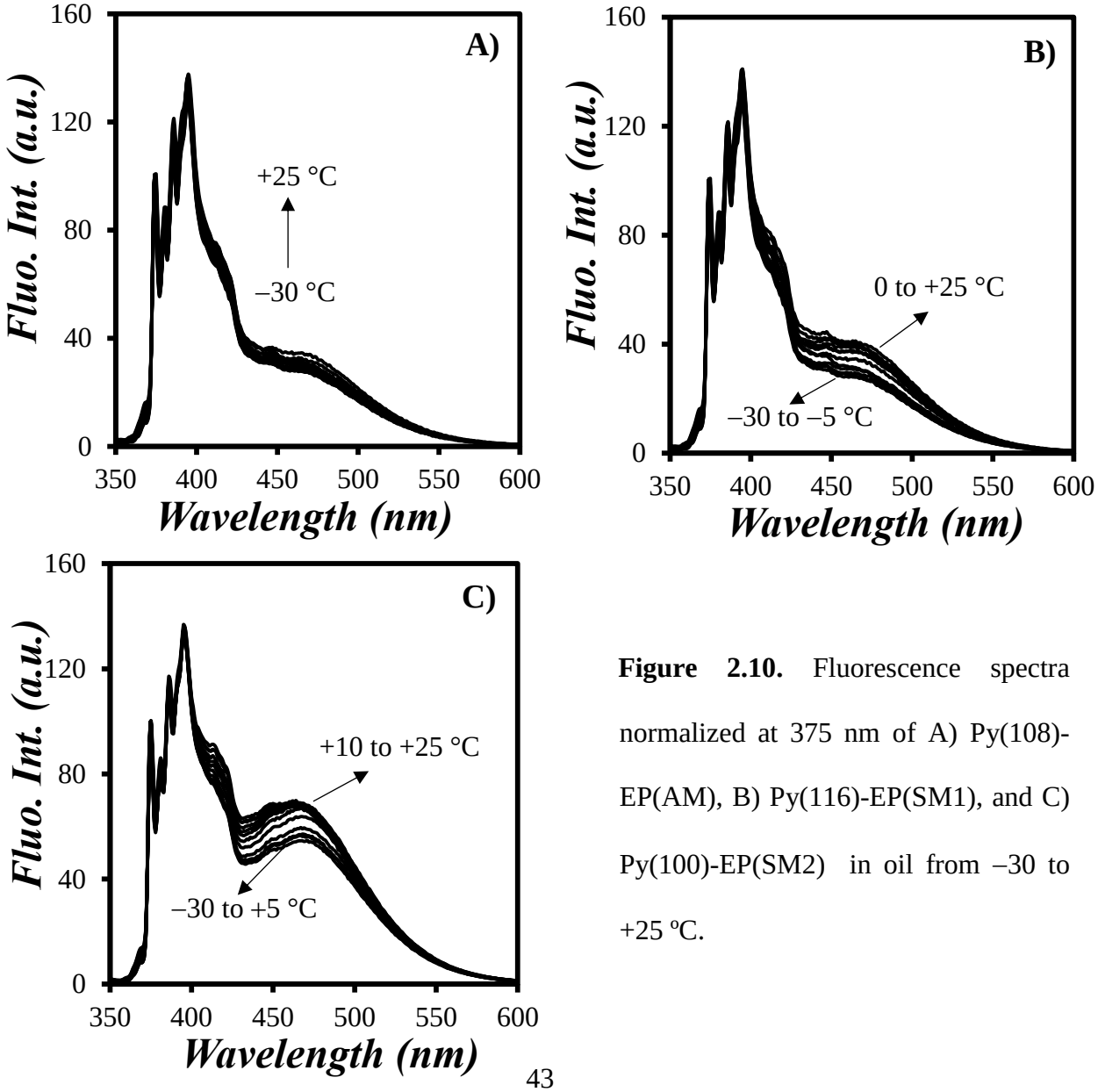

Figure 2.10. Fluorescence spectra normalized at 375 nm of A) Py(108)-EP(AM), B) Py(116)-EP(SM1), and C) Py(100)-EP(SM2) in oil from –30 to +25 ºC.

The I_E/I_M(inter & intra) and I_E/I_M(intra) ratios were calculated using the fluorescence spectra that were acquired at high and low concentrations of the Py-EP samples. The I_E/I_M ratios were plotted as a function of temperature for each of the samples in Figure 2.11. For Py(108)-EP(AM) solutions in oil, the I_E/I_M ratios increased continuously with increasing temperature at both high and low concentrations in a manner similar to what had been observed in toluene. As discussed before, this behavior is indicative of an increase in the rate constant of excimer formation by diffusion k_{diff} resulting from the decrease in the solvent viscosity with increasing temperature. At low temperatures in oil, the I_E/I_M ratio for a 10 $g.L^{-1}$ solution of the Py(116)-EP(SM1) and Py(100)-EP(SM2) samples increased with increasing temperature, similarly to what was found for the amorphous sample. The increase in I_E/I_M was then followed by a decrease from −10 °C to 5 °C for Py(116)-EP(SM1), and from 0 °C to +20 °C for Py(100)-EP(SM2). At higher temperatures, the I_E/I_M ratios increased with the temperature for both semicrystalline samples. The anomalous behavior of the Py(116)-EP(SM1) and Py(100)-EP(SM2) solutions at intermediate temperatures could be similarly assigned to the hydrodynamic volume expansion of the polymeric coils happening upon melting the crystalline microdomains as well as the dissociation of the Py-EP(SM) aggregates. The break points obtained for the I_E/I_M ratios of the Py-EP(SM) samples in oil appeared at 0 and +5 °C for Py(116)-EP(SM1) and Py(100)-EP(SM2) representing a +5 °C shift in comparison to the break points encountered for these copolymers in toluene, probably due to the better solvating ability of toluene towards the succinimide ring exists in Py-EP samples.[16]

The 0.01 $g.L^{-1}$ solutions of the Py-EP(SM) mixed with 10 $g.L^{-1}$ of the respective unlabeled EP(SM) copolymers in oil yielded an I_E/I_M profile that increased slightly with increasing temperature and showed hardly any change at temperature where the break point for I_E/I_M had been observed for the 10 $g.L^{-1}$ Py-EP(SM) solutions. Such an observation confirmed that under

these conditions, the Py-EP(SM1) and Py-EP(SM2) molecules were perfectly isolated from each other due to the presence of a large amount of unlabeled EP(SM) and formed excimer solely by intramolecular interactions.

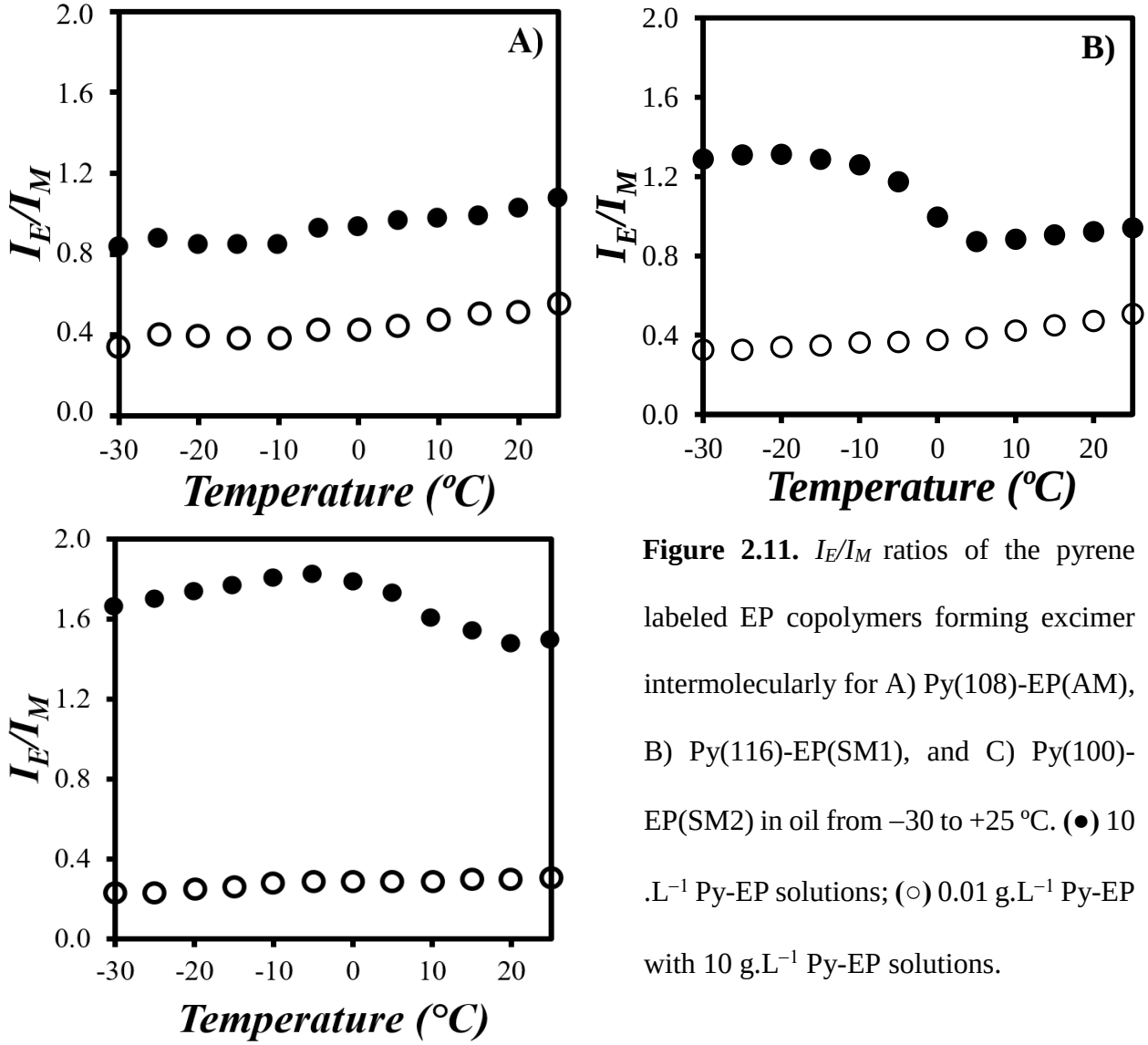

Figure 2.11. I_E/I_M ratios of the pyrene labeled EP copolymers forming excimer intermolecularly for A) Py(108)-EP(AM), B) Py(116)-EP(SM1), and C) Py(100)-EP(SM2) in oil from −30 to +25 ºC. **(●)** 10 .L^{-1} Py-EP solutions; **(○)** 0.01 g.L^{-1} Py-EP with 10 g.L^{-1} Py-EP solutions.

The I_E/I_M ratios in oil were combined according to Eq. 2.5 to yield f_{inter}, which was plotted as a function of temperature in Figure 2.12. Consistently with the behavior of Py(108)-EP(AM) in toluene, f_{inter} remained constant around 0.53 ± 0.05 with temperature for the this sample in oil (Figure 2.6).

The f_{inter} value of 0.56 for Py(108)-EP(AM) in oil was substantially larger than what had been observed in toluene, suggesting that more intermolecular interactions were occurring in oil. For the 10 g.L^{-1} Py(116)-EP(SM1) solution in oil, f_{inter} decreased from 0.73 ± 0.02 at high temperature to 0.53 ± 0.04 at low temperature. The inflexion point of the transition in f_{inter} of this sample was observed at T = 0 ± 5 ºC. In a similar manner, the f_{inter} for Py(100)-EP(SM2) decreased from 0.82 ± 0.03 at high temperature to 0.70 ± 0.01 at low temperature with the inflexion point of T = +10 ± 5 ºC.

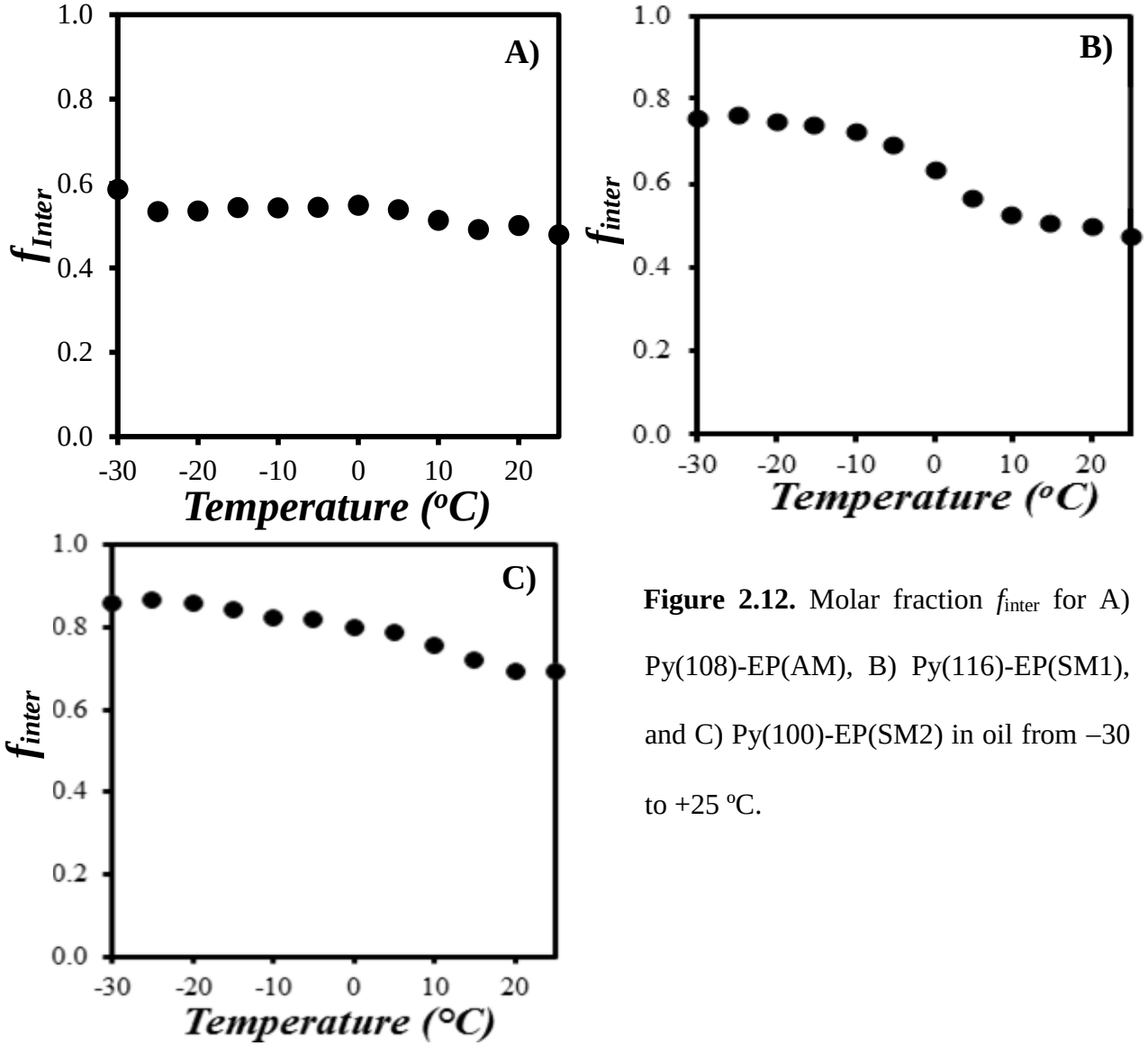

Figure 2.12. Molar fraction f_{inter} for A) Py(108)-EP(AM), B) Py(116)-EP(SM1), and C) Py(100)-EP(SM2) in oil from –30 to +25 ºC.

As listed in Table 2.4, two distinct regimes were also observed for the f_{inter} values of both Py-EP(SM) samples in oil, where in the case of Py-EP(AM), f_{inter} remained constant consistent with a single regime in oil similar to what had been obtained in toluene previously.

Table 2.4. Summary of the molar fractions (f_{inter}) obtained for a solution of 10 g.L^{-1} Py-EP samples in oil.

Sample	T_C (°C)	λ_{py}	Temp (°C)			
			–30 to –10	–10 to +5	+5 to +15	+15 to +25
Py-EP(SM1)	0	116	0.75 ± 0.02	-	0.53 ± 0.04	
Py-EP(SM2)	+10	100	0.82 ± 0.03		-	0.70 ± 0.01
Py-EP(AM)	-	108	0.53 ± 0.05			

2.10 Comparison of the Molar Fraction f_{inter} of Py-EPs in Oil and Toluene

The f_{inter} profiles obtained for the 10 g.L^{-1} solutions of Py(108)-EP(AM), Py(116)-EP(SM1), and Py(100)-EP(SM2) in oil and toluene were plotted in Figure 2.13 for comparison. Figure 2.13 also includes the plots obtained earlier for the 10 g.L^{-1} solutions for Py(108)-EP(AM), Py(116)-EP(SM1) in the presence of 10 g.L^{-1} wax in toluene.[1,3,21]

The presence of wax led to an increase in f_{inter} for both Py(108)-EP(AM) and Py(116)-EP(SM1) in toluene over the entire temperature range. This behavior had been interpreted as wax promoting intermolecular interactions between EP copolymers in toluene. Since engine oils contain a few weight percents of wax, the increased f_{inter} value observed for all EP copolymers in oil could be attributed to the presence of wax in oil. Another reason for the larger f_{inter} value in oil versus toluene could also be due to strong polar interactions between the succinimide pendants prone to happen in aliphatic solvents, that was inferred from the large f_{agg} values in Table 2.2. While the characterization of the interactions between EP copolymers and wax provides valuable

information about the interactions between different components found in oil, pyrene aggregation via succinimide interactions might pose a problem since it might induce unwanted interpolymeric interactions. This might affect the ability of the procedure to probe more detailed associative interactions taking place in oil.

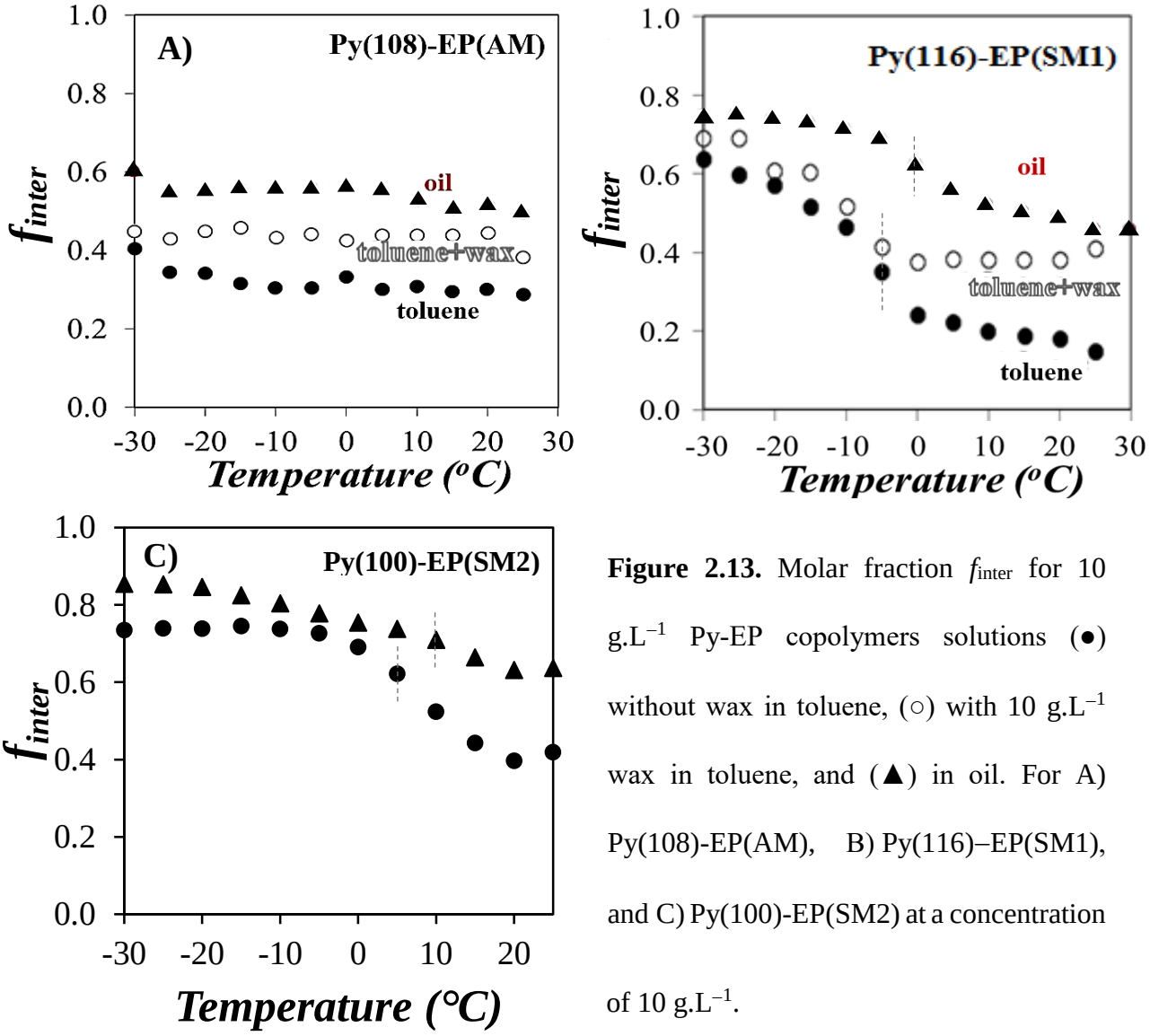

Figure 2.13. Molar fraction f_{inter} for 10 g.L^{-1} Py-EP copolymers solutions (●) without wax in toluene, (○) with 10 g.L^{-1} wax in toluene, and (▲) in oil. For A) Py(108)-EP(AM), B) Py(116)–EP(SM1), and C) Py(100)-EP(SM2) at a concentration of 10 g.L^{-1}.

Figure 2.13A and B also showed a 4 ± 1 °C increase in the crystallization temperature (T_C) of the Py-EP(SM) solutions in oil compared to what had been obtained in toluene and a mixture

of toluene and wax.[20] This behavior could be assigned to the different solvent quality of toluene towards these polymers compared to oil.[16] This conclusion is also reflected by the trends obtained with the intrinsic viscosity measurements in Figure 2.5, which already suggested that the oil was a worse solvent than toluene to solubilize the EP(SM) samples, resulting in much more pronounced transition at the crystallization temperature for the EP(SM) samples in oil. Indeed, crystallization of the Py-EP(SM) samples in toluene occurred at lower temperatures than in oil as observed experimentally in Figure 2.13.

2.11 Effect of PPD on the Level of Interpolymeric Interactions between Py-EP Copolymers in Oil

The effective concentration range of poly(alkyl methacrylate)s (PAMAs) used as PPD agents is usually found to be between ~0.1 and ~1.5 wt% in engine oils. Consequently, 2 $g.L^{-1}$ of two PPDs was added to solutions of high (10 $g.L^{-1}$) and low (0.01 $g.L^{-1}$) concentrations of Py(108)-EP(AM) and Py(100)-EP(SM2) in oil. To prevent intermolecular interactions for the 0.01 $g.L^{-1}$ Py-(EP) solutions, 10 $g.L^{-1}$ unlabled EPs was added to them to obtain the I_E/I_M(intra) ratio. The fluorescence spectra were acquired as a function of temperature for the Py(108)-EP(AM) and Py(100)-EP(SM2) solutions in the presence of the pour point depressants PPD1 and PPD2 in oil and were plotted in Figure 2.14.

Surprisingly, the fluorescence spectra of Py(100)-EP(SM2) showed a distortion of the fifth band (I_V) of the pyrene monomer emission at 415 nm. Such behavior in the fluorescence spectra of Py-EPs is often attributed to the presence of pyrene aggregates whose formation appreared to have been promoted by the additioon of the PPDs.[21]

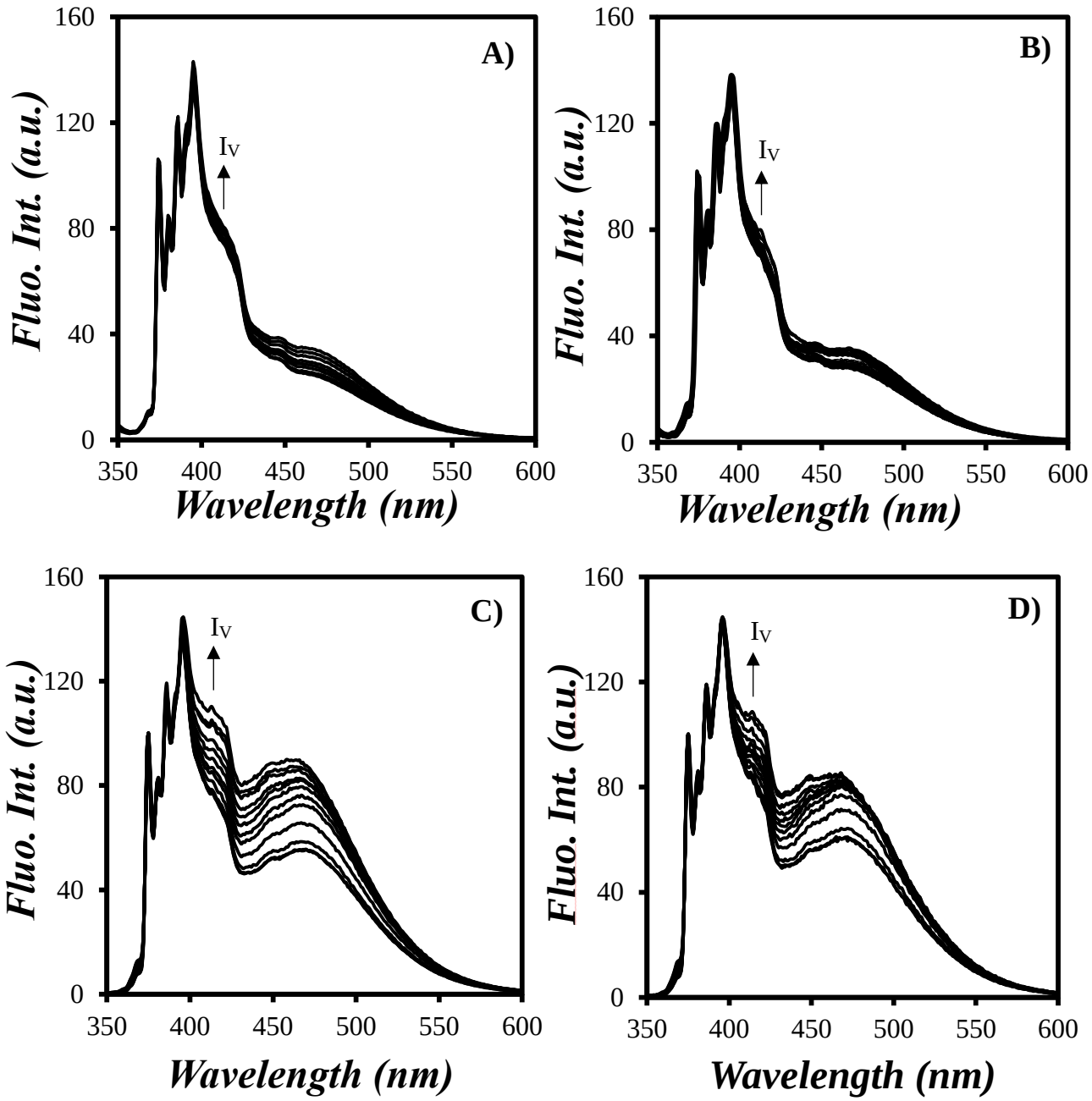

Figure 2.14. Fluorescence spectra of solutions of A) 10 g.L^{-1} Py(108)-EP(AM) with 2 g.L^{-1} PPD1, B) 10 g.L^{-1} Py(108)-EP(AM) with 2 g.L^{-1} PPD2, C) 10 g.L^{-1} Py(100)-EP(SM2) with 2 g.L^{-1} PPD1, and D) 10 g.L^{-1} Py(100)-EP(SM2) with 2 g.L^{-1} PPD2 acquired from –30 to +25 ^{o}C in oil.

The presence of pyrene aggregates that formed excimer instantaneously, and which were identified in the fluorescence spectra in Figure 2.14, should be accounted for in the calculation of I_E/I_M. However I_E, being calculated by taking the integral of the fluorescence signal between 500 and 530 nm, might not appropriately represent the aggregated pyrenes that also emit at 415 nm.[21] As illustrated in Figure 2.15, the shift in excimer emission to lower wavelengths was more pronounced for the Py(100)-EP(SM2) solution than for the Py(108)-EP(AM) solution in oil. Consequently, aggregated pyrenes might affect the I_E/I_M ratios, and thus the molar fraction f_{inter} derived from them, to a greater extent for the semicrystalline EP sample than for the amorphous EP sample. To ensure that the aggregated pyrenes did not influence the I_E/I_M ratios, the following procedure was implemented.

The fluorescence spectrum of a 3×10^{-6} mol.L^{-1} solution of 1-pyrenemethylsuccinimide (Py-MSI), used as a model compound, was normalized to that of the Py-EP at 375 nm and subtracted from the fluorescence spectrum of the 10 g.L^{-1} solution of Py(100)-EP(SM2) in toluene and in oil with PPD1. Since the fluorescence spectrum of the model compound is only representative of the pyrene monomer emission, this procedure enables one to isolate the emission from the pyrene excimer in the fluorescence spectrum of Py(100)-EP(SM2).

As shown in Figure 2.15, the 10 g.L^{-1} Py(100)-EP(SM2) solution in toluene, yielded a symmetric excimer fluorescence spectrum that was centered around 480 nm. The excimer fluorescence spectrum converged to zero at wavelengths below 394 nm and thus, did not have any effect on the I_M calculation, which was obtained by integrating the fluorescence intensity of the monomer peak I_I between 372 and 379 nm. By contrast, the excimer emission of the same sample in oil with PPD1 (or PPD2) was centered around 466 nm and did not yield a symmetric profile, indicative of a high level of pyrene aggregation. Whether the excimer emission of Py(100)-

EP(SM2) would interfere with the fluorescence of the pyrene monomer centered at 375 nm is debatable, but it is usually assumed in similar instances that the emission at 375 nm is only due to the pyrene monomer.[22]

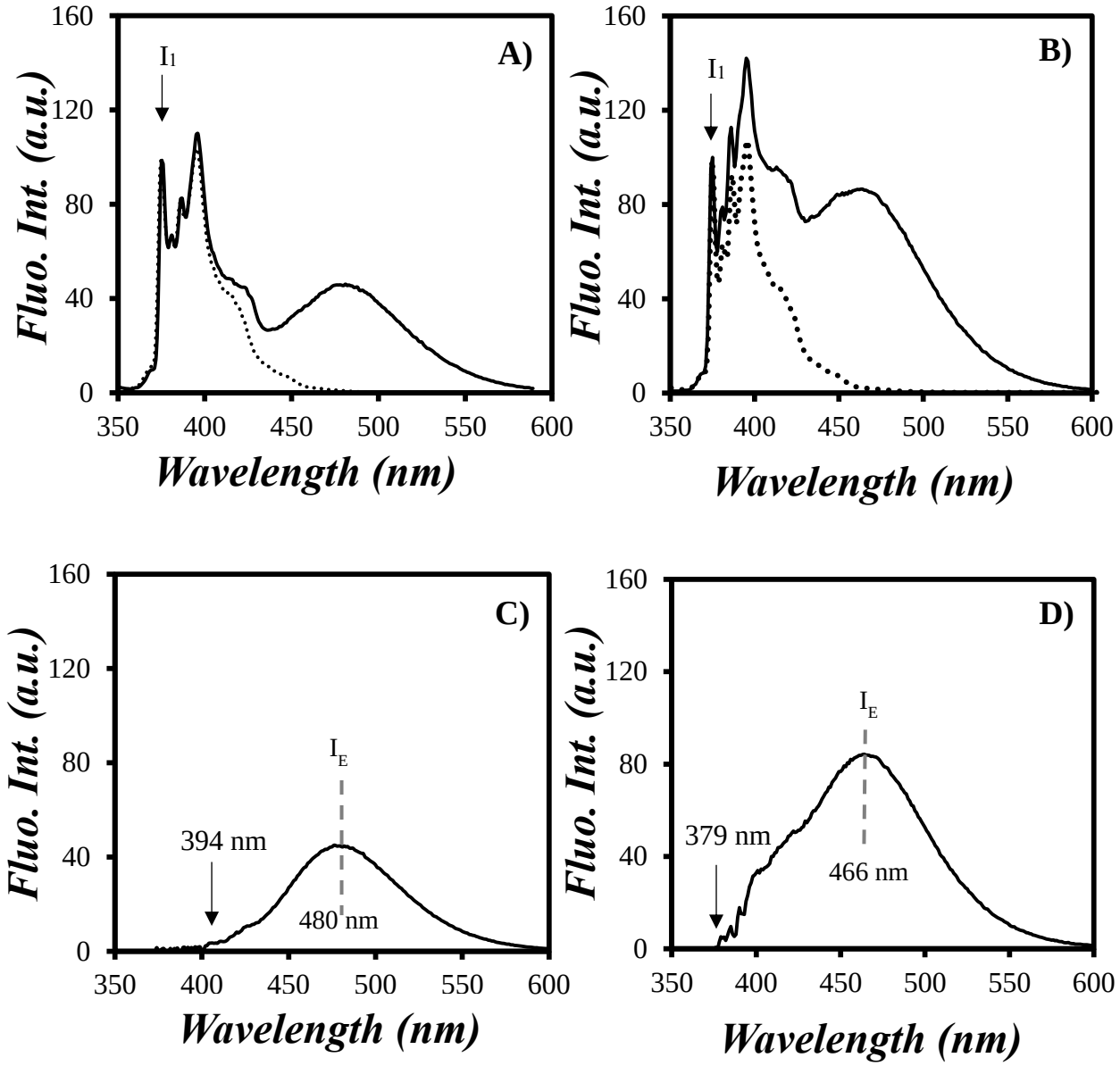

Figure 2.15. Fluorescence spectra of solutions of (⋯) 3×10^{-6} mol.L^{-1} Py-MSI and (—) 10 g.L^{-1} Py(100)-EP(SM2) A) in toluene, B) with 2 g.L^{-1} PPD1 in oil, and excimer spectra of 10 g.L^{-1} Py(100)-EP(SM2) in C) toluene, and D) with 2 g.L^{-1} PPD1 in oil.

The results were first discussed by considering the traditional approach where the I_E/I_M ratios are calculated by integrating the fluorescence intensity of the excimer from 500 to 530 nm. The I_E/I_M ratios of the solution in oil containing 10 g.L^{-1} Py(108)-EP(AM) with 2 g.L^{-1} PPD1 or PPD2, and 10 g.L^{-1} Py(100)-EP(SM2) with 2 g.L^{-1} PPD1 or PPD2 were plotted as a function of temperature in Figure 2.16. The I_E/I_M ratios for both high and low concentrations of the amorphous sample with 2 g.L^{-1} PPD1 or 2 g.L^{-1} PPD2 showed an overall increase with increasing temperature, with some fluctuation at −17.5 ± 2.5 ºC. These fluctuations might reflect the crystallization of the PPD molecules. For the solution containing 10 g.L^{-1} Py(100)-EP(SM2) with 2 g.L^{-1} PPD1, a break point appeared in I_E/I_M(inter & intra) at +10 ºC corresponding to the crystallization of Py(116)-EP(SM2) in oil. As was expected from the 0.04 g.L^{-1} solution of Py(100)-EP(SM2) with 10 g.L^{-1} EP(SM2) and 2 g.L^{-1} PPD1 in oil, a continuous increase in I_E/I_M(intra) was observed over the entire temperature range.

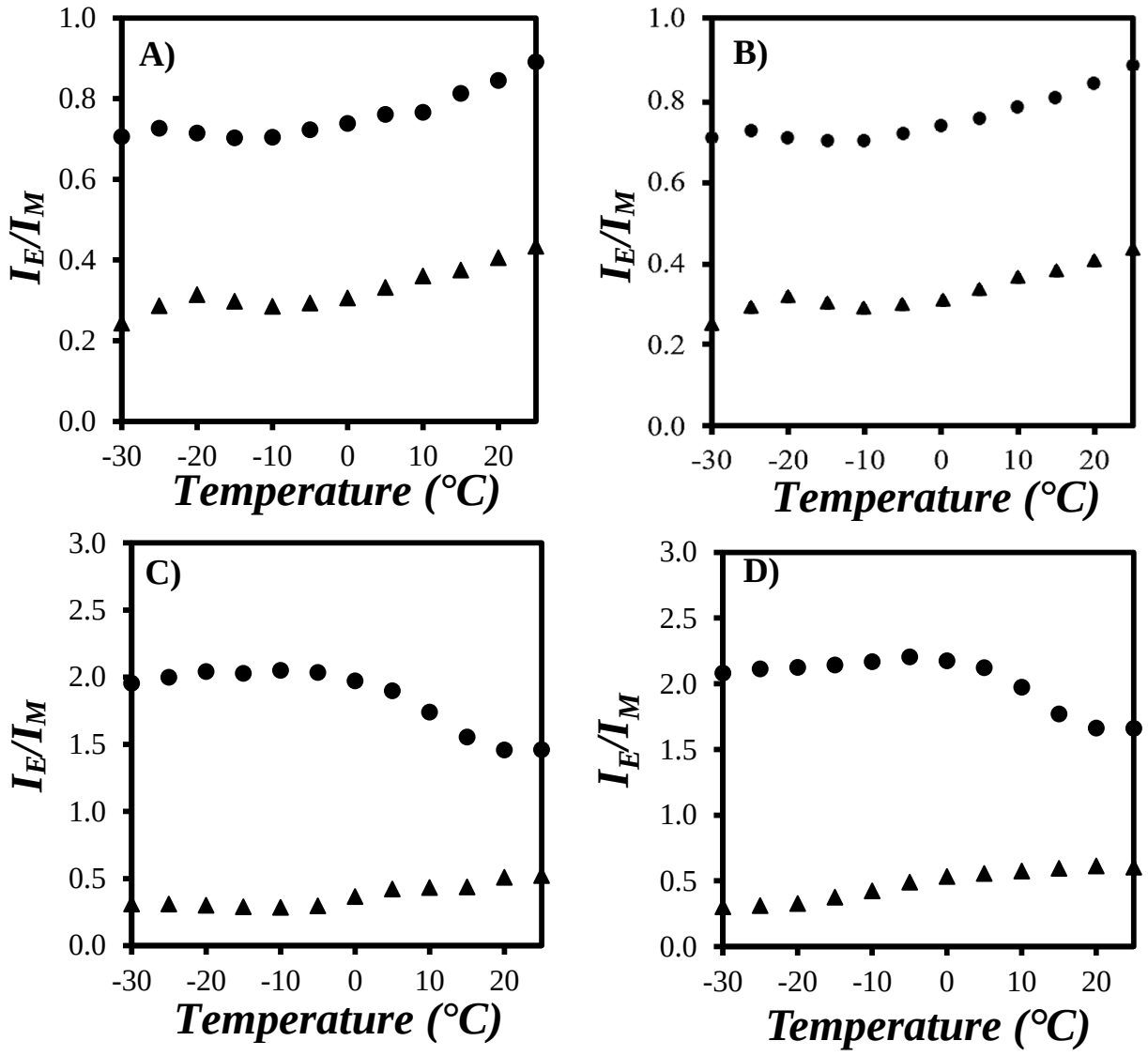

Figure 2.16. Plots of (●) I_E/I_M(inter & intra) and (▲) I_E/I_M(intra) as a function of temperature for mixtures of A) 2 g.L^{-1} of PPD1 with either 10 g.L^{-1} Py(108)-EP(AM) or 0.04 g.L^{-1} Py(108)-EP(AM) and 10 g.L^{-1} EP(AM), B) 2 g.L^{-1} of PPD2 with either 10 g.L^{-1} Py(108)-EP(AM) or 0.04 g.L^{-1} Py(108)-EP(AM) and 10 g.L^{-1} EP(AM), C) 2 g.L^{-1} of PPD1 with either 10 g.L^{-1} Py(116)-EP(SM2) or 0.04 g.L^{-1} Py(100)-EP(SM2) and 10 g.L^{-1} EP(SM2), and D) 2 g.L^{-1} of PPD2 with either 10 g.L^{-1} Py(100)-EP(SM2) or 0.04 g.L^{-1} Py(100)-EP(SM2) and 10 g.L^{-1} EP(SM2) from –30 to +25 ^{o}C in oil.

The ratios I_E/I_M(inter & intra) and I_E/I_M(intra) were combined according to Equation 2.5 to yield $f_{inter,}$ which was plotted as a function of temperature in Figure 2.17. For the 10 g.L^{-1} Py(108)-EP(AM) solution containing PPD1 or PPD2, f_{inter} decreased from 0.67 ± 0.02 at –30 ^{o}C to 0.56 ± 0.01 at –20 ^{o}C, and remained more or less constant from –20 to +25 ^{o}C. In the case of the 10 g.L^{-1} Py(100)-EP(SM2) solution with 2 g.L^{-1} PPD1, f_{inter} remained constant and equal to 0.84 ± 0.01 from –30 to –5 ^{o}C, and showed a continuous decrease at higher temperatures before plateauing at 0.64 ± 0.01 from +20 to +25 ^{o}C. Similarly f_{inter} for the 10 g.L^{-1} Py(100)-EP(SM2) solution with 2 g.L^{-1} PPD2 exhibited a continuous decrease from 0.85 ± 0.01 at –30 ^{o}C to 0.63 ± 0.01 where it remained from +20 to +25 ^{o}C. The profiles obtained for Py(100)-EP(SM2) with PPD1 and PPD2 showed some differences, with PPD1 inducing stronger intermolecular interactions for Py(100)-EP(SM2) at temperatures above –20 ^{o}C.

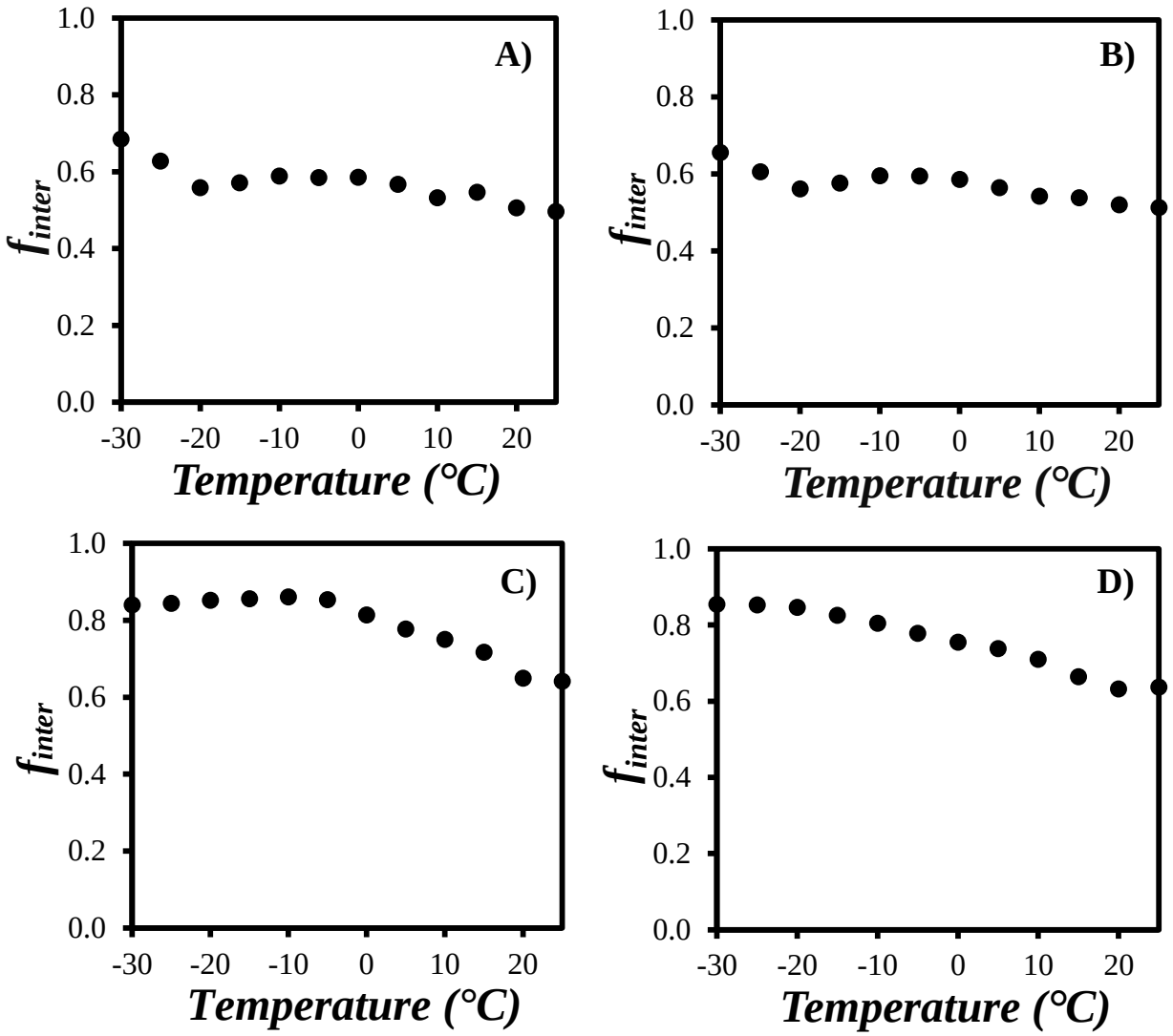

Figure 2.17. Molar fraction f_{inter} of A) 10g.L^{-1} Py(108)-EP(AM) with 2 g.L^{-1} PPD1, B) 10 g.L^{-1} Py(108)-EP(AM) with 2 g.L^{-1} PPD2, C) 10 g.L^{-1} Py(100)-EP(SM2) with 2 g.L^{-1} PPD1, and D) 10 g.L^{-1} Py(100)-EP(SM2) with 2 g.L^{-1} PPD2 in oil, from –30 to +25 ^{o}C.

2.12 Comparison of the f_{inter} Plots of Py-EP Samples Obtained Using Different Integration Boundaries for I_E

To ensure that the blue shift in the excimer emission of the Py(100)-EP(SM2) sample resulting from the high level of aggregation did not affect the f_{inter} values calculated by integrating the excimer intensity from 500 to 530 nm, a second wavelength range from 400 nm to 530 nm was

also used to calculate I_E at high and low Py(100)-EP(SM2) concentrations in oil. This sample had shown the strongest distortion in the I_V band of the fluorescence spectra in Figure 2.14. The obtained I_E values were then used to calculate the f_{inter} molar fraction of the 10 g.L^{-1} solution of Py(100)-EP(SM2) in the presence of PPD1 or PPD2. As compared in Figure 2.18, little-to-no change was observed for the f_{inter} values obtained using different integration boundaries for I_E. This result suggests that the integration boundaries applied to calculate I_E do not affect the final f_{inter} value much. Since the procedure using the 500 – 530 nm range was much simpler to implement in practice, it was applied to the rest of this thesis.

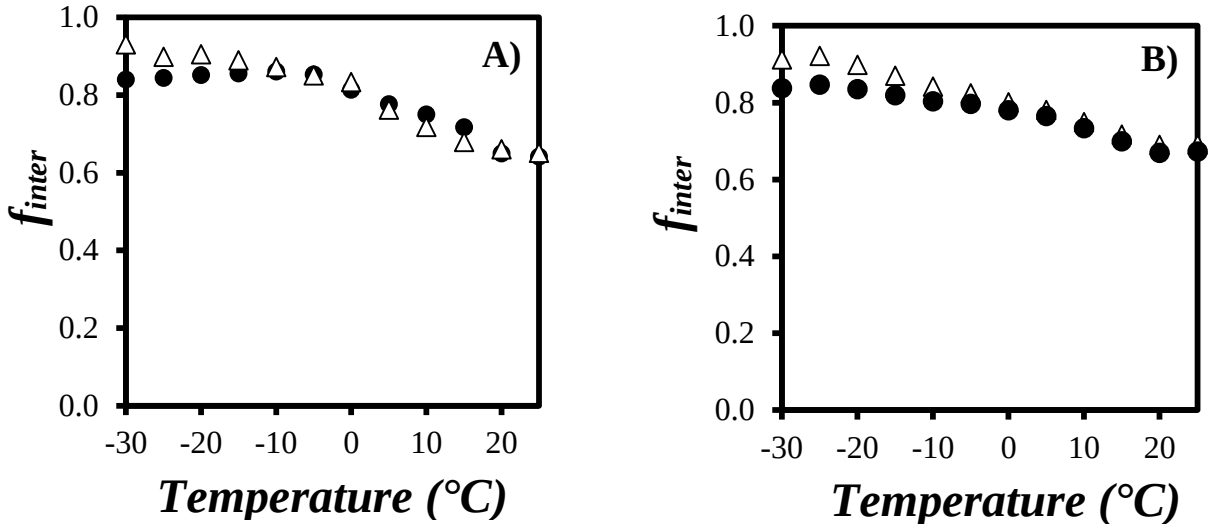

Figure 2.18. Plots of the molar fraction f_{inter} as a function of temperature for the solution of 10 g.L^{-1} Py(100)–EP(SM2) in oil with 2 g.L^{-1} of A) PPD1 and B) PPD2 calculated from the ratio (●) I_E(500-530 nm)/I_M(372-379 nm) or (Δ) I_E(400-530 nm)/I_M(372-379 nm).

2.13 Comparison of the f_{inter} Plots of Py-EP Samples Before and After the Addition of the PPDs in Oil

The f_{inter} profiles of the 10 g.L^{-1} solutions of Py-EP samples in the presence and absence of the

PPDs were compared in Figure 2.19. The presence of PPDs led to a small increase in f_{inter} for both Py(108)-EP(AM) and Py(100)-EP(SM2) by promoting intermolecular interactions between EP copolymers in oil over the entire temperature range. Such an effect of PPD on the f_{inter} of the Py(100)-EP(SM2) molecules was found to be more pronounced in the presence of PPD1 in the solution. While a difference is clearly seen in Figure 2.19 between the effect of PPD1 and PPD2, drawing a conclusion about the origin of this effect was complicated by the absence of information about the chemical composition of the PPDs and the fact that the behavior differences might reflect differences between the interactions of the PPDs with the succinimide groups of the Py(100)-EP(SM2) sample.

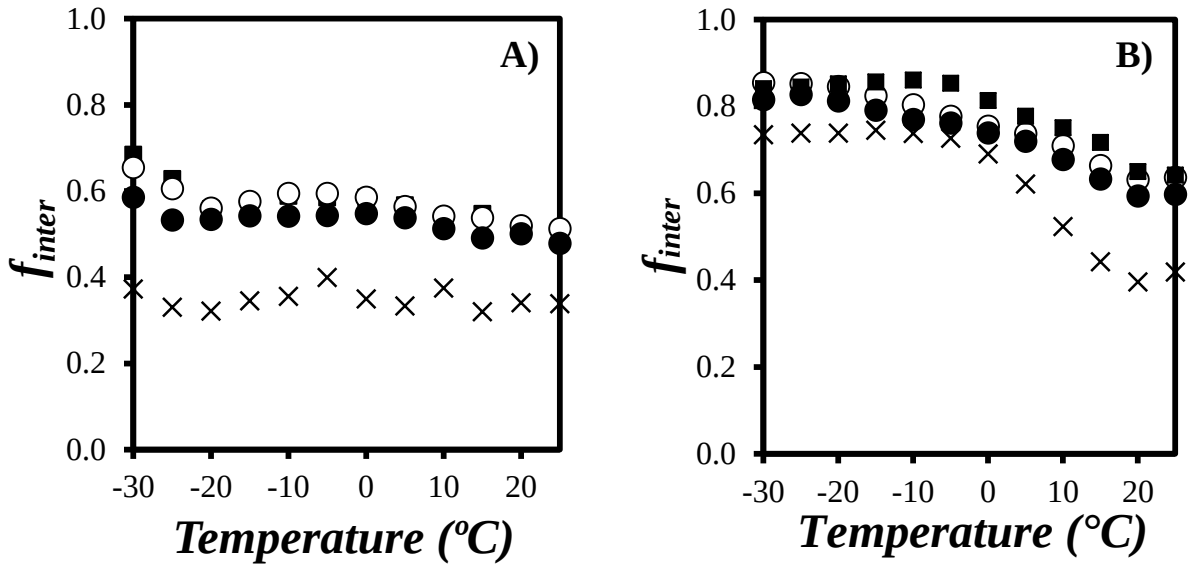

Figure 2.19. Plots of the molar fraction f_{inter} as a function of temperature for the solution of A) 10 g.L^{-1} Py(108)–EP(AM) and B) 10 g.L^{-1} Py(100)–EP(SM2) (●) without PPD, (■) with 2 g.L^{-1} PPD1, and (○) with 2 g.L^{-1} PPD2 in oil from –30 to +25 ºC. (×) Py–EP copolymers with no additive in toluene.

2.14 Conclusions

Maleation and pyrene labeling of an amorphous (EP(AM)) and two semicrystalline (EP(SM)) VIIs were carried out to prepare the Py-EP samples for the fluorescence measurements. The chemical composition of the maleated and pyrene-labeled EP copolymers were confirmed by Fourier transform infrared (FTIR), UV-Vis absorption, and ^{13}C NMR spectroscopies. A method that was introduced earlier to quantitatively characterize the level of intermolecular interactions between VIIs in toluene was then applied to the same Py-EP samples in oil. The fluorescence spectra showed that sufficient pyrene excimer fluorescence was generated, although less excimer was produced in oil as compared to toluene due to the higher viscosity of the oil. The molar fraction f_{inter} was determined and monitored for both EP copolymers in oil as a function of temperature. The comparison of the f_{inter} plots being obtained before and after the addition of the PPDs did not show much difference between the f_{inter} ratios at the corresponding temperatures, suggesting that the presence of PPD induced little additional intermolecular interactions between the Py-EP samples in comparison to those displayed by the Py-EP samples alone in oil.

Based on the transition points observed in the plots of f_{inter} vs temperature, both types of EP(SM) samples underwent crystallization at low temperatures in oil. This observation was further confirmed by the intrinsic viscosity measurements, that showed that the microcrystallization of EP(SM1) and EP(SM2) in engine oil took place at 0 °C and 10 °C, respectively. Consistently with the intrinsic viscosity measurements, the EP(AM) sample exhibited no such transition due to its inability to crystalize, even at low temperatures in oil.

Despite the close f_{inter} values for the Py-EP(SM) samples below the crystallization temperature in oil and toluene, the fractions of intermolecular interactions above this temperature in oil were higher than those observed for the same samples in toluene. This phenomenon was

attributed to the lower solvent quality of the oil for the succinimide group in Py-EP copolymers as compared to toluene, that promoted intermolecular interactions.

Analysis of the TRF measurements also suggested that the Py-EP copolymers underwent more pyrene aggregation in oil as compared to toluene. The increased pyrene aggregation was attributed to the insolubility of the succinimide group joining pyrene to the EP backbone. Because the succinimide groups could induce undesired intermolecular interactions between the Py-EP samples in oil, they might compromise the conclusions reached with f_{inter}. With this in mind, the fluorescence experiments were repeated using unlabeled EP copolymers and a pyrene-labeled PAMA sample, where the introduction of the pyrene label to the macromolecule would not induce unwanted interactions. These experiments are described in Chapters 3 and 4.

Chapter 3

Probing the Interactions between Pour Point Depressants (PPDs) and Viscosity Index Improvers (VIIs) in Engine Oil Using Fluorescently Labeled PPDs

3.1 Outline

The level of interpolymeric interactions, that take place between the pyrene-labeled poly(alkyl methacrylate) (Py-PAMA) molecules, used as a mimic of power point depressants (PPDs), was characterized by fluorescence. Fluorescence experiments were conducted with a pyrene-labeled poly(dodecyl methacrylate) with a pyrene content of 5.6 mol% (Py(5.6)-$PC_{12}MA$) and poly(octadecyl methacrylate) with a pyrene content of 6.7 mol% (Py(6.7)-$PC_{18}MA$). The fluorescence spectra of solutions of the pyrene-labeled samples in engine oil were acquired as a function of temperature and analyzed to obtain f_{inter}, the molar fraction of pyrene labels that formed excimer intermolecularly upon encounter between an excited and a ground-state pyrene. The fraction f_{inter} is a measure of the level of intermolecular interactions between Py-PAMA macromolecules and it was plotted as a function of solution temperature. The f_{inter}-vs-T profiles obtained for Py(5.6)-$PC_{12}MA$ and Py(6.7)-$PC_{18}MA$ showed a sharp transition between –35 and –30 ^{o}C and between +10 and +15 ^{o}C, respectively, indicating an increase in intermolecular interactions at temperatures lower than the transition. This behavior suggested that the alkyl side chains of both samples underwent crystallization. Since the crystallization of the octadecyl side chains of Py(6.7)-$PC_{18}MA$ occurred at a temperature which was more accessible, that sample was selected to monitor its interactions with an amorphous (EP(AM)) and a semicrystalline (EP(SM)) ethylene-propylene copolymer. Addition of EP(AM) resulted in an increase in interpolymeric interactions between Py(6.7)-$PC_{18}MA$ macromolecules at all solution temperatures studied. The addition of EP(SM) increased f_{inter} for Py(6.7)-$PC_{18}MA$ at high temperatures, but at lower temperatures where EP(SM) formed microcrystals, f_{inter} for Py(6.7)-$PC_{18}MA$ returned to its original value when no EP(SM) was present in solution. The implications of this result are discussed.

3.2 Introduction

The ability of an engine oil to flow at low temperatures is essential for the proper operation of internal combustion engines. However the presence of wax, which helps maintain a higher viscosity of the engine oil at high temperatures, hinders oil flow at low temperatures by forming crystals. Since wax crystals grow in size as the temperature decreases, they aggregate and form a 3D network. Expansion of the 3D network of wax crystals in the oil results in the formation of a gel which prevents oil flow, a regime that is quickly followed by engine failure.[1] The lowest temperature at which the oil is still capable of flowing is called the pour point (PP).[1] Additives used to lower the PP of an engine oil are referred to as pour point depressants (PPDs). Alkyl aromatic polymers and poly(alkyl methacrylate)s (PAMAs) are the two main types of PPDs used by the lubricants industry.[2] Both types of PPDs interact with wax in a way that perturbs the growth of wax crystals, and thus delays the formation of a wax crystal network to lower solution temperatures. Since the late 1930s, PAMAs have become an important polymeric additive that is employed to effectively reduce the PP of engine oils. The main reason for the widespread acceptance of PAMA by the oil additive industry resides in the easy variation in chemical composition that can be introduced into PAMAs. As illustrated in Figure 3.1, a typical PAMA used as PPD is constituted of two different alkyl methacrylate monomers units, where the number of carbon atoms in the alkyl side chains can vary from 1 to 22.[1,2]

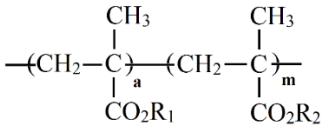

Figure 3.1. Chemical structure of poly(alkyl methacrylate)s used as PPDs and constituted of two alkyl methacrylate monomers with side chains R_1 and R_2.

PPDs and viscosity index improvers (VIIs) are the two main polymeric additives used in engine oils.[1-5] The two major differences between these two additives are their concentration for use in engine oils and their chemical composition.[2] With regard to PPD concentration, low concentrations of this additive might not be able to sufficiently reduce the engine oil PP, whereas higher concentrations might result in its crystallization in oil, accompanied by a loss of its activity. Therefore, the concentration of a PPD in engine oil needs to be optimized.[2] As demonstrated in Figure 3.2, the addition of a PPD up to a concentration of 0.25 wt% reduces the PP of a Group 1 base oil from −18 to −37 °C (Region I). However, a further increase in the PPD concentration up to ~0.75 wt% results in no significant change in the PP of the oil (Region II). Higher concentrations of PPD would lead to crystallization of the PPD in the oil, which is known as the pour point reversion phenomenon (Region III), where the PP temperature increases back to its original level.[1]

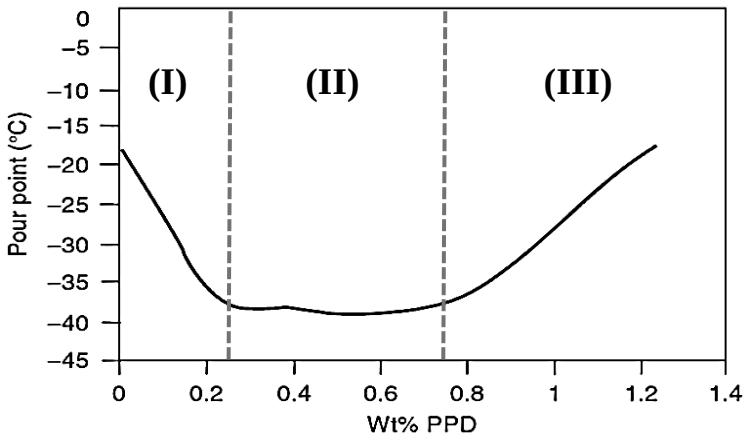

Figure 3.2. Effect of PPD concentration on the pour point of Group I base oil.[1]

VIIs are meant to counteract the inherent decrease in oil viscosity that occurs upon increasing the oil temperature.[4-6] The change in oil viscosity with increasing temperature is called the viscosity index (VI), a low VI corresponding to an oil whose viscosity changes substantially with temperature.[3] Since the good operation of an engine depends on the even flow of the oil regardless of temperature, the oil industry is interested in controlling the oil viscosity within a

narrow range, hence the need to increase the VI of the oil by using VIIs. VIIs are polymers such as ethylene-propylene (EP) copolymers, that accomplish this task by undergoing a coil expansion with increasing temperature.[2,3,6] Since the viscosity of a polymer solution increases when the fraction of the solution volume occupied by the polymer increases, a polymer whose coil expands in oil upon increasing the solution temperature will counteract the decrease in viscosity associated with the higher temperature.

The different oil additives used in the industry all have a specific purpose, PPDs and VIIs being designed to lower the PP and increase the VI of the oil, respectively, they need to achieve their task optimally without detrimental interactions with one another. For this reason, techniques that provide information on the level of interpolymeric interactions between polymeric additives used by the oil industry are particularly interesting. By fluorescently labeling a polymer with the dye pyrene, this laboratory has established that pyrene excimer fluorescence (PEF) can be applied to provide the molar fraction (f_{inter}) of pyrene labels attached onto a polymer that form excimer intermolecularly, a measure of the level of interpolymeric interactions.[6] In this chapter, f_{inter} of two pyrene-labeled PAMAs (Py-PAMAs) used as mimics for PPDs was determined as a function of temperature in a group II engine oil. Poly(dodecyl methacrylate) and poly(octadecyl methacrylate) were labeled with 5.6 and 6.7 mol% of 1-pyrenebutyl methacrylate and referred to as Py(5.6)-$PC_{12}MA$ and Py(6.7)-$PC_{18}MA$, respectively. The fluorescence spectra of the Py-PAMA solutions in oil were acquired and PEF was employed to determine f_{inter} as a function of oil temperature. After establishing that Py(6.7)-$PC_{18}MA$ was better suited for this study, its interactions were characterized from plots of f_{inter}-versus-temperature in the presence and absence of an amorphous (EP(AM)) and a semicrystalline (EP(SM)) EP copolymer. How the behavior of Py(6.7)-$PC_{18}MA$ was affected by the presence of the EP copolymers in oil is described hereafter.

3.3 Experimental

Chemicals. 1-Pyrenebutanol (99%) and poly(lauryl methacrylate) solution ($PC_{12}MA$ 25 wt% in toluene, with number-(M_n) and weight-(M_w) average molecular weight equal to 290 and 570 $kg.mol^{-1}$, respectively) were purchased from Sigma-Aldrich and were employed without further purification. Py(5.6)-$PC_{12}MA$ and Py(6.7)-$PC_{18}MA$ were prepared by copolymerization of 1-pyrenebutyl methacrylate and the respective alkyl methacrylate, and their synthesis and characterization have been described earlier.[7] A Group II engine oil and two ethylene-propylene copolymers, one semicrystalline and one amorphous, were supplied by Afton. These copolymers were referred to as EP(SM2) and EP(AM), respectively. Their properties and chemical compositions have been characterized in Chapter 2.

Synthesis of $PC_{18}MA$. Stearyl methacrylate ($C_{18}MA$) purchased from Sigma was washed three times with a 10% NaOH solution and dried over anhydrous $MgSO_4$. The recovered monomer was then polymerized using conventional free radical polymerization with azobisisobutyronitrile (AIBN) as initiator. To a dry Schlenk tube, $C_{18}MA$ (4.68 g, 0.014 mol), AIBN (0.0023 g, 14 μmol) and 46 mL of tetrahydrofuran (THF) were added. The tube was placed on ice and the solution was degassed with dry nitrogen for 1 hour. The tube was sealed and placed in an oil bath at 65 °C for 18 hours. The polymer was precipitated in methanol and then re-dissolved in THF. This precipitation cycle was repeated three more times to obtain a pure white solid.

Gel Permeation Chromatography (GPC). M_n and M_w for the Py-PAMA and PAMA samples were determined with a Viscotek GPC device equipped with a 305 Triple Detector Array that included a differential refractive index (DRI), viscosity, and light scattering detector using a 1 mL/min flow rate. A Polymer Char high-temperature gel permeation chromatograph (GPC) was used to calculate the molecular weight distribution of the EP samples at 145 °C and with a flow rate of 1

mL/min of 1,2,4-trichlorobenzene (TCB).[8] The GPC instrument was equipped with three detectors, namely a 15° angle light scattering, differential refractive index, and differential viscosity detectors.

***UV-Visible Spectrophotometer* (*UV-Vis*).** A Cary 100 UV-Vis and a Cary 5000 UV-Vis spectrophotometer were used to obtain the absorbance/transmittance of all the solutions in the 200–600 nm wavelength range using quartz cells with 0.1 and 10 mm path length.

Steady-State Fluorometer. The SSF spectra of the Py-PAMA solutions were acquired using a Photon Technology International (PTI) LS-100 fluorometer with a PTI 814 photomultiplier detection system and an Ushio UXL-75Xe xenon arc lamp. For low concentrations of the Py-PAMAs, between 0.01 and 0.1 $g.L^{-1}$, a square cell was used to acquire the fluorescence spectra with the right-angle geometry. For higher Py-PAMA concentrations such as 10 $g.L^{-1}$, a triangular cell was used with the front-face geometry to avoid the inner filter effect when acquiring the fluorescence spectra. To ensure the removal of oxygen from the solution, all the solutions in oil were degassed for 50-60 minutes under a gentle flow of N_2 before the cell was sealed with a Teflon stopper.[9] The solutions were excited at a wavelength of 344 nm, and their emission spectra were acquired between 350 and 600 nm. Background corrections were also applied to remove the contribution from light scattered by the polymer solutions in oil.

Cryostat (Optistat DN). A cryostat from Oxford Instruments (Optistat DN) was used to run the fluorescence measurements at temperatures ranging from –45 (± 0.2) °C to +25 (± 0.2) °C. To this end, the fluorescence cell containing the degassed solutions was inserted inside the cryostat and the instrument was placed in the steady-state fluorometer. The solutions were cooled to the lowest temperature required for their f_{inter} study. The temperature of each solution was then increased in 5 °C increments until the maximum temperature (+25 °C) was reached. The solution was left in

the cryostat for 5 min after the set temperature of the cryostat had been reached, to ensure accuracy and stability of the solution temperature. The fluorescence spectrum was then acquired at that temperature.

Time-Resolved Fluorescence. The Py-PAMA solutions were excited at 344 nm with an IBH time-resolved fluorometer equipped with a 340 nm nano-LED light. Model free analysis (MFA) was used to fit the acquired fluorescence decays, after applying light scattering and background corrections. The monomer and excimer fluorescence decay curves for the Py-PAMA solutions were fit globally to yield the average rate constant $<k>$ of pyrene excimer formation by diffusive encounters and the molar fractions f_{diff}, f_{free}, and f_{agg} of the pyrene labels that formed excimer by diffusion, did not form excimer and behaved as if they were free in solution, and were aggregated and formed excimer by direct excitation, respectively. The global MFA for each pair of monomer and excimer decays was considered good if the obtained χ^2 was smaller than 1.30 where the residuals and their autocorrelations were randomly distributed around zero. An in-depth description of the MFA of the fluorescence decays acquired with pyrene-labeled macromolecules can be found in earlier publications.[10,11]

Pyrene Labeling. The two Py-PAMAs were pyrene-labeled poly(dodecyl methacrylate) and poly(octadecyl methacrylate) which were prepared earlier by Dr. Farhangi.[12] The chemical structure, M_n, M_w, and PDI of these polymers are shown in Figure 3.3 and Table 3.1. The pyrene content of Py(5.6)-PC_{12}MA and Py(6.7)-PC_{18}MA equaled 216 and 195 $\mu mol.g^{-1}$ corresponding to 5.6 and 6.7 mol% pyrene-labeling, respectively. The pyrene content was low enough to not affect the behavior of the polymers in solution.

Py-$PC_{12}MA$ Py-$PC_{18}MA$

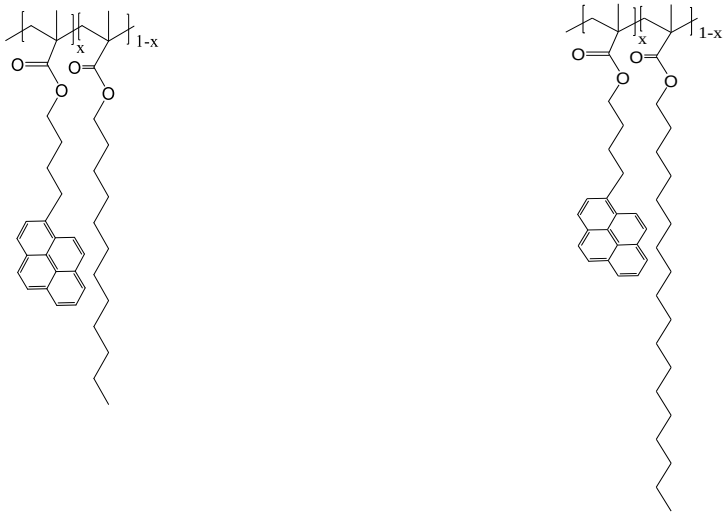

Figure 3.3. Chemical structure of the pyrene-labeled poly(dodecyl methacrylate) (left, Py(5.6)-$PC_{12}MA$, x = 0.056) and poly(octadecyl methacrylate) (right, Py(6.7)-$PC_{18}MA$, x = 0.067) used as PPD mimics.

Table 3.1. Summary of the GPC results for the polymers used in this study.[6]

Sample	M_n ($g.mol^{-1}$)	M_w($g.mol^{-1}$)	PDI(M_n/ M_w)
Py(5.6)-$PC_{12}MA$ a)	507,000	862,000	1.70
Py(6.7)-$PC_{18}MA$ a)	719,000	1071,000	1.49
$PC_{12}MA$ b)	290,000	570,000	1.97
$PC_{18}MA$ c)	617,000	1243,000	2.01
EP(AM) d)	59,000	125,000	2.11
EP(SM2) c)	22,800	145,900	6.40

a) Farhangi et al.[12]; b) Information from Sigma Aldrich, c) this study; d) Pirouz et al.[6]

3.4 Interpolymeric Interactions for the Py-PAMA Samples in Oil

3.4.1. Behavior of Py(5.6)-$PC_{12}MA$ in oil probed by fluorescence

Since engine oils usually contain between 0.1 and 1.5 wt% of PAMA used as PPD,[13] the fluorescence spectrum of a 2 $g.L^{-1}$ Py(5.6)-$PC_{12}MA$ solution in oil was initially acquired as a

function of temperature (Figure 3.4). The intensity of the monomer at 375 nm (I_M) was normalized to 100 for all spectra. Figure 3.4A showed two distinct regimes for the fluorescence spectra depending on whether the fluorescence spectrum was acquired at temperatures that were higher or lower than –30 °C. For both regimes, the intensity of the excimer (I_E) relative to that of the monomer at 375 nm (I_M) decreased continuously with decreasing temperature, as would be expected for pyrene excimer formation by diffusion. As the solvent viscosity increased due to the decrease in temperature, excimer formation by diffusive encounters between the pyrene labels was hindered. Between –35 and –30 °C however, a clear change in the spectral features was observed for the 2 $g.L^{-1}$ Py(5.6)-$PC_{12}MA$ solution in oil upon decreasing the temperature, which implied that excimer formation had undergone a significant and precipitous change. The fifth band (I_V) in the fluorescence spectrum of the monomer at 415 nm increased substantially at –30 ^oC upon lowering the solution temperature, which led to an increase in excimer intensity (I_E) at this temperature.

The step increase in I_E was due to a contraction of the polymer coil taking place between –35 and –30 °C, which was attributed to the crystallization of the dodecyl side chains of Py(5.6)-$PC_{12}MA$. Since this effect appeared to be similar to that observed during the crystallization of semicrystalline pyrene-labeled ethylene-propylene copolymers (Py-EP) in toluene,[6] the procedure that was originally developed to determine f_{inter} for Py-EP copolymers in apolar solvents was implemented for the Py(5.6)-$PC_{12}MA$ sample. To this end, the fluorescence spectra of a mixture of 0.01 $g.L^{-1}$ Py(5.6)-$PC_{12}MA$ sample and 2 $g.L^{-1}$ unlabeled $PC_{12}MA$ were also acquired in oil to obtain the behavior of the fluorescently labeled polymer under conditions where excimer would be generated intramolecularly. Such a low concentration of Py(5.6)-$PC_{12}MA$ ensured that each pyrene-labeled polymer was surrounded by unlabeled chains when the polymer underwent

crystallization, so that the labeled polymer could not form excimer intermolecularly. As shown in Figure 3.4B, I_E increased continuously from −45 to +25 °C, showing no indication of a transition, and thus of intermolecular interactions.

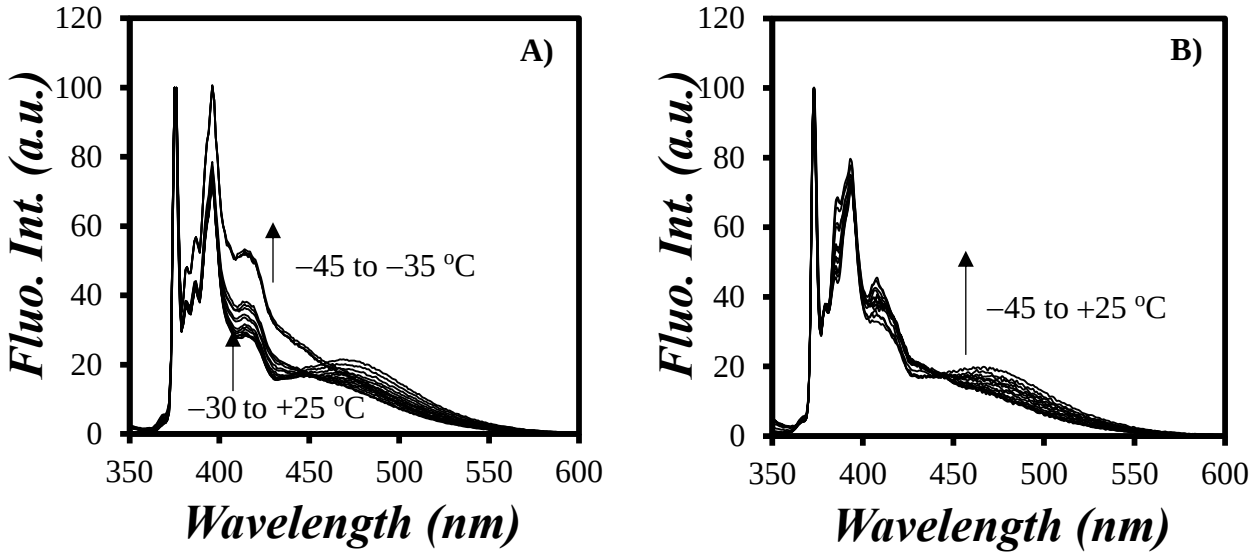

Figure 3.4. Fluorescence spectra of solutions of A) 2 g.L^{-1} Py-PC$_{12}$MA and B) 0.01 g.L^{-1} Py(5.6)-PC$_{12}$MA and 2 g.L^{-1} PC$_{12}$MA in oil acquired from −45 to +25 °C.

As for the Py-EP study described in Chapter 2, the ratios I_E/I_M(inter & intra) and I_E/I_M(intra) obtained at, respectively, high and low Py(5.6)-PC$_{12}$MA concentrations were plotted as a function of temperature in Figure 3.5A. The I_E/I_M(inter & intra) ratio was calculated by integrating the fluorescence intensity of the excimer from 500 to 530 nm for I_E, as it was demonstrated in Chapter 2 that this wavelength range yielded representative f_{inter} values even though it did not include the I_V band at 415 nm, which showed a substantial change in the fluorescence spectra in Figure 3.4A. The I_E/I_M(inter & intra) ratio showed a clear step increase between −35 and −30 °C as the solution temperature was lowered. The I_E/I_M ratios were combined according to Equation 2.5 to yield f_{inter}, which was plotted as a function of temperature in Figure 3.5B. Two temperature regimes were clearly visible between −45 and −35 °C on the one hand, and −30 and +25 °C on the other hand. In

the lower temperature regime, f_{inter} remained more or less constant around 0.44 ± 0.01, while it decreased to 0.20 ± 0.02 in the higher temperature regime. The step increase of f_{inter} at −30 °C indicated an increase in intermolecular interactions which was attributed to a decrease in the solubility of Py(5.6)-PC_{12}MA, whose dodecyl side chains were believed to have undergone crystallization.

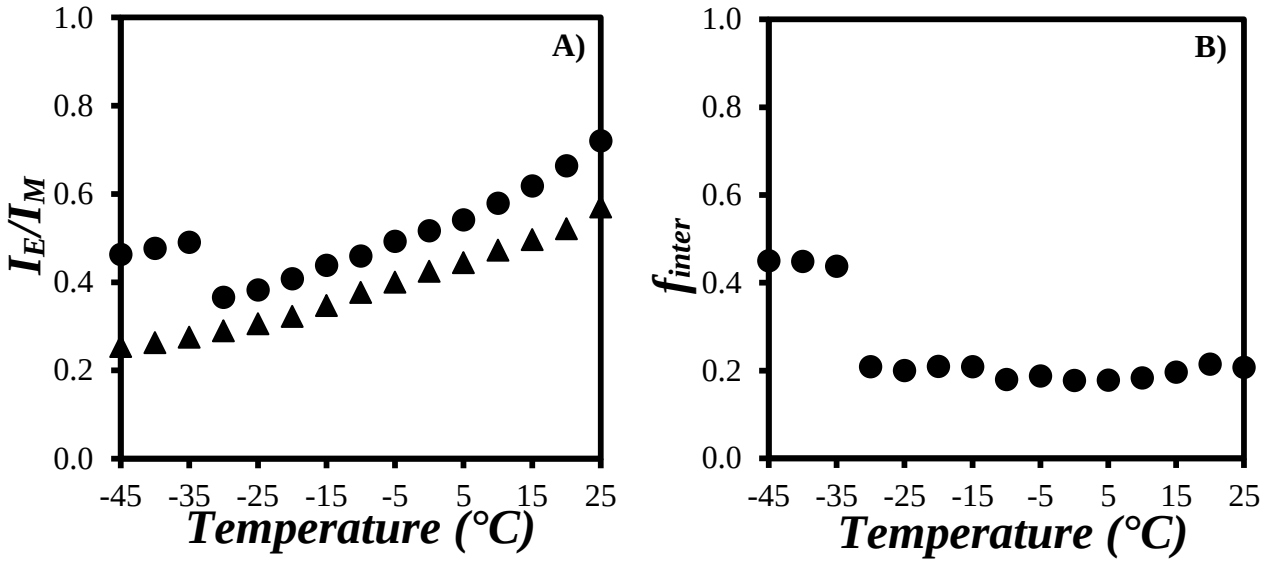

Figure 3.5. Plots of A) the I_E/I_M ratio for (●) 2 g.L^{-1} Py(5.6)-PC_{12}MA solution in oil and (▲) a mixture of 0.01 g.L^{-1} Py(5.6)-PC_{12}MA and 2 g.L^{-1} PC_{12}MA in oil and B) the molar fraction f_{inter} for the 2 g.L^{-1} Py(5.6)-PC_{12}MA solution in oil as a function of temperature.

3.4.2 Behavior of Py(6.7)-PC_{18}MA in oil probed by fluorescence

A similar set of experiments to that conducted with Py(5.6)-PC_{12}MA in oil was carried out with the Py(6.7)-PC_{18}MA sample. The fluorescence spectra of two solutions, one with 2 g.L^{-1} Py(6.7)-PC_{18}MA and the other with 0.01 g.L^{-1} Py(6.7)-PC_{18}MA, without excess unlabeled PC_{18}MA, were acquired as a function of temperature. The spectra are presented in Figure 3.6A and B. Two distinct regimes were encountered at temperatures lower and higher than +10 °C for both concentrations. In both temperature regimes, the intensity of the excimer (I_E) relatively to that of the monomer

(I_M) increased continuously with the temperature. As for Py(5.6)-$PC_{12}MA$, the boundary between the two regimes was marked by a step increase in I_E at +10 °C upon increasing the temperature. While the continuous increase in I_E was attributed to an increase in diffusive encounters between pyrene labels due to a decrease in viscosity, the step increase in I_E observed at +10 °C was attributed to the contraction of the polymer coil due to the crystallization of the octadecyl side chains of Py(6.7)-$PC_{18}MA$. Interestingly, the transition attributed to $PC_{18}MA$ crystallization was detected at +10 °C for both the low 0.01 $g.L^{-1}$ and high 2.0 $g.L^{-1}$ Py(6.7)-$PC_{18}MA$ concentrations.

To assess whether $PC_{18}MA$ could crystallize in oil, a 10 $g.L^{-1}$ $PC_{18}MA$ solution in oil was prepared and its behavior was characterized by differential scanning calorimetry. As shown in Figure S3.1 in Supporting Information, the solution showed a sharp exotherm at 10.6 °C upon decreasing the solution temperature, reflecting the crystallization of $PC_{18}MA$ in oil. The excellent agreement between the transition observed in the fluorescence spectra and the exotherm found in the DSC trace at 10.6 °C provides strong evidence of the crystallization of $PC_{18}MA$ in oil at low temperature.

Since the crystallization of $PC_{18}MA$ corresponds to a decrease in solubility of the polymer, intermolecular interactions between Py(6.7)-$PC_{18}MA$ were expected to occur in oil even at 0.01 $g.L^{-1}$ polymer concentration, as suggested by the clear change in the I_V band at 415 nm observed at 10 °C in Figure 3.6B. To prevent this from happening, a mixture of 0.01 $g.L^{-1}$ Py(6.7)-$PC_{18}MA$ and 2 $g.L^{-1}$ $PC_{18}MA$ was prepared in oil and its fluorescence spectrum was acquired as a function of temperature as shown in Figure 3.6C. The clear transition observed at +10 °C in Figure 3.6A and B was not found in Figure 3.6C, demonstrating that intermolecular interactions between Py(6.7)-$PC_{18}MA$ molecules had been eliminated upon adding an excess of $PC_{18}MA$. Instead, the spectra in Figure 3.6C showed a continuous increase in I_E from −30 to +25 °C,

reflecting an increase in excimer formation by diffusive encounters due to the decrease in viscosity experienced by the oil with increasing temperature.

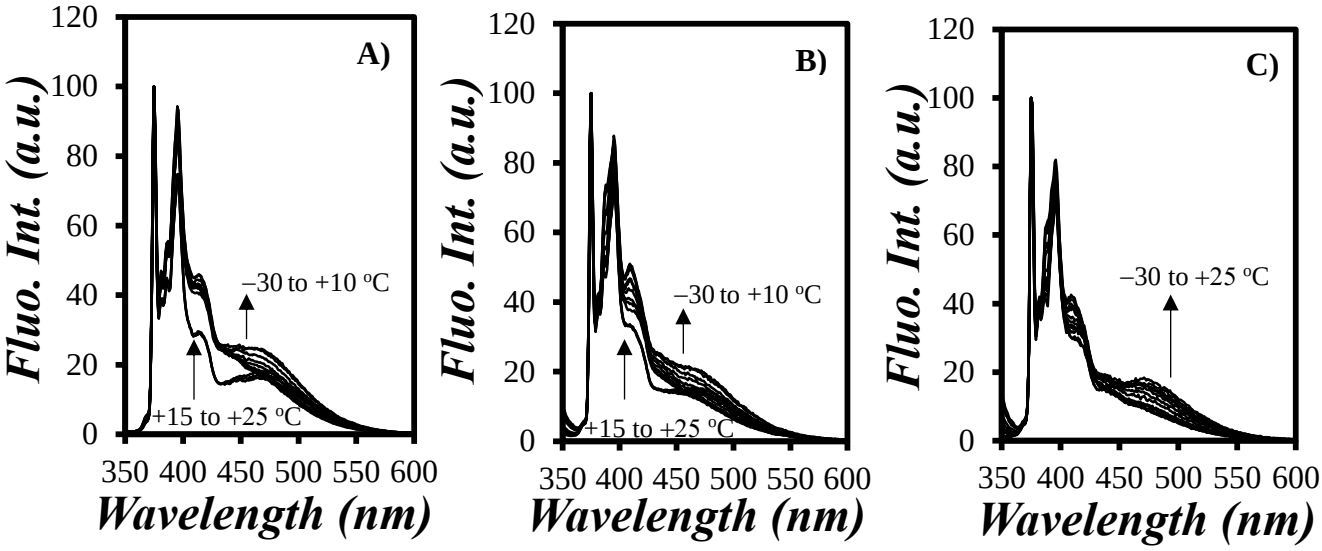

Figure 3.6. Fluorescence spectra of solutions in oil of A) 2 g.L^{-1} Py(6.7)-PC$_{18}$MA, B) 0.01 g.L^{-1} Py(6.7)-PC$_{18}$MA, and C) 0.01 g.L^{-1} Py(6.7)-PC$_{18}$MA and 2 g.L^{-1} PC$_{18}$MA in oil taken at temperatures ranging from −30 to +25 °C.

The I_E/I_M ratios of the solutions in oil containing 2 g.L^{-1} Py(6.7)-PC$_{18}$MA, 0.01 g.L^{-1} Py(6.7)-PC$_{18}$MA, and a mixture of 0.01 g.L^{-1} Py(6.7)-PC$_{18}$MA and 2 g.L^{-1} PC$_{18}$MA were plotted as a function of temperature in Figure 3.7. The I_E/I_M ratios increased in a similar manner with increasing temperature for all three solutions in oil over the entire temperature range. Only the two solutions containing 2 g.L^{-1} and 0.01 g.L^{-1} Py(6.7)-PC$_{18}$MA with no excess of unlabeled PC$_{18}$MA showed a clear step increase between +10 and +15 °C, which corresponds to the crystallization of PC$_{18}$MA. The 0.01 g.L^{-1} Py(6.7)-PC$_{18}$MA solution with a 2 g.L^{-1} PC$_{18}$MA showed no transition, indicating that pyrene excimer formation occurred intramolecularly over the entire temperature range, thus yielding I_E/I_M(intra) in oil.

The I_E/I_M ratio for the 2 g.L^{-1} Py(6.7)-PC$_{18}$MA solution in oil was always larger than that of the mixture of 0.01 g.L^{-1} Py(6.7)-PC$_{18}$MA and 2 g.L^{-1} PC$_{18}$MA at a same temperature (Figure 3.6A). This behavior simply reflected that more intermolecular interactions were observed for this high concentration of Py(6.7)-PC$_{18}$MA.

Interestingly, Figure 3.6B showed that the 0.01 g.L^{-1} Py(6.7)-PC$_{18}$MA solution and the mixture of 0.01 g.L^{-1} Py(6.7)-PC1$_8$MA with 2 g.L^{-1} PC$_{18}$MA yielded similar I_E/I_M ratios at temperatures above +15 ^{o}C. At lower temperatures, the I_E/I_M ratio was higher for the solution containing only 0.01 g.L^{-1} Py(6.7)-PC$_{18}$MA. Such an observation indicated that the 0.01 g.L^{-1} Py(6.7)-PC$_{18}$MA solution in oil formed excimer only intramolecularly above its crystallization temperature so that it yielded the ratio I_E/I_M(intra), whereas at lower temperatures, the I_E/I_M ratio of the 0.01 g.L^{-1} Py(6.7)-PC$_{18}$MA solution yielded I_E/I_M(inter & intra).

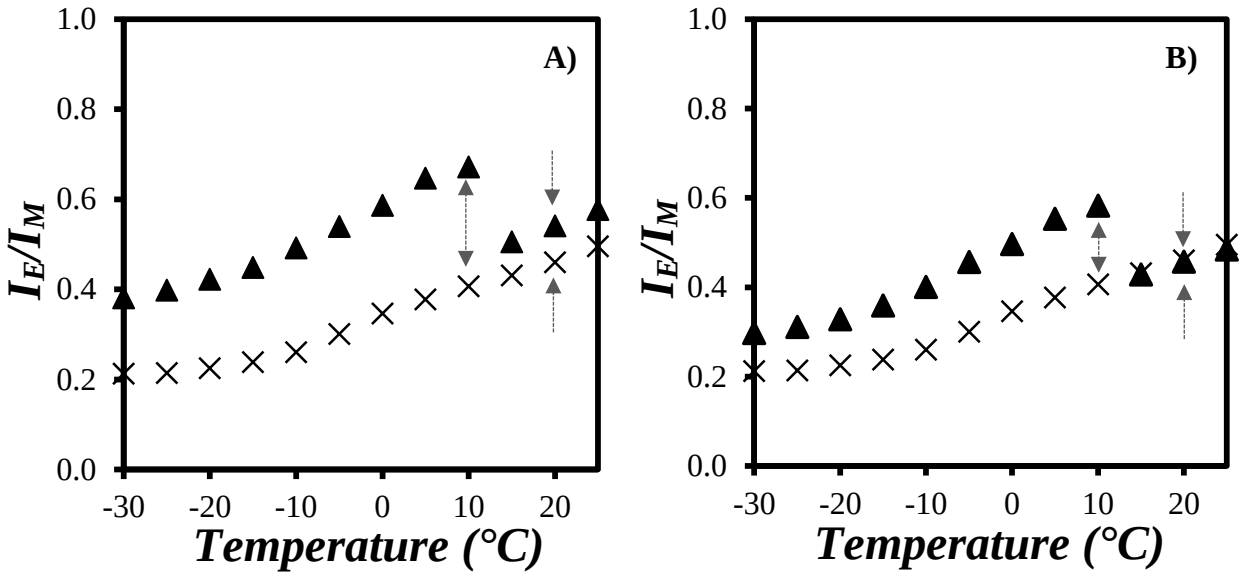

Figure 3.7. Comparison of the I_E/I_M plots of A) (▲) the 2 g.L^{-1} Py(6.7)-PC$_{18}$MA solution and B) (▲) the 0.01 g.L^{-1} Py(6.7)-PC$_{18}$MA with (×) the mixture of 0.01 g.L^{-1} Py(6.7)-PC$_{18}$MA and 2 g.L^{-1} PC$_{18}$MA in oil as a function of temperature.

The I_E/I_M(inter & intra) and I_E/I_M(intra) ratios in Figure 3.7 were combined to yield f_{inter}, which was plotted as a function of temperature in Figure 3.8. For both the high and low concentrations of Py(6.7)-PC_{18}MA, two regimes were observed at temperatures below and above the crystallization temperature (T_C). According to the f_{inter} plot of the 2 g.L^{-1} Py(6.7)-PC_{18}MA solution, f_{inter} decreased from 0.45 ± 0.04 at temperatures lower than +15 °C (T_C = +12.5 ± 2.5 °C) to 0.15 ± 0.01 at higher temperatures, remaining more or less constant in each temperature regime.

In the case of the 0.01 g.L^{-1} Py(6.7)-PC_{18}MA solution in oil, no intermolecular interactions took place at temperatures higher than T_C where f_{inter} equaled 0.00±0.01. However, at temperatures lower than +10 °C, f_{inter} increased to 0.14 ± 0.04, indicating the presence of intermolecular interactions between Py(6.7)-PC_{18}MA chains induced by crystallization at low temperatures, even at this low 0.01 g.L^{-1} Py(6.7)-PC_{18}MA concentration.

The results described in Figure 3.7 for f_{inter} at 0.01 and 2 g.L^{-1} Py(6.7)-PC_{18}MA concentrations indicate that, first, f_{inter} takes large values at all temperatures for the 2 g.L^{-1} solution due to increased intermolecular interactions at high concentration; second, f_{inter} equals zero for the 0.01 g.L^{-1} solution at temperatures above crystallization when Py(6.7)-PC_{18}MA forms excimer intramolecularly; and third, f_{inter} presents the same transition at +10 °C at both concentrations, reporting on the crystallization of the octadecyl side chains. These results reflect the expected behavior of these polymeric samples and demonstrate the robustness and validity of the method implemented to determine f_{inter}. They also generalize the procedure to polymers other than the EP copolymers studied so far.[6,14]

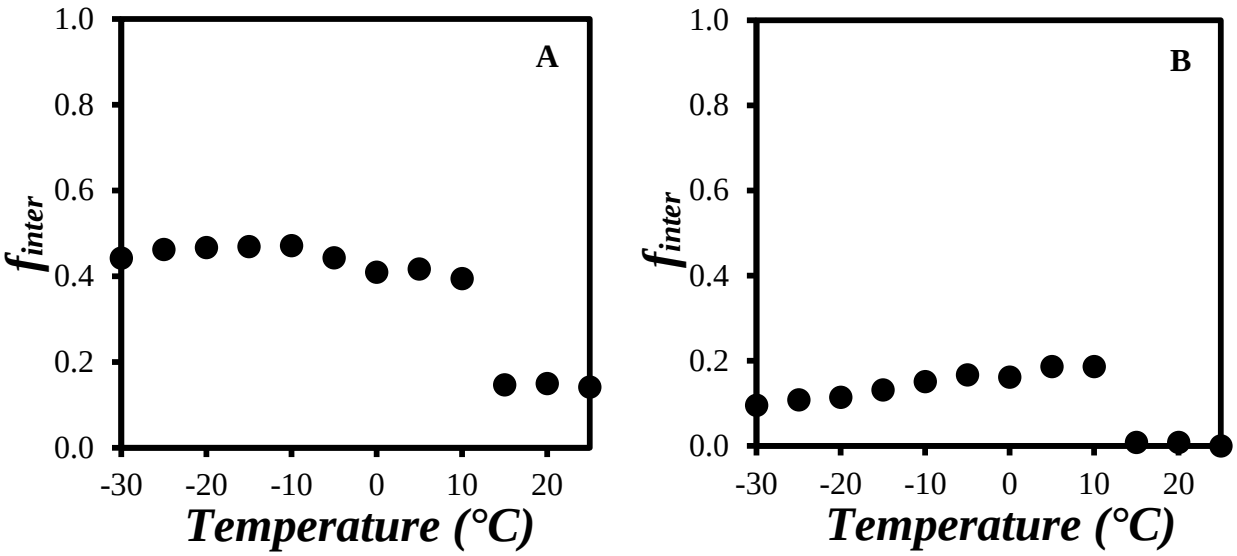

Figure 3.8. Plots of f_{inter} as a function of temperature for A) the 2 g.L^{-1} Py(6.7)-PC$_{18}$MA solution and B) the 0.01 g.L^{-1} Py(6.7)-PC$_{18}$MA solution in oil.

3.5 Comparing the f_{inter} Profiles for Py(5.6)-PC$_{12}$MA and Py(6.7)-PC$_{18}$MA in Oil

For a similar pyrene content of 216 μmol.g^{-1} for Py(5.6)-PC$_{12}$MA and 195 μmol.g^{-1} for Py(6.7)-PC$_{18}$MA and a same polymer concentration of 2 g.L^{-1} in oil, f_{inter} took a similar value independently of the alkyl chain length of the Py-PAMA sample, since both the Py(5.6)-PC$_{12}$MA and Py(6.7)-PC$_{18}$MA solutions yielded similar f_{inter} values below and above their crystallization points in oil (Figure 3.9, Table 3.2).

Table 3.2. Summary of the f_{inter} values obtained for the 2 g.L^{-1} solutions for two Py-PAMA samples.

	Temp (°C)				
	–45 to –35	–35 to –30	–30 to +10	+10 to +15	+15 to +25
Py-PC$_{12}$MA	0.44 ± 0.01	Crystallization	0.20 ± 0.02		
Py-PC$_{18}$MA	-		0.45 ± 0.04	Crystallization	0.15 ± 0.01

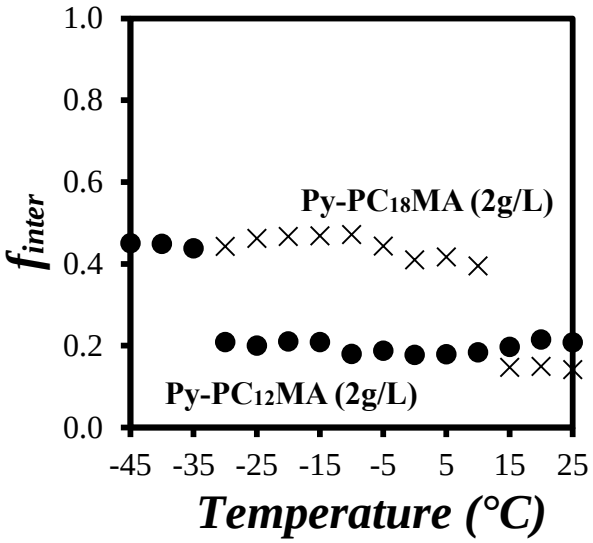

Figure 3.9. Molar fraction f_{inter} of a 2 g.L^{-1} solution of (•) Py(5.6)-PC$_{12}$MA and (×) Py(6.7)-PC$_{18}$MA in oil from –45 to +25 ^{o}C.

However, there was a significant difference between the crystallization temperature (T_C) of –32.5 ± 2.5 ^{o}C and +12.5 ± 2.5 ^{o}C obtained for the 2 g.L^{-1} solutions of Py(5.6)-PC$_{12}$MA and Py(6.7)-PC$_{18}$MA in oil, respectively. This represented a +45 ± 5 ^{o}C difference in T_C. As demonstrated in Figure 3.10, a similar temperature difference could be observed between the melting points of the alkanes having a similar chemical composition as the alkyl side chains of the PAMA samples, found to equal –9.6 ± 0.4 ^{o}C and +30.0 ± 2.0 ^{o}C for n-dodecane and n-octadecane, respectively. This represented a 39.6 ± 2.4 ^{o}C temperature difference in T_C for the two alkanes, comparable to the T_C difference between the C$_{12}$ and C$_{18}$ alkyl side chains of the PAMA in oil.

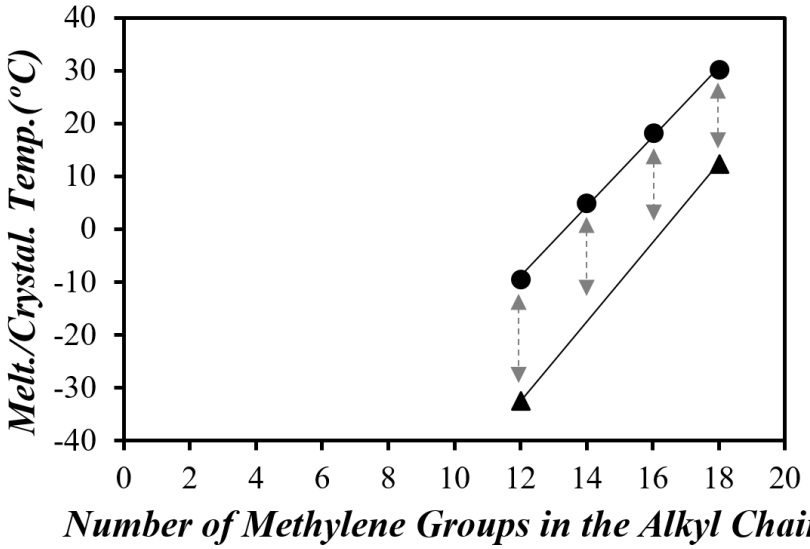

Figure 3.10. Plots of (▲) T_C values of the Py-PAMAs in oil and (●) T_C values of alkanes as a function of the number of carbon atoms in the side chain.

In summary, the fluorescence experiments have identified that Py(5.6)-PC_{12}MA and Py(6.7)-PC_{18}MA undergo a crystallization-induced coil contraction at –30 and +15 °C, respectively. Since the temperature range from room temperature (+25 °C) down to the crystallization temperature was much narrower for Py(6.7)-PC_{18}MA than for Py(5.6)-PC_{12}MA and thus would require less experimental work to cover, Py(6.7)-PC_{18}MA was selected to probe the interactions taking place between EP copolymers and Py-PAMAs.

3.6 Level of Interpolymeric Interactions (f_{inter}) of PC_{18}MA in the Presence of EP Copolymers in Oil

Now that the solution behavior of Py(6.7)-PC_{18}MA in oil had been well characterized as a function of temperature, the effect that another oil additive might have on the PAMA behavior could be investigated. To this end, mixtures of 10 $g.L^{-1}$ naked EP(AM) or EP(SM2) copolymers with either 2 $g.L^{-1}$ of Py(6.7)-PC_{18}MA, or a mixture of 0.01 $g.L^{-1}$ Py(6.7)-PC_{18}MA and 2 $g.L^{-1}$ PC_{18}MA were prepared in oil. The fluorescence spectra of the solutions were acquired as a function of

temperature. The spectra for the concentrated Py(6.7)-PC_{18}MA solutions with either EP(AM) or EP(SM2) are shown in Figures 3.11A and B, respectively, where the intensity of the monomer at 375 nm (I_M) was normalized to 100 for all solutions. As was observed earlier with the Py(6.7)-PC_{18}MA solutions only, two distinct regimes could be identified depending on whether the solution temperature was above or below the crystallization temperature of Py-PC_{18}MA. As the temperature decreased from +25 to –30 °C, I_E decreased continuously but showed a step increase at +10 °C. As explained earlier, the continuous decrease in I_E observed with decreasing temperature was a consequence of the increase in viscosity that reduced pyrene diffusive encounters. The step increase in I_E at +10 °C was the result of a contraction of the polymer coil that brought the pyrene labels in closer proximity, leading to a step increase in excimer formation.

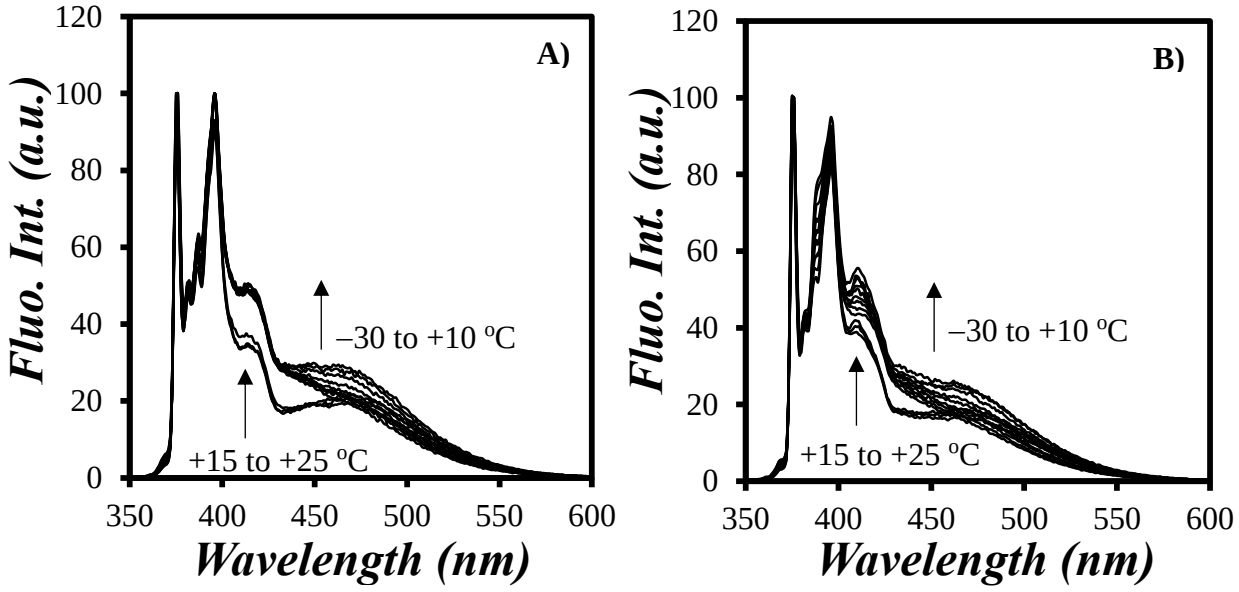

Figure 3.11. Fluorescence spectra of a mixture of 2 g.L^{-1} Py(6.7)-PC_{18}MA and A) 10 g.L^{-1} EP(AM) and B) 10 g.L^{-1} EP(SM2) in oil as a function of temperature from –30 to +25 °C.

The fluorescence spectra shown in Figure 3.11 for the 2 g.L^{-1} Py(6.7)-PC_{18}MA solution were analyzed to yield the I_E/I_M(inter & intra) ratio. The fluorescence spectra of the solutions

containing 0.01 g.L^{-1} Py(6.7)-PC$_{18}$MA and 2 g.L^{-1} PC$_{18}$MA with 10 g.L^{-1} EP copolymer were also acquired as a function of temperature to yield I_E/I_M(intra). I_E/I_M(inter & intra) and I_E/I_M(intra) were plotted as a function of temperature in Figures 3.12A and B for the solutions with EP(AM) and EP(SM2), respectively. They presented the general trends discussed earlier, with a continuous increase in the I_E/I_M ratios observed with temperature due to an increase in diffusive encounters between the pyrene pendants. The main difference in behavior between the dilute and concentrated Py(6.7)-PC$_{18}$MA solutions was the break point observed at +10 °C for the concentrated Py(6.7)-PC$_{18}$MA solution, which corresponded to the crystallization of the side chains.

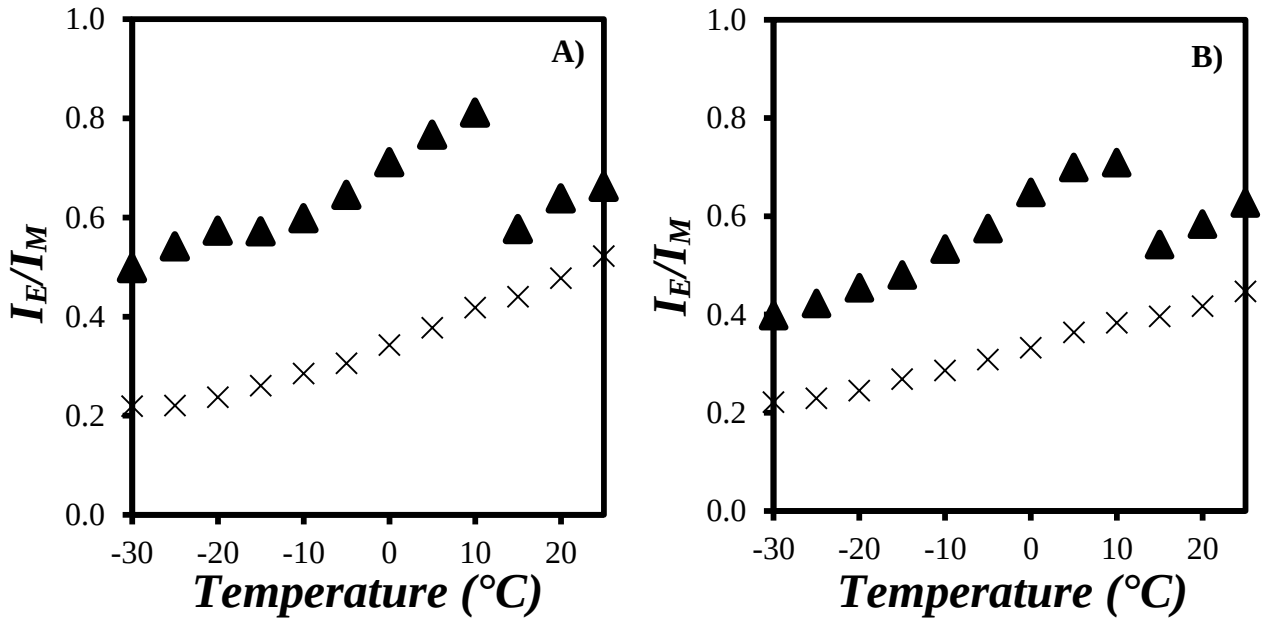

Figure 3.12. Plots of (▲) I_E/I_M(inter & intra) and (×) I_E/I_M(intra) as a function of temperature for mixtures of 10 g.L^{-1} of A) EP(AM) or B) EP(SM2) with either 2 g.L^{-1} Py(6.7)-PC$_{18}$MA or a mixture of 0.01 g.L^{-1} Py(6.7)-PC$_{18}$MA and 2 g.L^{-1} PC$_{18}$MA.

The ratios I_E/I_M(inter & intra) and I_E/I_M(intra) were combined according to Equation 2.5 to yield f_{inter} which was plotted as a function of temperature in Figure 3.13. For the 2 g.L^{-1} Py(6.7)-PC$_{18}$MA solution containing the EP(AM) copolymer, f_{inter} decreased slightly from 0.56 at –30 °C

to 0.48 at +10 °C, before undergoing a step decrease between +10 and +15 °C, and plateauing at 0.23 ± 0.02 for temperatures between +15 and +25 °C. As for the 2 g.L^{-1} Py(6.7)-PC$_{18}$MA solution with 10 g.L^{-1} EP(SM2), f_{inter} remained constant and equal to 0.46 ± 0.03 and 0.28 ± 0.01 in the high and low temperature ranges, respectively.

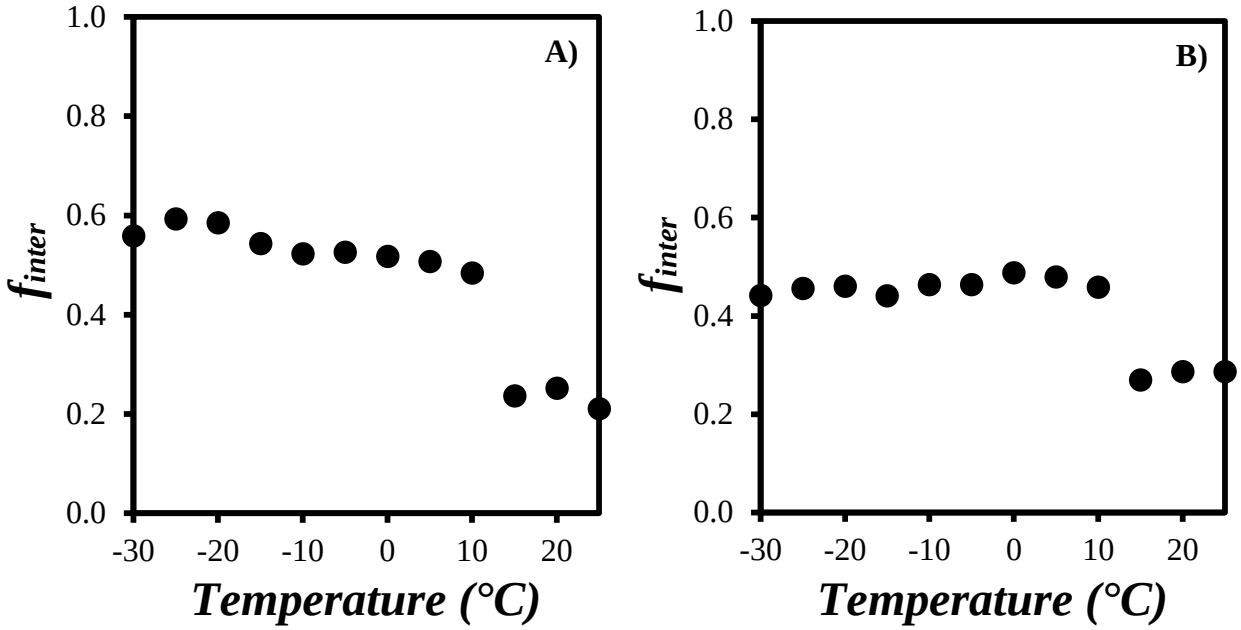

Figure 3.13. Molar fraction f_{inter} for a 2 g.L^{-1} Py(6.7)-PC$_{18}$MA solution in oil with A) 10 g.L^{-1} EP(AM) and B) 10 g.L^{-1} EP(SM2) obtained at temperatures between –30 and +25 °C.

3.7 Comparison of the f_{inter} Plots of Py(6.7)-PC$_{18}$MA Before and After Addition of EP Copolymers

The f_{inter} profiles of the 2 g.L^{-1} solutions of Py(6.7)-PC$_{18}$MA in the presence and absence of the EP copolymers were compared in Figure 3.14. A small increase could be observed in f_{inter} at temperatures higher than +15 °C after the addition of both EP copolymers. This result indicates that the addition of EP copolymers, promotes intermolecular interactions between Py(6.7)-PC$_{18}$MA macromolecules. This suggests that Py(6.7)-PC$_{18}$MA associates with the EP copolymers,

that act as binders and induce Py(6.7)-$PC_{18}MA$ aggregation, resulting in larger f_{inter} values. At +15 °C, where the side chains of Py(6.7)-$PC_{18}MA$ crystallize, f_{inter} showed a step increase for all the solutions, but f_{inter} remained larger for the solution with, rather than without, EP copolymers. However, whereas f_{inter} remained larger with EP(AM) than without EP copolymer at all temperatures, the f_{inter} values for the solutions with 10 $g.L^{-1}$ EP(SM2) was found to decrease with decreasing temperature, until it matched the f_{inter} values of the 2 $g.L^{-1}$ Py-$PC_{18}MA$ solution without EP copolymers at temperatures lower than −5 °C.

As shown in Chapter 2, the crystallization of EP(SM2) occurred over a broad temperature range between −10 and +10 °C in Figure 2.12, as compared to the sharp transition observed for Py(6.7)-$PC_{18}MA$ in oil. The trends shown in Figure 3.14 suggest that as EP(SM2) slowly crystallized with decreasing temperature, it could no longer promote the interactions between the Py(6.7)-$PC_{18}MA$ macromolecules, whose f_{inter} value returned to that of the 2 $g.L^{-1}$ Py(6.7)-$PC_{18}MA$ solution without EP copolymer. Furthermore, since the crystallization of EP(SM2) took place with longer oligoethylene sequences, the dissociation of EP(SM2) from Py(6.7)-$PC_{18}MA$ that took place as EP(SM2) crystallized implied that the long oligoethylene sequences of EP(SM2) promoted the association with Py(6.7)-$PC_{18}MA$, probably via the linear alkyl side chains. As these longer oligoethylene sequences became unavailable upon crystallization of EP(SM2), f_{inter} decreased progressively with decreasing solution temperature from +10 to −5 °C, where it reached the f_{inter} value corresponding to the 2 $g.L^{-1}$ Py(6.7)-$PC_{18}MA$ solution without EP copolymer. At this stage, the oligoethylene sequences could no longer bind the alkyl side chains of the Py(6.7)-$PC_{18}MA$ macromolecules.

By contrast EP(AM), which did not crystallize over the temperature range studied, promoted intermolecular interactions between Py(6.7)-$PC_{18}MA$ macromolecules over the entire

temperature range, showing the largest f_{inter} value in Figure 3.14. The results also indicate that the crystallization of Py(6.7)-PC_{18}MA at +15 °C did not affect the interactions between Py(6.7)-PC_{18}MA and EP(SM2), but that crystallization of EP(SM2) between −10 and +10 °C reduced the interactions between the two polymers.

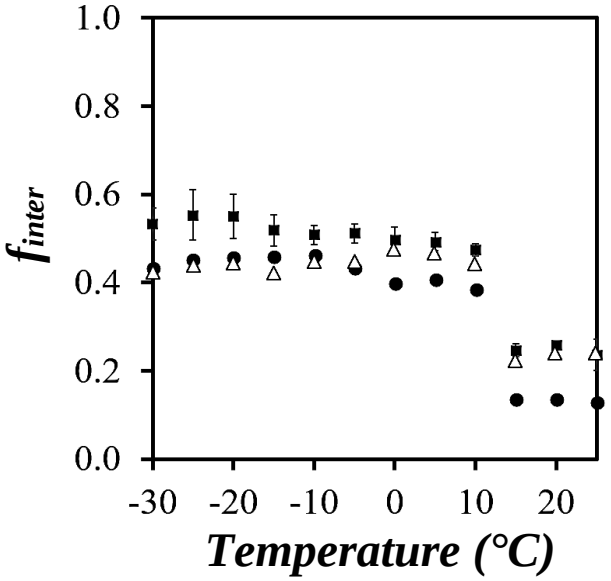

Figure 3.14. Plots of the molar fraction f_{inter} as a function of temperature for 2 g.L^{-1} Py-PC_{18}MA solutions in oil (●) without EP copolymer, (■) with 10 g.L^{-1} EP(AM), and (Δ) with 10 g.L^{-1} EP(SM2).

3.8 Molar Fractions of the Different Pyrene Species of the Py(6.7)-PC_{18}MA Solution in Oil

Fluorescence decay measurements were conducted using an IBH time-resolved fluorometer equipped with a Cryostat to determine the molar fraction of pyrene species that were aggregated in solution. The monomer and excimer decays were acquired for a solution of 2 g.L^{-1} Py(6.7)-PC_{18}MA in oil at temperatures ranging from −30 to +25 °C. Additionally, the monomer decay of a solution of 3×10^{-6} mol.L^{-1} 1-pyrenebutanol, used as a model compound, was acquired at the

same temperatures to obtain the pyrene monomer lifetime (τ_M). Using the model free analysis (MFA), the molar fractions of those pyrenes that formed excimer by diffusion (f_{diff}), were isolated and did not form excimer (f_{free}), and formed excimer by direct excitation of a dimer constituted of two pyrene labels that were either well-stacked (f_{E0}) or poorly stacked (f_D) ($f_{agg} = f_D + f_{E0}$), and the average rate constant of pyrene excimer formation <k> were retrieved from the monomer and excimer fluorescence decays for the 2 g.L^{-1} Py(6.7)-PC$_{18}$MA solution in oil. They are reported in Table 3.3. This table also lists the I_E/I_M(inter & intra) ratios that were calculated in the temperature range from –30 to +25 °C using Equation 1.3 in Chapter 1.

Table 3.3. I_E/I_M ratios, <k>, and molar fractions of the different pyrene species found by MFA of the fluorescence decays of the 2 g.L^{-1} Py(6.7)-PC$_{18}$MA solution in oil.

Sample Description	Temp.(°C)	τ_M (ns)	f_{diff}	f_{free}	f_{agg}	f_D	f_{E0}	<k> (10^6 s^{-1})	I_E/I_M
Py(6.7)-PC$_{18}$MA (2 g/L) in Oil(II)	-30	236	0.748	0.063	0.189	0.088	0.101	4.2	0.372
	-25	236	0.771	0.060	0.169	0.093	0.077	3.6	0.364
	-20	232	0.797	0.025	0.178	0.088	0.091	4.2	0.362
	-15	230	0.774	0.063	0.163	0.095	0.068	4.1	0.363
	-10	222	0.778	0.055	0.168	0.099	0.068	4.9	0.373
	-5	217	0.734	0.094	0.172	0.102	0.070	4.9	0.416
	0	227	0.784	0.047	0.169	0.097	0.072	5.1	0.424
	+5	223	0.805	0.036	0.159	0.121	0.038	5.6	0.429
	+10	222	0.767	0.068	0.164	0.083	0.068	3.9	0.424
	+15	221	0.707	0.158	0.135	0.050	0.158	4.7	0.244
	+20	221	0.673	0.186	0.141	0.043	0.186	4.5	0.268
	+25	220	0.741	0.128	0.130	0.058	0.128	3.6	0.273

The parameters listed in Table 3.3 indicate that the rate constant <k> and the molar fraction f_{diff} showed hardly any change at the crystallization temperature (T_C = +12.5 ± 2.5 °C), whereas f_{free} and f_{agg}, which remained constant within experimental error in both temperature regimes, increased from 0.057 ± 0.019 to 0.157 ± 0.024 and decreased from 0.170 ± 0.009 to 0.136 ± 0.005 reaching the transition temperature, respectively. Such an observation suggests that a portion of the Py(6.7)-PC_{18}MA coils that were previously trapped and aggregated in the microcrystals generated by the octadecyl side chains were released to the solution after melting of the microcrystals, which led to less aggregated pyrenes (f_{agg} decreased) and more isolated pyrenes along the backbone (f_{free} increased). The decrease in f_{agg} and the increase in f_{free} seemed to balance out, resulting in constant f_{diff} and <k> values that represented excimer formation by diffusion between the pyrene labels. Most importantly, f_{agg} was lower than 0.19 at all temperatures. This level of pyrene aggregation is reasonable for a polymer randomly labeled with pyrene. In turn, it indicates that 80 mol% of the pyrene labels were not aggregated and could report effectively on the level of interpolymeric interactions, as reflected by the f_{inter} plots in Figure 3.14. Consequently, the Py-PAMA samples should be much less affected by the pyrene aggregation observed for the Py-EP samples in Chapter 2.

The I_E/I_M(inter & intra) ratios, that were retrieved from the analysis of the monomer and excimer decays of the 2 g.L^{-1} Py(6.7)-PC_{18}MA solution in oil, were plotted as a function of temperature and compared in Figure 3.15 to those obtained from the steady-state fluorescence (SSF) measurements of the same solution. It is worth pointing out that using Equation 1.3 provides an absolute measure of the I_E/I_M ratio, whereas the I_E/I_M ratios obtained by SSF are relative. The behaviors obtained for the I_E/I_M ratios determined by SSF and TRF showed the same transition between +10 and +15 °C, indicating that both techniques described the same effect.

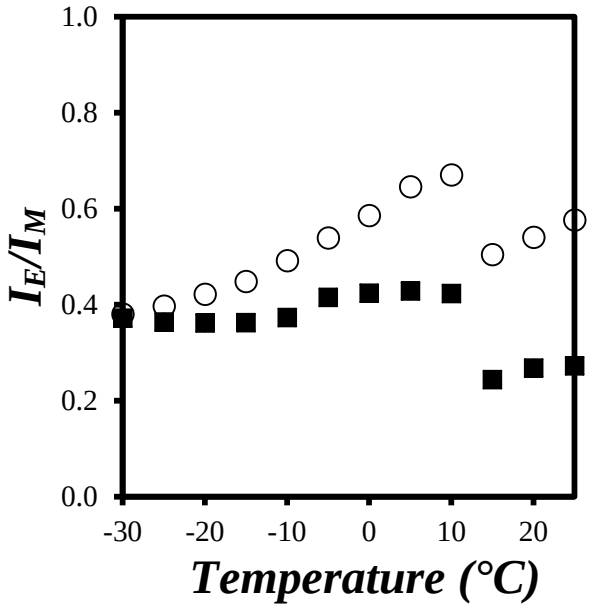

Figure 3.15. I_E/I_M plots of the 2 g.L^{-1} Py-PC$_{18}$MA solution in oil as a function of temperature obtained by (○) SSF and (■) TRF.

3.9 Conclusions

Two types of Py-PAMAs with different alkyl chain lengths were used as PPD mimics in oil. To probe the interactions taking place between polymer chains at the molecular level, time-resolved and steady-state fluorescence experiments were conducted on the Py-PAMA samples. A break point was observed in the f_{inter}-vs-T profiles for the Py-PAMA samples in oil, which reflected contraction of the polymer coils due to the crystallization of the alkyl side chains. The temperature where the transition occurred depended on the side chain length, as would be the case for alkanes of different lengths. A PAMA polymer with a longer alkyl side chain yielded a higher crystallization temperature in solution.

Having developed a good understanding of the behavior of the Py(6.7)-PC$_{18}$MA solution in oil as a function of temperature, the interactions of Py(6.7)-PC$_{18}$MA with EP copolymers were

investigated. Mixtures of Py(6.7)-$PC_{18}MA$ and EP(AM) copolymers resulted in an increase in intermolecular interactions at all temperatures, indicating that Py(6.7)-$PC_{18}MA$ bound onto the EP(AM) copolymers, thus promoting interpolymeric interactions. A similar behavior was observed with the semicrystalline EP(SM2) sample at high temperatures, where EP(SM2) was soluble. But as the temperature decreased from +15 to −10 ^{o}C, EP(SM2) underwent crystallization which reduced interpolymeric interactions between the Py(6.7)-$PC_{18}MA$ molecules, which dissociated from the EP(SM2)/Py(6.7)-$PC_{18}MA$ aggregates into the solution, thus resulting in a lower level of interpolymeric interactions. This was reflected by f_{inter}, which went back to the same level of interpolymeric interactions as the Py(6.7)-$PC_{18}MA$ solution without EP copolymer at solution temperature lower than −10 ^{o}C, when EP(SM2) had completed crystallization in oil.

Chapter 4

Probing the Interactions between Pour Point Depressants (PPDs), Viscosity Index Improvers (VIIs), and Wax in Octane Using Fluorescently Labeled PPDs

4.1 Outline

A poly(octadecyl methacrylate) sample fluorescently labeled with 6.7 mol% of pyrene (Py(6.7)-$PC_{18}MA$), used as a mimic of power point depressant (PPD), was employed to investigate how Py(6.7)-$PC_{18}MA$ interacts with ethylene-propylene (EP) copolymers used as viscosity index improvers (VIIs) and wax found in engine oil. Octane was selected as the solvent for these experiments to ascertain the effect that wax, which is an inherent component of engine oils, had on the interactions between PPDs and VIIs. The fluorescence spectra for Py(6.7)-$PC_{18}MA$ solutions in octane were acquired at low and high concentrations for Py(6.7)-$PC_{18}MA$ and analyzed to obtain the molar fraction (f_{inter}) of pyrene labels that formed excimer intermolecularly, a measure of the level of intermolecular interactions between Py(6.7)-$PC_{18}MA$ molecules in the solution. The f_{inter}-versus-T profile obtained for Py(6.7)-$PC_{18}MA$ alone in octane confirmed that Py(6.7)-$PC_{18}MA$ formed microcrystals as the solution temperature was lowered below 0 ^{o}C. The effect induced by the addition of wax and an amorphous (EP(AM)) and a semicrystalline (EP(SM2)) EP copolymer on the interactions experienced by Py(6.7)-$PC_{18}MA$ were characterized by monitoring f_{inter} as a function of temperature, and comparing the different f_{inter}-versus-T plots obtained after the addition of the different components with the f_{inter}-versus-T plot obtained for Py(6.7)-$PC_{18}MA$ alone. These studies demonstrated that wax and EP(AM) increased the level of intermolecular interactions between the Py(6.7)-$PC_{18}MA$ molecules at all temperatures in octane. EP(SM2) increased the interactions between Py(6.7)-$PC_{18}MA$ molecules at high temperature, where it was soluble in octane, but f_{inter} reverted to its value in the absence of EP(SM2) at low temperatures, where EP(SM2) had crystallized.

4.2 Introduction

Waxes are long chain hydrocarbons derived from petroleum with chemical formula C_nH_{2n+2}, that crystallize at low temperature.[1] Despite the removal of a substantial amount of wax during the refining of base oil, a small amount of these long chain hydrocarbons is left in the oil to maintain its viscosity within a desired range. For example, the oil sample used in Chapters 2 and 3 contained around 10 wt% of wax. Therefore, a wax-free apolar solvent would be beneficial as an oil substitute since it could be used to characterize the effect that the presence and absence of wax might have on the level of intermolecular interactions between other oil additives such as pour point depressants (PPDs) and viscosity index improvers (VIIs). The solvent substitute should have a chemical composition similar to that of oil and would need to remain liquid over the temperature range of –30 to +25 ^oC that was targeted by our experiments. A typical engine oil is a mixture consisting mainly of saturated 18-to-34 carbon atom-long hydrocarbons.[2] Accordingly, an 18-to-34 carbon atom-long alkane would be an ideal solvent substitute for oil. However, since the freezing point of alkanes with more than 9 carbon atoms is higher than –30 ^oC, which represents the lower boundary of the temperature range where our experiments were conducted, it only left nonane or octane as possible solvents. Since octane was more widely available, it was selected as oil substitute in this study.

The presence of wax in octane is expected to hinder its flow by forming microcrystals at low temperatures. As discussed in the previous chapter, the tendency of wax crystals to form a 3D network increases when the solution temperature is lowered. Network formation by wax crystals eventually thickens the oil to the point where it can no longer be pumped. The effect that wax had at low temperatures on the behavior of a poly(octadecyl methacrylate) sample labeled with 6.7 mol% pyrene (Py(6.7)-PC_{18}MA) in octane was characterized by fluorescence, by probing its level

of intermolecular interactions with the parameter f_{inter} in the presence or absence of EP copolymers. The results of this study are described hereafter.

4.3 Experimental

Materials: The amorphous (EP(AM)) and semicrystalline (EP(SM2)) EP copolymers were provided by Afton and their molecular weight distribution and ethylene content have been provided in Chapter 2. The synthesis and characterization of Py(6.7)-$PC_{18}MA$ have been described in an earlier publication[3] and that of $PC_{18}MA$ was presented in Chapter 3. Octane (99%) was purchased from Aldrich. Wax was extracted from a group II oil as follows. A homogenous 5 : 95 oil : methyl ethyl ketone (MEK) mixture was prepared at room temperature and it was placed in a –20 ^{o}C freezer for 24 hrs to ensure the crystallization of the solid wax. The crystallized wax was retrieved from the mixture using suction filtration on a filter paper. The obtained product was then kept in a vacuum oven at 70 ^{o}C for 2 hrs to ensure the complete removal of MEK from the wax.[4]

Instrumentation: The fluorescence spectra of the Py(6.7)-$PC_{18}MA$ solutions were acquired with a PTI LS-100 steady-state fluorometer using an excitation wavelength of 344 nm. The solutions with low and high Py(6.7)-$PC_{18}MA$ concentrations were placed in a square or triangular quartz cell with circular opening on top, to allow their degassing by bubbling nitrogen through a needle for 30 min before sealing them quickly with either a Teflon cap or a rubber septum. The fluorescence cells containing the degassed solutions were then placed in an Oxford Optistat DN fitted in the sample chamber of the fluorometer. Right angle and front-face geometries were employed to acquire the fluorescence spectra for the solutions having a low and a high Py(6.7)-$PC_{18}MA$ concentration, respectively.

4.4 Level of Interpolymeric Interactions (f_{inter}) of Py-PC_{18}MA in Octane

The fluorescence spectrum of a 2 $g.L^{-1}$ Py(6.7)-PC_{18}MA solution was initially acquired in octane as a function of temperature (Figure 4.1). The fluorescence intensity at 375 nm, corresponding to the 0-0 transition of pyrene, was used to represent the pyrene monomer fluorescence intensity (I_M) and was normalized to 100 for all fluorescence spectra. As shown in Figure 4.1A, two well-defined regimes could be identified at temperatures lower and higher than the crystallization temperature of Py-PC_{18}MA, estimated to equal 0 °C in octane. In both temperature regimes, the intensity of the excimer (I_E) at 480 nm relatively to the normalized monomer intensity (I_M) decreased continuously with decreasing temperature as expected. This phenomenon results from the increase in solvent viscosity with decreasing temperature, that consequently reduces pyrene excimer formation by diffusion. The transition at 0 ^oC in Figure 4.1A was mostly identified from the obvious distortion that appeared in the fifth band of the pyrene monomer (I_V) at 414 nm, which transitioned from a low to a high value at this temperature. This transition was attributed to the formation of poorly stacked pyrene aggregates resulting from the crystallization of the octadecyl side chains of PC_{18}MA.

Additionally, the fluorescence spectrum for a solution of 0.05 $g.L^{-1}$ Py(6.7)-PC_{18}MA and 2 $g.L^{-1}$ unlabeled PC_{18}MA was acquired in octane. Under these conditions, the labeled polymer would be incapable of forming excimer intermolecularly upon crystallizing in octane, as crystallization would generate polymeric aggregates where single Py(6.7)-PC_{18}MA would be isolated in a large excess of unlabeled PC_{18}MA. Contrary to Figure 4.1A that showed a marked change in I_V for the pyrene monomer, no such change was observed for the fluorescence spectra acquired with a low concentration of Py(6.7)-PC_{18}MA in octane. Instead, the normalized spectra

showed a continuous increase in I_E at 480 nm when the solution temperature was increased from −30 to +25 °C.

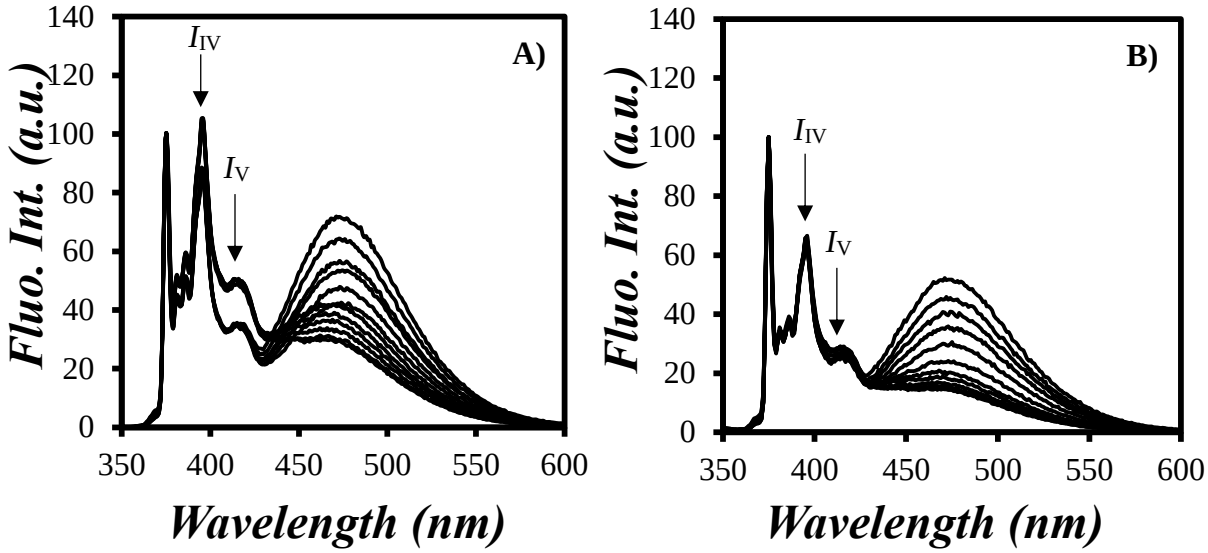

Figure 4.1. Fluorescence spectra of solutions of A) 2 g.L^{-1} Py(6.7)-PC_{18}MA and B) 0.05 g.L^{-1} Py(6.7)-PC_{18}MA with 2 g.L^{-1} PC_{18}MA in octane acquired as a function of temperature from −30 to +25 °C.

The I_E/I_M(inter & intra) and I_E/I_M(intra) ratios were calculated from the fluorescence spectra obtained at high and low concentrations of Py(6.7)-PC_{18}MA in octane. These ratios were plotted as a function of temperature in Figure 4.2A and were employed to calculate f_{inter} in Figure 4.2B. Despite the obvious transition point in the fluorescence spectra of the 2 g.L^{-1} Py(6.7)-PC_{18}MA solution in octane, identified by the change in I_V in Figure 4.1A, the f_{inter}-versus-temperature profile in Figure 4.2B showed a less defined transition at the corresponding temperature.

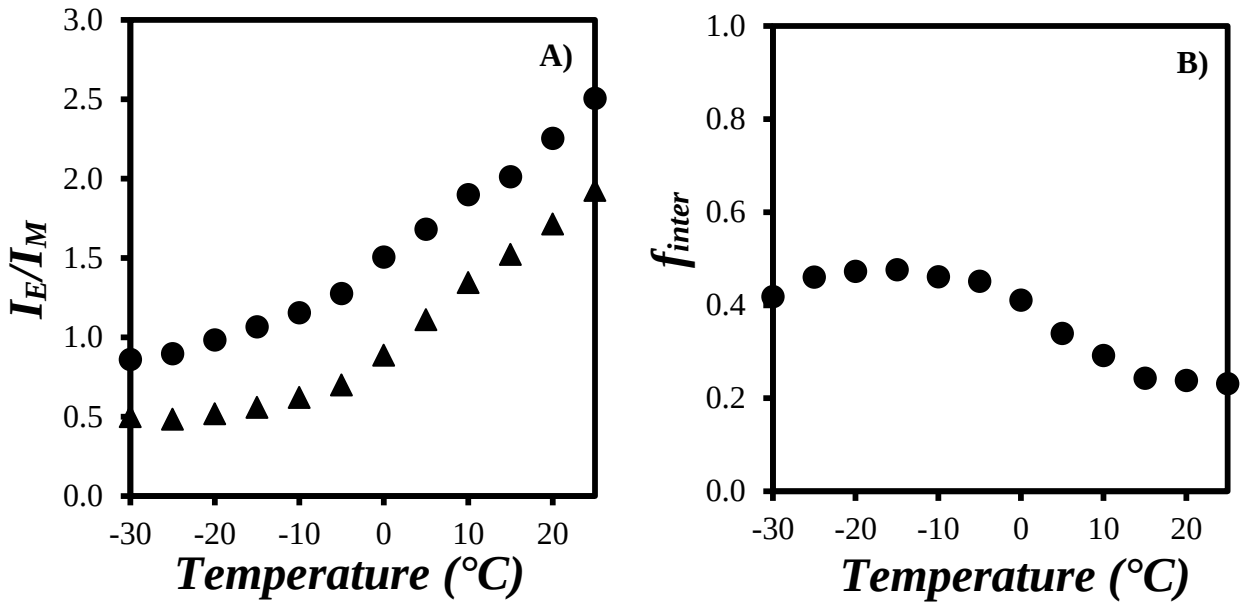

Figure 4.2. Plots of A) the I_E/I_M ratios of solutions of (●) 2 g.L^{-1} Py-PC$_{18}$MA and (▲) 0.05 g.L^{-1} Py-PC$_{18}$MA and 2 g.L^{-1} PC$_{18}$MA in octane and B) the molar fraction f_{inter} for the 2 g.L^{-1} Py-PC$_{18}$MA solution in octane as a function of temperature.

The change in spectral features observed in the fluorescence spectra was attributed to the formation of aggregates of poorly stacked pyrene labels at temperatures below the crystallization temperature of ~0 °C in octane (see f_{agg} in Table 3.4 for Py(6.7)-PC$_{18}$MA in oil). Normally, the pyrene excimer exhibits a broad and structureless emission centered at 480 nm.[3] However, it was pointed out in Chapter 2 that a high level of aggregation of poorly stacked pyrene labels generated by a pyrene-labeled polymer can result in the emission of these pyrene aggregates at lower wavelengths, as illustrated by the I_V band of the pyrene monomer at ~415 nm. Consequently, one might think that the selection of the 500-530 nm wavelength range for the integration of the excimer fluorescence to yield I_E might not best reflect the emission of these poorly stacked pyrene aggregates whose contribution is clearly seen in the I_V band in the fluorescence spectra at ~415 nm in Figure 4.1A.

However, when the entire excimer contribution was considered as in Chapter 2, where the excimer fluorescence intensity was isolated, by subtracting the monomer contribution from the fluorescence spectrum, and integrated from 420 to 530 nm, little difference was observed in the f_{inter}-vs-T profiles regardless of the wavelength range used to integrate the excimer signal. Consequently the standard procedure, consisting in integrating the fluorescence intensity of the excimer from 500 to 530 nm, was applied to calculate the f_{inter} profile presented in Figure 4.2B. The f_{inter}-versus-T profile for the 2 g.L^{-1} solution of Py(6.7)-PC$_{18}$MA in octane exhibited a transition point at 0 ± 2 ^{o}C, that marked the boundary between the two distinct regimes at temperatures below and above the crystallization temperature of Py(6.7)-PC$_{18}$MA in octane. The fraction f_{inter} equaled 0.46 ± 0.03 from −30 to −5 ^{o}C, before decreasing at 0 ^{o}C to a plateau value of 0.24 ± 0.03 in the temperature range from +10 to +25 ^{o}C.

4.5 Level of Interpolymeric Interactions (f_{inter}) of Py(6.7)-PC$_{18}$MA in the Presence of Wax in Octane

The wax that had been extracted from the Group II oil was added at a concentration of 10 g.L^{-1} to the 2 g.L^{-1} Py(6.7)-PC$_{18}$MA solution in octane. The fluorescence spectra of the solution were acquired as a function of temperature and the intensity of the monomer (I_M) at 375 nm was normalized to 100 as shown in Figure 4.3A. Two distinct temperature regimes could be identified from the change in fluorescence intensity of the I_V band, at temperatures lower and higher than the 0 °C crystallization temperature of Py(6.7)-PC$_{18}$MA in octane. The excimer emission at ~480 nm showed a continuous decrease in intensity with decreasing temperature, as a result of the increase in viscosity that took place upon lowering the solution temperature.

The transition in the I_V band of the pyrene monomer was not observed at 0 ^{o}C in Figure 4.3B for the fluorescence spectra acquired with a solution of 0.05 g.L^{-1} Py(6.7)-PC$_{18}$MA, 2 g.L^{-1}

unlabeled $PC_{18}MA$, and 10 $g.L^{-1}$ wax in octane. Instead, the fluorescence spectra normalized at 375 nm showed a continuous decrease in excimer intensity (I_E) with increasing temperature from –30 to +25 °C as usually observed for pyrene excimer formed by diffusive encounters in solution.

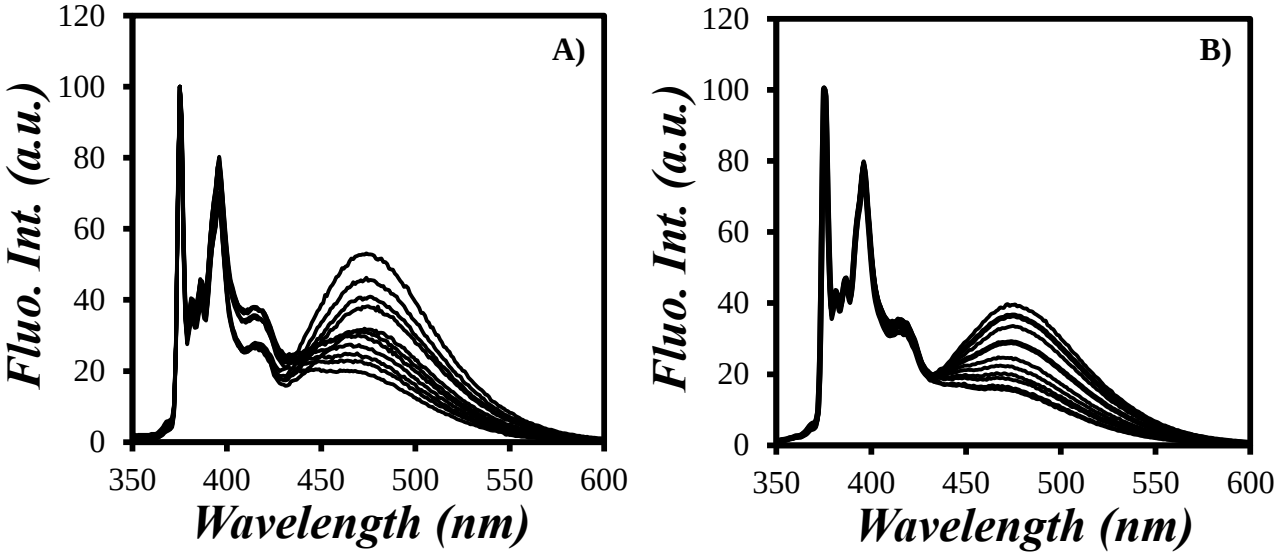

Figure 4.3. Fluorescence spectra of solutions of A) 2 $g.L^{-1}$ Py(6.7)-$PC_{18}MA$ and 10 $g.L^{-1}$ wax and B) 0.05 $g.L^{-1}$ Py(6.7)-$PC_{18}MA$, 2 $g.L^{-1}$ $PC_{18}M$ A, and 10 $g.L^{-1}$ wax in octane as a function of temperature from –30 to +25 °C.

The I_E/I_M(inter & intra) and I_E/I_M(intra) ratios were plotted as a function of temperature in Figure 4.4A. I_E/I_M(intra) took a lower value than I_E/I_M(inter & intra) for all temperatures between –30 to +25 °C, thus reflecting the increase in excimer formation due to intermolecular interactions at higher Py(6.7)-$PC_{18}MA$ concentration. The I_E/I_M ratio at both concentrations increased with increasing temperature as a result of increased excimer formation by diffusion.

The molar fraction f_{inter} obtained from the I_E/I_M(inter & intra) and I_E/I_M(intra) ratios in Figure 4.4A was plotted as a function of temperature in Figure 4.4B. The f_{inter}-vs-T profile obtained for a 2 $g.L^{-1}$ Py(6.7)-$PC_{18}MA$ solution in octane showed similar features in the presence and

absence of wax. f_{inter} increased slightly from 0.46 ± 0.03 without wax to 0.49 ± 0.03 with wax over the temperature range from −30 to −5 °C. For temperatures between +10 and +25 °C, f_{inter} showed a more substantial increase from 0.24 ± 0.03 without wax to 0.32 ± 0.03 with wax. This significant increase in f_{inter} at temperatures higher than 0 °C was attributed to the binding of Py(6.7)-PC_{18}MA onto wax that promoted their aggregation. The effect might have been less pronounced at lower temperatures, probably due to the crystallization of PC_{18}MA that led to the polymer forming polymer-polymer contacts instead of polymer-wax contacts, that were observed more prevalently at higher temperatures.[1] Interactions observed between Py(6.7)-PC_{18}MA and wax are reasonable, since PC_{18}MA was used as a PPD mimic and PAMAs used as PPDs are well-known to interact with wax in oil in order to reduce the size of the wax crystals.

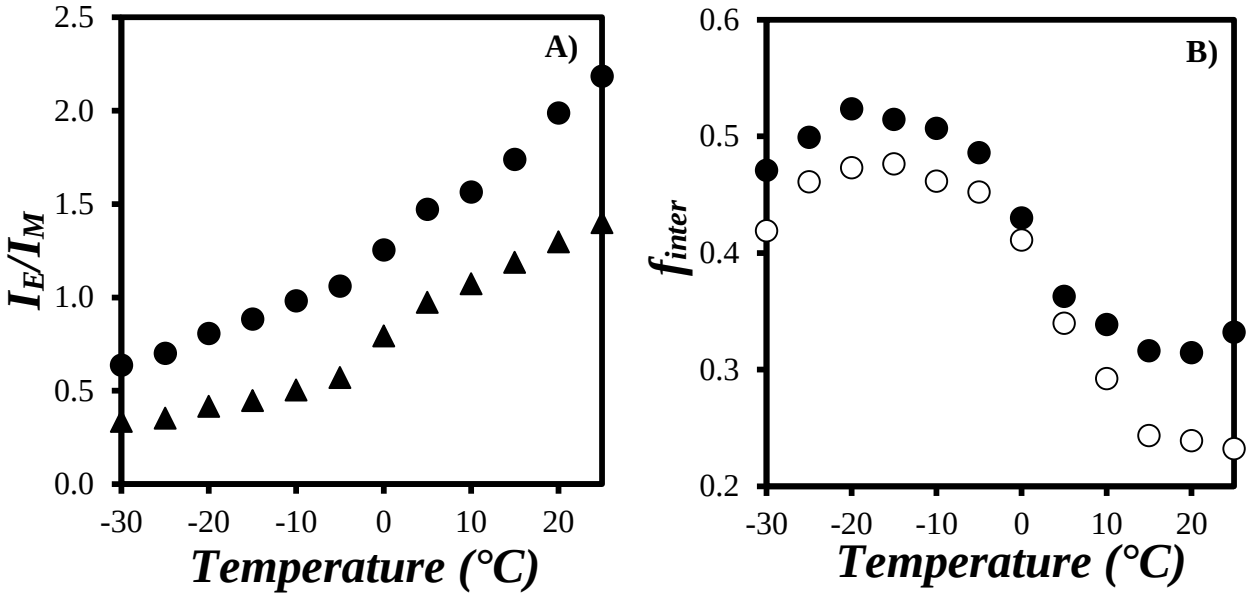

Figure 4.4. Plots of A) the I_E/I_M ratios of solutions of (●) 2 g.L^{-1} Py(6.7)-PC_{18}MA and 10 g.L^{-1} wax and (▲) 0.05 g.L^{-1} Py(6.7)-PC_{18}MA, 2 g.L^{-1} PC_{18}MA, and 10 g.L^{-1} wax and B) the molar fraction f_{inter} for 2 g.L^{-1} Py(6.7)-PC_{18}MA in the presence of 10 g.L^{-1} wax in octane as a function of temperature. (○) Data obtained for Py(6.7)-PC_{18}MA without wax.

4.6 Level of Interpolymeric Interactions of Py(6.7)-PC_{18}MA in the Presence of Wax and EP Copolymers in Octane

Having characterized the effect of wax on the interactions between Py(6.7)-PC_{18}MA chains in octane, the effect induced by the presence of EP copolymers on the interactions of Py(6.7)-PC_{18}MA was investigated. Two EP copolymers, namely the EP(AM) and EP(SM2) copolymers that were already encountered in the previous chapters, were added to a solution of 2 $g.L^{-1}$ Py(6.7)-PC_{18}MA and 10 $g.L^{-1}$ wax in octane. The the different interactions taking place in solution were monitored as a function of temperature.

4.6.1 Addition of EP(AM)

EP(AM) (10 $g.L^{-1}$) was added to a solution of 2 $g.L^{-1}$ Py(6.7)-PC_{18}MA and 10 $g.L^{-1}$ wax in octane. The fluorescence spectra for the solutions were acquired at different temperatures and for all spectra, the monomer peak at 375 nm was normalized to 100 as shown in Figure 4.5. The same two regimes were observed at temperatures lower and higher than 0 ^{o}C, which was the temperature where Py(6.7)-PC_{18}MA crystallized in octane. The distortion of the I_V band in the monomer spectra was clearly visible in all fluorescence spectra acquired between –30 and –5 ^{o}C, reflecting the presence of aggregated pyrene species that emitted at lower wavelengths. Another evidence of the existence of pyrene aggregation at low temperatures was the occurrence of a 13 nm (480 nm → 467 nm) blue shift for the excimer emission maximum as compared to the spectra in Figure 4.5C, obtained at low Py(6.7)-PC_{18}MA concentration in the presence of an excess of unlabeled PC_{18}MA, that mostly reflected excimer formation by diffusion.

A blue shift was also observed for the wavelength at the maximum of the excimer fluorescence intensity at temperatures between 0 and +25 ^{o}C (Figure 4.5B), from 480 nm for the dilute Py(6.7)-PC_{18}MA solution, where excimer formed mainly by diffusion, to 473 nm for the

concentrated Py(6.7)-PC_{18}MA solution. The blue shift found for the 2 $g.L^{-1}$ Py(6.7)-PC_{18}MA solution reflected the existence of pyrene aggregates, even in the range of temperatures above the crystallization temperature of PC_{18}MA.

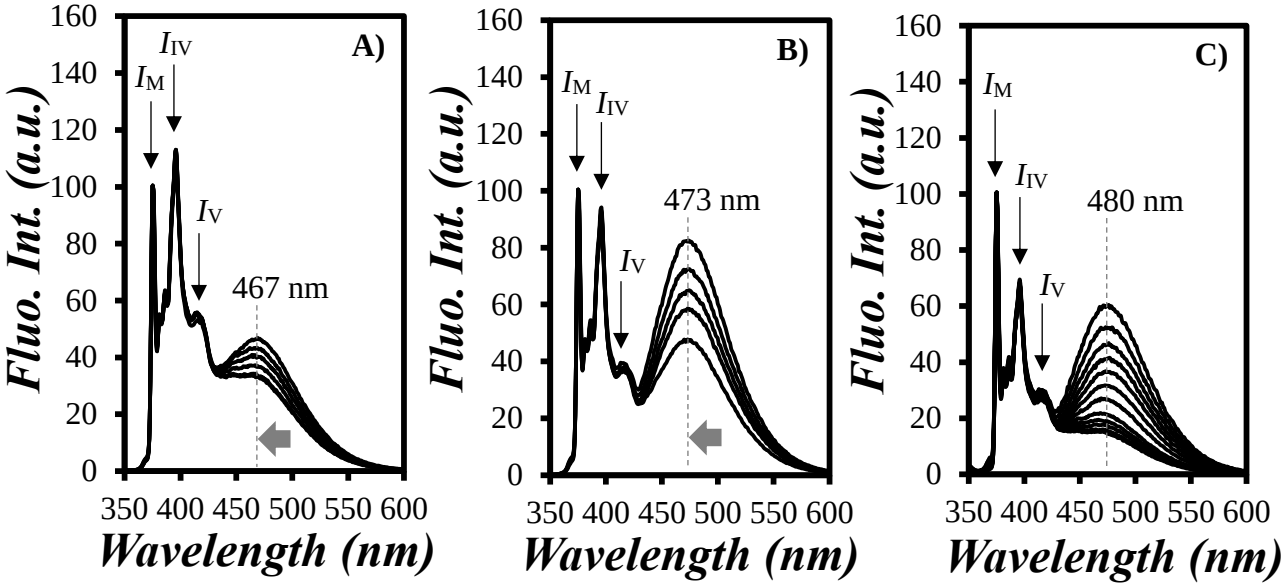

Figure 4.5. Fluorescence spectra of solutions of 2 $g.L^{-1}$ Py(6.7)-PC_{18}MA, 10 $g.L^{-1}$ EP(AM), and 10 $g.L^{-1}$ wax from A) –30 to –5 °C and B) 0 to +25 °C, and C) 0.05 $g.L^{-1}$ Py-PC_{18}MA, 2 $g.L^{-1}$ PC_{18}MA, 10 $g.L^{-1}$ EP(AM), and 10 $g.L^{-1}$ wax from –30 to +25 °C in octane.

The ratios I_E/I_M(inter & intra) and I_E/I_M(intra) were calculated from the fluorescence spectra of the solutions and plotted as a function of temperature in Figure 4.6A. They were used to calculate f_{inter}, which is plotted as a function of temperature in Figure 4.6B. f_{inter} equaled 0.57 ± 0.02 from –30 to –10 °C and exhibited a break point at ~ 0 °C, before decreasing to a constant value of 0.38 ± 0.02 between +5 and +25 °C. These f_{inter} values were substantially larger than those found without EP(AM), indicating that the presence of EP(AM) increased the intermolecular interactions between Py(6.7)-PC_{18}MA chains.

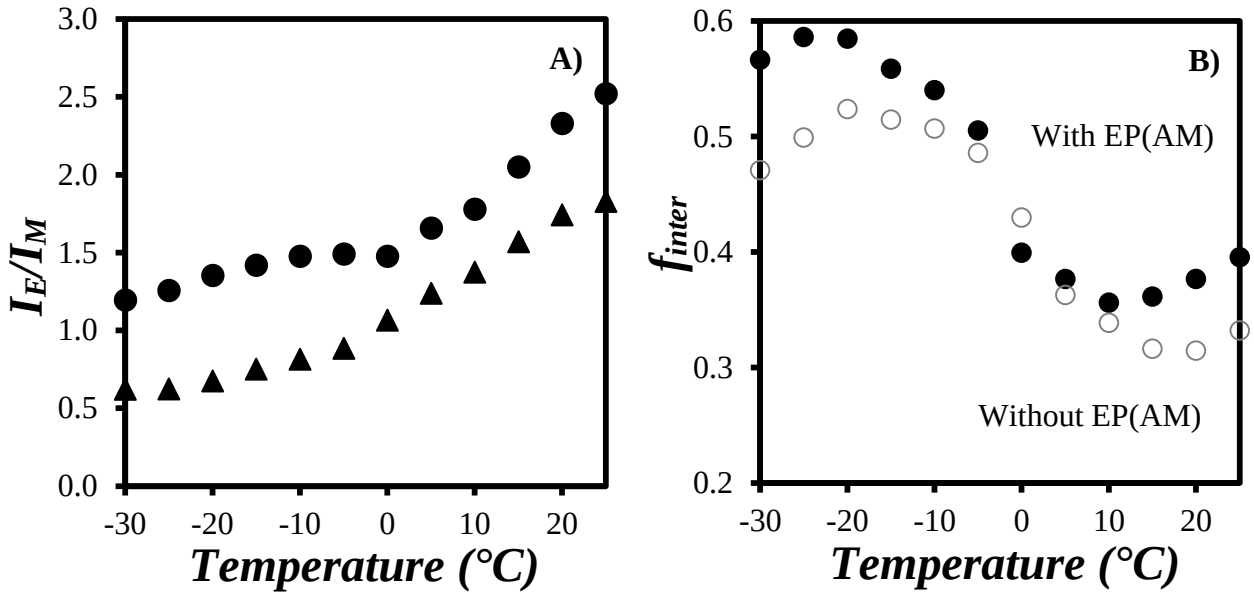

Figure 4.6. Plots of A) the I_E/I_M ratios of solutions of (●) 2 g.L^{-1} Py-PC$_{18}$MA, 10 g.L^{-1} EP(AM), and 10 g.L^{-1} wax and (▲) 0.05 g.L^{-1} Py-PC$_{18}$MA, 2 g.L^{-1} PC$_{18}$MA, 10 g. L^{-1} EP(AM), and 10 g.L^{-1} wax, and B) the molar fraction f_{inter} for 2 g.L^{-1} Py-PC$_{18}$MA in the presence of 10 g.L^{-1} EP(AM) and 10 g.L^{-1} wax as a function of temperature in octane.

4.6.2 Addition of EP(SM2)

The same experiments were also conducted with the semicrystalline EP(SM2) sample, which was added at a concentration of 10 g.L^{-1} to a solution containing 10 g.L^{-1} of wax, and either 2 g.L^{-1} Py-PC$_{18}$MA or a mixture of 0.05 g.L^{-1} of Py(6.7)-PC$_{18}$MA and 2 g.L^{-1} PC$_{18}$MA in octane. The fluorescence spectra for the solution were acquired at temperatures between –30 and +25 ^{o}C (Figure 4.7A-C). The fluorescence spectra showed the typical behavior expected for a 2 g.L^{-1} for Py(6.7)-PC$_{18}$MA solution in octane, exhibiting two different regimes at temperatures above and below the ~0 ^{o}C crystallization temperature of Py(6.7)-PC$_{18}$MA in octane. As was observed for the experiments conducted with 10 g.L^{-1} EP(AM), the presence of a similar amount of EP(SM2) copolymer significantly increased the level of aggregation of Py(6.7)-PC$_{18}$MA in octane, which

resulted in an increase in pyrene aggregation. This led to a blue shift in the excimer emission, as shown in Figure 4.7A-B, and an increase in the fluorescence intensity of the I_{IV} and I_V bands in the monomer fluorescence spectrum.

When the fluorescence of a 0.05 g.L^{-1} Py(6.7)-PC$_{18}$MA solution with a 2 g.L^{-1} excess of PC$_{18}$MA, 10 g.L^{-1} wax, and 10 g.L^{-1} EP(SM2) was studied, each Py(6.7)-PC$_{18}$MA molecule was expected to be surrounded by unlabeled PC$_{18}$MA chains, which prevented intermolecular interactions between Py(6.7)-PC$_{18}$MA macromolecules. Consequently, the corresponding fluorescence spectra shown in Figure 4.7C showed a maximum in excimer fluorescence at 480 nm, and lower I_{IV} and I_V bands that resembled those expected for 1-pyrenebutanol in octane.

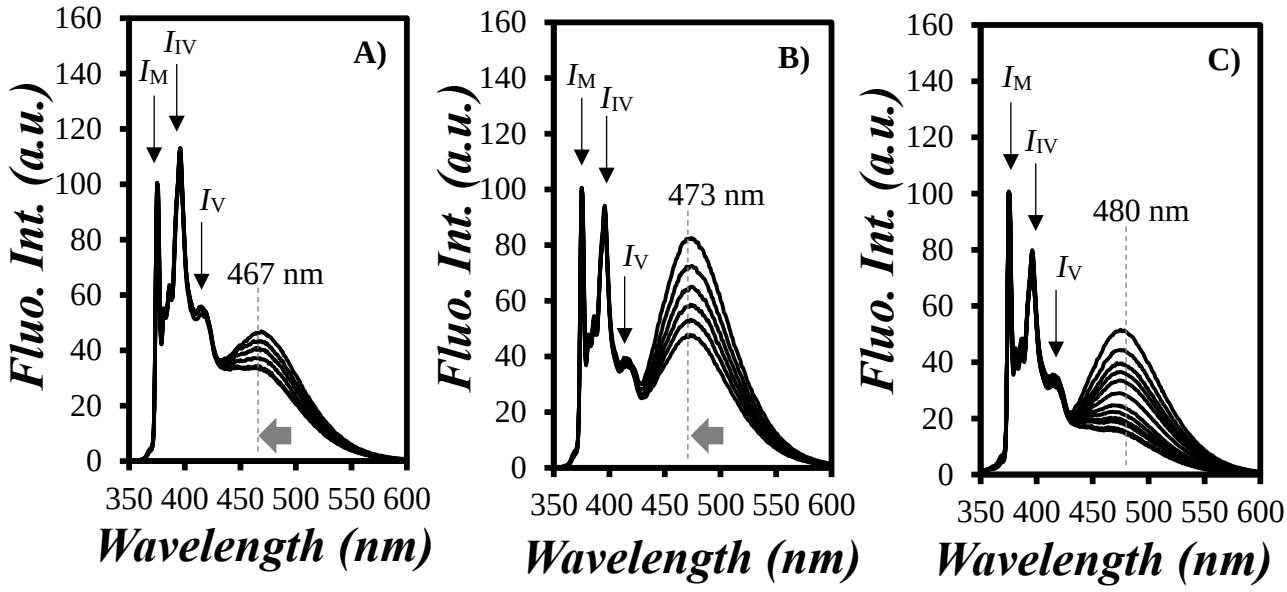

Figure 4.7. Fluorescence spectra of solutions in octane of 2 g.L^{-1} Py(6.7)-PC$_{18}$MA, 10 g.L^{-1} EP(SM2), and 10 g.L^{-1} wax from A) –30 to –5 °C and B) 0 to +25 °C, and C) 0.05 g.L^{-1} Py(6.7)-PC$_{18}$MA, 2 g.L^{-1} PC$_{18}$MA, 10 g.L^{-1} EP(SM2), and 10 g.L^{-1} wax from –30 to +25 °C.

The I_E/I_M(inter & intra) and I_E/I_M(intra) ratios were calculated from the fluorescence spectra presented in Figure 4.7A-C. They are shown in Figure 4.8A and were used to determine

f_{inter}, which was plotted as a function of temperature in Figure 4.8B. f_{inter} showed the typical features expected from a 2 g.L^{-1} Py(6.7)-PC$_{18}$MA solution in octane, with a transition at 0 °C corresponding to the crystallization of the octadecyl side chain of Py(6.7)-PC$_{18}$MA in octane.

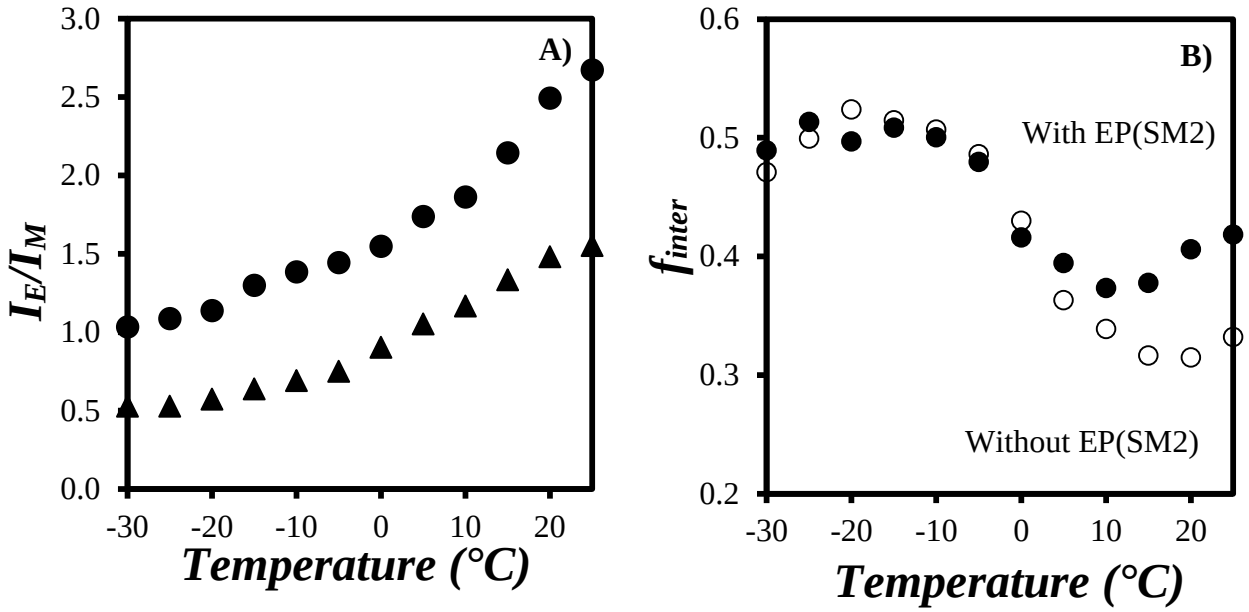

Figure 4.8. Plots of A) the I_E/I_M ratios of solutions in octane of (●) 2 g.L^{-1} Py-PC$_{18}$MA, 10 g.L^{-1} EP(SM2), and 10 g.L^{-1} wax and (▲) 0.05 g.L^{-1} Py-PC$_{18}$MA, 2 g.L^{-1} PC$_{18}$MA, 10 g.L^{-1} EP(SM2), and 10 g.L^{-1} wax and B) the molar fraction f_{inter} for 2 g.L^{-1} Py-PC$_{18}$MA in the presence of 10 g.L^{-1} EP(SM2) and 10 g.L^{-1} wax, as a function of temperature.

The f_{inter}-vs-T profiles for the 2 g.L^{-1} Py(6.7)-PC$_{18}$MA containing 10 g.L^{-1} wax and 10 g.L^{-1} of amorphous or semicrystalline EP copolymers exhibited similar features, with high and low f_{inter} values being observed below and above the 0 °C transition, respectively. The main difference in the two profiles was the f_{inter} value of 0.50 ± 0.02 obtained between –30 and –5 °C in the presence of EP(SM2), that was lower than that of 0.57 ± 0.02 found in the presence of EP(AM). Based on the trends shown in Figure 4.8B, EP(AM) led to stronger intermolecular interactions

between Py(6.7)-PC_{18}MA chains than EP(SM2) at low temperatures. This might be a consequence of the crystallization of EP(SM2) in octane, which would lead to stronger interactions between EP(SM2) polymers than between Py-PC_{18}MA and EP(SM2).

4.7 Comparison of the f_{inter} Plots of Py(6.7)-PC_{18}MA Before and After the Addition of Wax and the EP Copolymers in Octane

The f_{inter}-versus-T profiles for the 2 g.L^{-1} solutions of Py(6.7)-PC_{18}MA, in the presence and absence of wax and the EP copolymers, were compared in Figure 4.9. The addition of 10 g.L^{-1} wax to the 2 g.L^{-1} Py-PC_{18}MA solution led to an increase in f_{inter} over the entire temperature range. This increase in f_{inter} for solutions with wax was more pronounced at temperatures higher than 0 °C. This suggests that wax promoted the aggregation of Py(6.7)-PC_{18}MA in octane, which would be the behavior expected from an industrial PPD. The fact that a stronger increase in f_{inter} was observed at temperatures greater than 0 °C indicated that these interactions were stronger at temperatures above T_C, due to the melting of the microcrystals of the Py(6.7)-PC_{18}MA side chains, which seemed to promote wax–Py(6.7)-PC_{18}MA interactions.[4]

The addition of 10 g.L^{-1} EP(AM) to a solution of 2 g.L^{-1} Py(6.7)-PC_{18}MA and 10 g.L^{-1} wax led to another increase in the f_{inter} profile over the entire temperature range. This behavior suggested that EP(AM) promoted interactions between Py(6.7)-PC_{18}MA macromolecules. By contrast, the addition of a similar amount of EP(SM2) copolymer to a solution of 2 g.L^{-1} Py(6.7)-PC_{18}MA and 10 g.L^{-1} wax showed a difference in the f_{inter}-vs-T profile with respect to the solution without EP copolymer, but only in the temperature range from 0 to +25 °C. Such an observation suggests that Py(6.7)-PC_{18}MA would bind to oligoethylene sequences of the semicrystalline EP(SM2) copolymer at high temperatures. But at low temperatures, where EP(SM2) formed microcrystals,

these oligoethylene sequences previously available for the binding of Py(6.7)-$PC_{18}MA$ were now trapped in crystals and could no longer interact with Py(6.7)-$PC_{18}MA$, thus reducing f_{inter} to the value of the solution without EP(SM2).

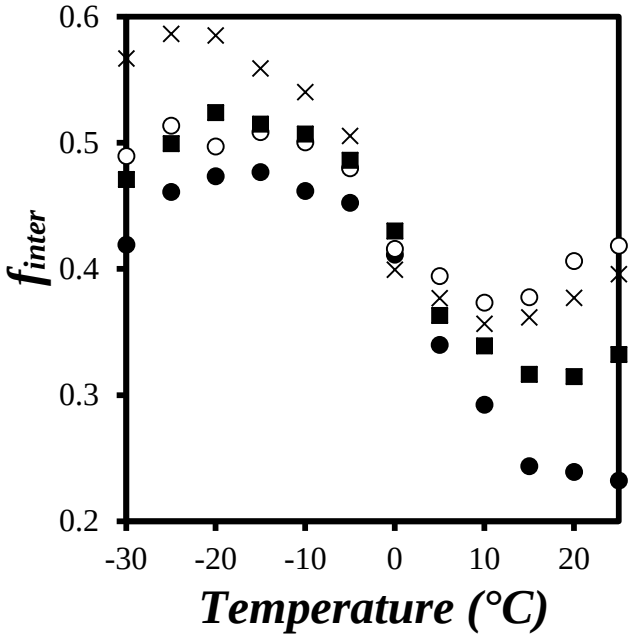

Figure 4.9. Plots for the molar fraction f_{inter} as a function of temperature for the 2 $g.L^{-1}$ Py(6.7)-$PC_{18}MA$ solution in octane (●) without wax and EP copolymers, (■) with 10 $g.L^{-1}$ wax, (×) with 10 $g.L^{-1}$ wax and 10 $g.L^{-1}$ EP(AM), and (○) with 10 $g.L^{-1}$ wax and 10 $g.L^{-1}$ EP(SM2).

The conclusions drawn from Figure 4.9 are consistent with the behavior that would be expected from industrial VIIs and PPDs, and agree with those drawn from the results obtained in oil and described earlier in Figure 3.14. Since the purpose of PPDs is to interact with the wax in engine oils, the increase in f_{inter} observed in Figure 4.9 for Py(6.7)-$PC_{18}MA$ in octane in the presence of wax was reasonable, as it suggests that this polymer interacts with wax over the entire temperature range studied. Similarly, since EP copolymers exhibit some long oligoethylene sequences similar to the long alkane chains constituting wax, the EP copolymers would be

expected to induce some interactions with PPDs, as was observed in Figure 4.9 with the increase in f_{inter} for the 2 g.L^{-1} Py(6.7)-PC$_{18}$MA and 10 g.L^{-1} wax solution upon addition of 10 g.L^{-1} EP copolymers at temperatures larger than 0 ^{o}C. At temperatures lower than 0 ^{o}C, only EP(AM) resulted in an increase in f_{inter}, as it did not crystallize and its longer oligoethylene sequences could still interact with Py(6.7)-PC$_{18}$MA. Since EP(SM2) formed microcrystals at temperatures lower than −5 ^{o}C, its longer oligoethylene sequences were no longer available to promote interactions between Py(6.7)-PC$_{18}$MA macromolecules and f_{inter} returned to its value in the absence of EP(SM2).

In summary, Py(6.7)-PC$_{18}$MA was found to interact with wax and EP(AM) at all temperatures and with EP(SM2) at temperatures above 0 ^{o}C. However, Py(6.7)-PC$_{18}$MA did not interact with EP(SM2) at temperatures lower than −5 ^{o}C, where EP(SM2) had begun forming microcrystals in octane. These conclusions are consistent with those drawn from the analysis of the f_{inter}-versus-temperature plots shown for Py(6.7)-PC$_{18}$MA in oil in Figure 3.14.

4.8 Conclusions

EP(AM) and EP(SM2) copolymers, as well as a wax sample that was extracted from an engine oil were added sequentially to a 2 g.L^{-1} solution of Py(6.7)-PC$_{18}$MA in octane, to study the effect that each of these components would have on the molar fraction f_{inter} of Py(6.7)-PC$_{18}$MA in the solution. The extent of interactions between Py(6.7)-PC$_{18}$MA macromolecules was probed by analysis of the steady-state fluorescence spectra acquired with the Py(6.7)-PC$_{18}$MA solutions. The behavior of the different Py(6.7)-PC$_{18}$MA solutions in octane was characterized by plotting the corresponding f_{inter} values as a function of temperature. The results obtained in this chapter suggested that wax also interacted with Py(6.7)-PC$_{18}$MA, used as a mimic of PPD in oil. EP(AM) and EP(SM2) copolymers were also found to promote interactions with Py(6.7)-PC$_{18}$MA in

octane, probably through binding of the octadecyl side chains for Py(6.7)-$PC_{18}MA$ to long oligoethylene sequences in the EP copolymers. Such an effect was observed over the entire temperature range investigated for the amorphous EP(AM) sample, which did not form microcrystals in the solution, whereas the crystallization of EP(SM) at low temperatures led to a reduction in the level of interactions between Py(6.7)-$PC_{18}MA$ macromolecules. These results are fully consistent with the behavior expected from VIIs and PPDs used as industrial additives in engine oils.

Chapter 5

Summary and Future Work

5.1. Summary of Thesis

Polymeric oil additives have been employed since the 1930's to improve the performance of oils used as lubricants in internal combustion engines.[1] The solution behavior of these polymeric additives, including viscosity index improvers (VIIs), pour point depressants (PPDs), and dispersants, must be properly understood to ensure that their addition to the base oil will result in a fluid that exhibits the expected lubricating properties within the intended operation time and temperature range. Ideally, each component of the oil is expected to operate optimally according to its specific purpose, the VII improving the viscosity index of the solution,[2,3] the PPD lowering the pour point of the oil,[4,5] and the dispersant stabilizing carbon-rich particulate matter in oil,[2] and do so without experiencing negative interferences from the other chemicals present in the oil. Accordingly, the goal of this thesis was to characterize the level of intermolecular interactions between poly(alkyl methacrylate)s (PAMAs) and ethylene-propylene (EP) copolymers used as mimics of PPD and VII in engine oil, respectively.

The interactions between different polymers found in engine oils were probed by fluorescently labeling one specific polymer, and monitoring how its level of intermolecular interactions, determined from the analysis of its fluorescence signal, would vary upon addition of different chemicals found in engine oils. To this end, each polymeric additive was labeled with the fluorophore pyrene to yield Py-EP and Py-PAMA. Pyrene excimer formation by the pyrene-labeled constructs was then analyzed to obtain a quantitative measure of the molar fraction (f_{inter}) of the polymeric additives that experienced intermolecular interactions in solution. f_{inter} was calculated from the I_E/I_M(inter & intra) and I_E/I_M(intra) ratios obtained from the fluorescence spectra acquired for the concentrated and dilute solutions of Py-EP and Py-PAMA, by applying Equation 1.2.[3]

In Chapter 2, two semicrystalline (EP(SM1), EP(SM2)) and one amorphous (EP(AM)) ethylene-propylene copolymers were maleated and labeled with pyrene, and their solution behavior was studied in toluene and oil. In toluene, the f_{inter} value of Py(108)-EP(AM) remained more or less constant with temperature. However, for the Py(116)-EP(SM1) and Py(100)-EP(SM2) copolymers, f_{inter} exhibited a significant increase in toluene at −5 and +5 °C, respectively, upon lowering the solution temperature from +25 to −30 °C. The increase in f_{inter} observed upon lowering the solution temperature was assigned to the increase in the local concentration of pyrene labels that took place upon the formation of microcrystals by the semicrystalline EP copolymers at the corresponding temperatures in toluene. The Py-EP copolymers exhibited a behavior in oil with respect to f_{inter} similar to that found in toluene. However, the overall f_{inter} values obtained for each Py-EP in oil was found to be larger than those obtained in toluene. This increase in f_{inter} value was certainly due in part to the presence of wax in oil, that promoted interactions between long oligoethylene sequences in the Py-EP samples, but also to the polar succinimide bonds linking the pyrene labels to the EP backbone, that led to some pyrene aggregation in oil. The overall increase in f_{inter} for Py(116)-EP(SM1) and Py(100)-EP(SM2) became less pronounced below their T_C, since the formation of microcrystals between long oligoethylene sequences in the EP copolymers were no longer available to interact with wax.

After having characterized the behavior of the amorphous and semicrystalline EP copolymers in oil using pyrene excimer fluorescence, two different PPDs were added to the solutions of Py(100)-EP(SM2) and Py(108)-EP(AM), to study how the presence of PPDs would affect the solution behavior of the EP copolymers. The similar f_{inter} profiles obtained before and after the addition of the PPDs suggested that these additives might not noticeably interact with the Py-EPs used as mimics of VIIs in oil. However, the Py-EP samples in oil showed high aggregation levels of the pyrene labels, due to interactions between the polar succinimide moieties connecting

the pyrene labels to the EP backbone. The strong level of aggregation between the pyrene labels could induce intermolecular interactions and artificially increase f_{inter} for the Py-EP samples. In turn, this could alter the conclusions drawn about the interactions between the Py-EP samples and the PPDs.

Since the fluorescence data obtained for the Py-EP samples in oil might be compromised, the problem was circumvented by studying the interactions between a poly(octadecyl methacrylate) labeled with 6.7 mol% pyrene (Py(6.7)-$PC_{18}MA$) and two EP copolymers. The ester bond connecting the pyrene label to the $PC_{18}MA$ backbone was much less polar than the succinimide bond used with the Py-EP samples, and was the same ester bond connecting each octadecyl side chain to the polymer backbone. The study of the interactions in oil between Py(6.7)-$PC_{18}MA$ and the EP copolymers, used as mimics of PPDs and VIIs, was described in the third chapter of the thesis. The procedure that was developed to determine f_{inter} for the Py-EP copolymers was applied to the Py(6.7)-$PC_{18}MA$ sample. A plot of f_{inter} for Py(6.7)-$PC_{18}MA$ showed a sharp transition between +10 and +15 ^{o}C, which was taken as evidence that the octadecyl side chains of $PC_{18}MA$ underwent crystallization in oil below +10 ^{o}C. Time-resolved fluorescence measurements also established that less than 20 % of the pyrene labels were aggregated in oil, contrary to what had been observed for the Py-EP samples where 37 to 62 % of the pyrene labels were aggregated. With such a low level of pyrene aggregation, intermolecular interactions between Py(6.7)-$PC_{18}MA$ were highly unlikely at low polymer concentration, as was established in Figure 3.8 at temperatures above +15 ^{o}C.

After having established the behavior of Py(6.7)-$PC_{18}MA$ in oil, 10 g.L^{-1} EP(AM) and EP(SM2) was added to a 2 g.L^{-1} Py(6.7)-$PC_{18}MA$ solution in oil to probe the intermolecular interactions between these two polymeric oil additives. The f_{inter} values were determined from the analysis of the fluorescence spectra of the solutions at temperatures between –30 and +25 ^{o}C. The

molar fraction f_{inter} increased upon addition of the amorphous EP(AM) sample over the entire temperature range, indicating that the presence of EP(AM) in the oil induced stronger intermolecular interactions between Py(6.7)-PC_{18}MA macromolecules. The binding of Py(6.7)-PC_{18}MA onto the EP copolymers was believed to be promoted by long oligoethylene stretches along the EP copolymers. The addition of EP(SM2) also led to an increase in f_{inter} for Py(6.7)-PC_{18}MA at temperatures above +15 ^{o}C in oil. But at temperatures lower than –5 ^{o}C, where EP(SM2) had finished crystallizing, f_{inter} for Py(6.7)-PC_{18}MA in the presence of EP(SM2) matched the f_{inter} value without EP(SM2). This result suggested that crystallization of EP(SM2) led to the release of the Py(6.7)-PC_{18}MA macromolecules into the solution, where they experienced the same level of intermolecular interactions as if EP(SM2) were not present.

Since engine oil is always laced with a small amount of wax to adjust the oil viscosity, the fluorescence experiments with Py(6.7)-PC_{18}MA and the EP copolymers were repeated in octane, a wax-free solvent, to which wax could be purposely added to assess its effect on the level of intermolecular interactions between Py(6.7)-PC_{18}MA and the EP copolymers. The molar fraction f_{inter} was determined for Py(6.7)-PC_{18}MA in the presence or absence of wax, EP(AM) and EP(SM2), and the results of this study were reported in Chapter 4. After having established that Py(6.7)-PC_{18}MA underwent crystallization at 0 ^{o}C in octane, 10 g.L^{-1} wax was added to a 2 g.L^{-1} Py(6.7)-PC_{18}MA solution in octane. The polymer underwent crystallization at the same temperature, but f_{inter} for the Py(6.7)-PC_{18}MA solution in octane with wax took substantially larger values over the entire temperature range between –30 and +25 ^{o}C as compared to the solution without wax. This led to the conclusion that wax promoted interactions between Py(6.7)-PC_{18}MA macromolecules, as would be expected from a PPD mimic. Indeed, PPDs are known to control the crystallization of wax by reducing the size of wax crystals through wax-PPD interactions, thus extending the low temperature range where the oil can flow. The fact that Py(6.7)-PC_{18}MA

interacted with engine wax in octane over the entire temperature range studied demonstrated that this macromolecule could be viewed as a representative PPD mimic.

The intermolecular interactions of Py(6.7)-PC_{18}MA and EP(AM) and EP(SM2) were then investigated in the presence of 10 $g.L^{-1}$ wax in octane. EP(AM) was found to increase the intermolecular interactions between Py(6.7)-PC_{18}MA macromolecules between –30 and +25 ^{o}C as compared to the Py(6.7)-PC_{18}MA solution with 10 $g.L^{-1}$ wax and without EP(AM). These interactions must have been promoted by the long oligoethylene stretches found in EP(AM). The molar fraction f_{inter} of Py(6.7)-PC_{18}MA experienced a similar increase in the presence of 10 $g.L^{-1}$ EP(SM2), as was observed with EP(AM) at temperatures above +10 ^{o}C. At temperatures lower than –5 ^{o}C, where EP(SM2) had crystallized in octane, Py(6.7)-PC_{18}MA was released into the octane solvent where it yielded an f_{inter} value that was similar to that obtained with wax and without EP copolymers. The enhancement in intermolecular interactions observed for Py(6.7)-PC_{18}MA in the presence of EP(AM) at all temperatures and EP(SM2) at temperature above +10 ^{o}C was consistent with the trends presented in Chapter 3 for Py(6.7)-PC_{18}MA in oil.

Perhaps the most unexpected result obtained with the f_{inter}-versus-temperature plots was that the crystallization of EP(SM2) led to the release of the Py(6.7)-PC_{18}MA macromolecules into the solution while the crystallization of the octadecyl side chains of Py(6.7)-PC_{18}MA did not release EP(AM) into the solution. This must be a consequence of differences in oligoethylene sequence lengths. EP(SM2) being a semicrystalline EP copolymer, it was expected to present longer oligoethylene sequences that would promote strong interactions between EP(SM2) copolymers, whose crystallization would induce the dissociation of the Py(6.7)-PC_{18}MA macromolecules from EP(SM2). By contrast, EP(AM) being an amorphous EP copolymer, it must exhibit a wider variety of oligoethylene sequences, many of which might be chemically compatible

with those of Py(6.7)-$PC_{18}MA$, thus leading to stronger intermolecular interactions that were not compromised by the crystallization of $PC_{18}MA$ in neither engine oil nor octane.

In summary, in this thesis pyrene excimer fluorescence was used to probe the interactions of important polymeric oil additives. It has expanded the scope of recent studies done by Pirouz et al. in toluene, used as an apolar mimic for oil,[3,4] by generalizing this novel analytical method to multicomponent systems. Such a study was accomplished by probing the intermolecular interactions between wax and mimics of VIIs and PPDs in the presence of each other, in engine oil and in octane. This thesis further supports the statement made earlier[3,4] that plots of f_{inter}-versus-T obtained from fluorescence measurements can be used confidently to measure the level of intermolecular interactions between different additives found in motor oil.

5.2 Future Work

VIIs, PPDs, dispersants, antioxidants, antiwears, and wax are some of the main components of the engine oils. In Chapters 2 – 4, the molar fraction f_{inter} between VIIs, PPDs, and wax was determined in oil and octane by the means of pyrene excimer formation. Therefore, the determination of f_{inter} in the presence of the remaining additives found in oils, notably dispersants, should be investigated in oil and octane. Additionally, most of the f_{inter} measurements for the VIIs and PPDs were conducted for temperatures ranging between −30 and +25 ^{o}C in oil. It would be interesting to repeat the fluorescence measurements at higher temperatures, that are more representative of the conditions found during the operation of an engine.

Supporting Information

Chapter 2

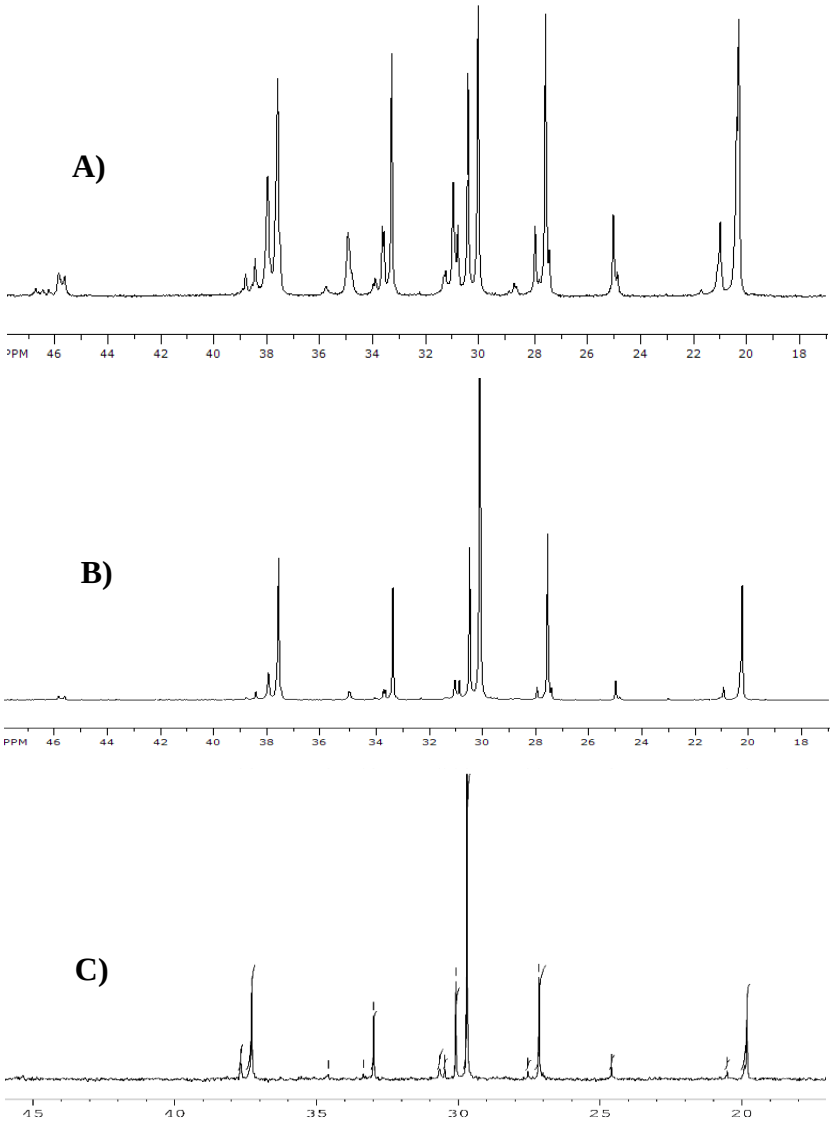

Figure S2.1. ^{13}C NMR spectrum for A) Py(108)-EP(AM)[1], B) Py(116)-EP(SM1)[1], and C) Py(100)-EP(SM2) in TCE−d_2.

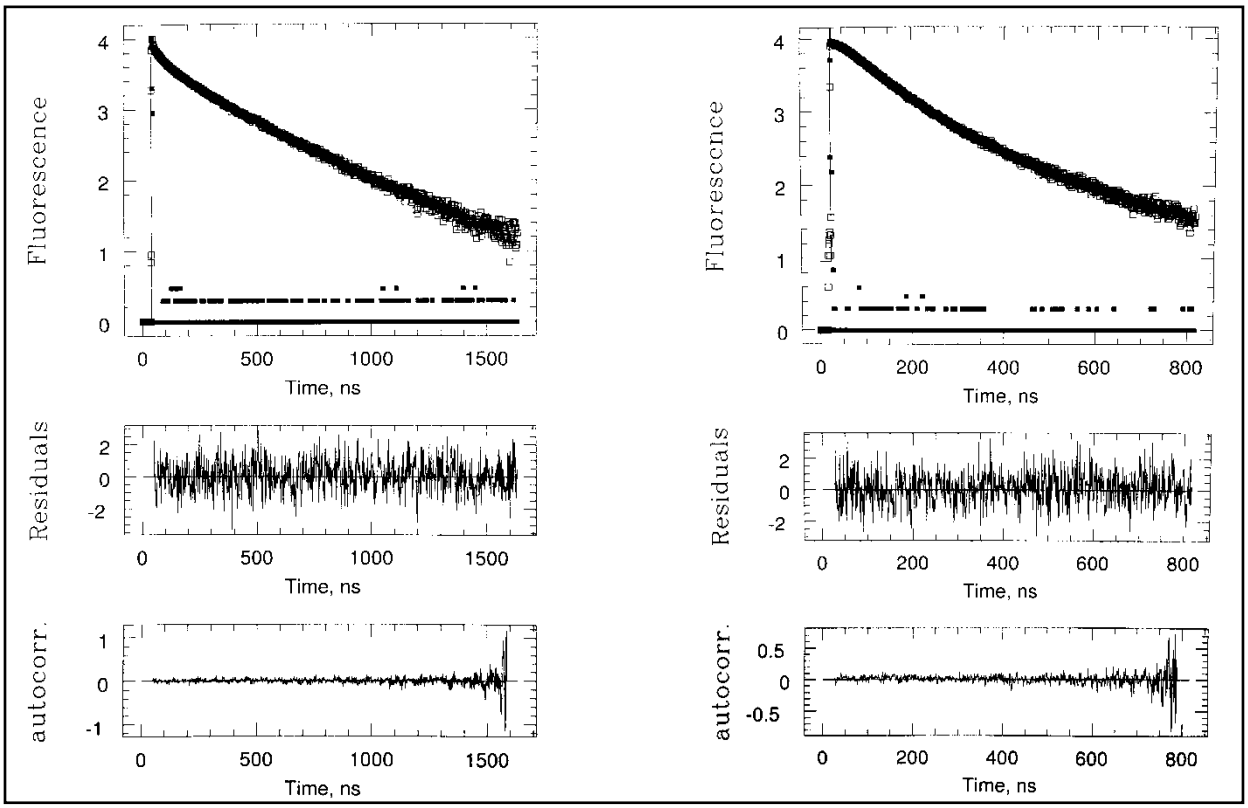

Figure S2.2. Monomer (left: λ_{ex} = 344 nm, λ_{em} = 375 nm; TPC = 2.04 ns/ch) and excimer (right; λ_{ex} = 344 nm, λ_{em} = 510 nm; TPC = 1.02 ns/ch) fluorescence decays for Py(108)-EP(AM) at +25 °C in toluene fitted according to the model free analysis (MFA).

Table S2.1. Pre-exponential factors and decay times retrieved from the MFA of the fluorescence decays acquired with the solutions of Py-EP samples (λ_{ex} = 344 nm, λ_{em} = 375 νμ, and $C_{Py\text{-}EP}$ = 10 g/L).

Sol.	Sample	a_{M1}	τ_1(ns)	a_{M2}	τ_2(ns)	a_{M3}	τ_3(ns)	a_M	τ_M(ns)	χ^2
toluene	Py(108)-EP(AM)	0.242	8.314	0.245	30.02	0.271	84.54	0.242	210	1.10
	Py(116)-EP(SM1)	0.309	14.590	0.166	38.59	0.266	89.60	0.259	210	1.07
	Py(100)-EP(SM2)	0.284	9.556	0.340	43.52	0.290	119.85	0.086	206	1.22
oil	Py(108)-EP(AM)	0.265	19.600	0.332	92.23	0.260	247.77	0.142	300	1.15
	Py(116)-EP(SM1)	0.356	26.775	0.220	105.81	0.228	197.06	0.196	302	1.29
	Py(100)-EP(SM2)	0.259	20.319	0.301	92.05	0.367	253.03	0.073	305	1.29

Table S2.1. (Continued) Pre-exponential factors and decay times retrieved from the MFA of the fluorescence decays acquired with the solutions of Py-EP samples (λ_{ex} = 344 nm, λ_{em} = 375 νμ, and $C_{Py\text{-}EP}$ = 10 g/L).

Sol.	Sample	f_{Ediff}	f_{EE0}	τ_{E0}	f_{ED}	τ_D
toluene	Py(108)-EP(AM)	0.711	0.199	48.62	0.089	129.45
	Py(116)-EP(SM1)	0.579	0.344	52.15	0.078	139.53
	Py(100)-EP(SM2)	0.615	0.297	48.94	0.087	121.78
oil	Py(108)-EP(AM)	0.469	0.455	61.18	0.076	186.53
	Py(116)-EP(SM1)	0.392	0.481	65.71	0.127	192.25
	Py(100)-EP(SM2)	0.344	0.559	64.28	0.097	183.56

Sol.	Sample	f_{diff}	f_{free}	f_{E0}	f_D	f_{agg}	$\langle\tau\rangle$	$\langle k\rangle$ (10^6 s^{-1})
toluene	Py(108)-EP(AM)	0.580	0.185	0.162	0.073	0.235	0.019	18.7
	Py(116)-EP(SM1)	0.481	0.168	0.286	0.065	0.351	0.017	16.6
	Py(100)-EP(SM2)	0.582	0.055	0.083	0.281	0.364	0.013	12.6
oil	Py(108)-EP(AM)	0.435	0.072	0.423	0.071	0.493	0.005	5.2
	Py(116)-EP(SM1)	0.358	0.087	0.439	0.116	0.555	0.007	6.9
	Py(100)-EP(SM2)	0.335	0.027	0.094	0.544	0.639	0.004	4.1

References

1. Pirouz, S.; Duhamel, J.; Jiang, S.; Duggal, A. Quantifying the Level of Intermacromolecular Interactions by Using Pyrene Excimer Formation, *Macromolecules* **2015**, *48*, 4620–4630.

Chapter 3

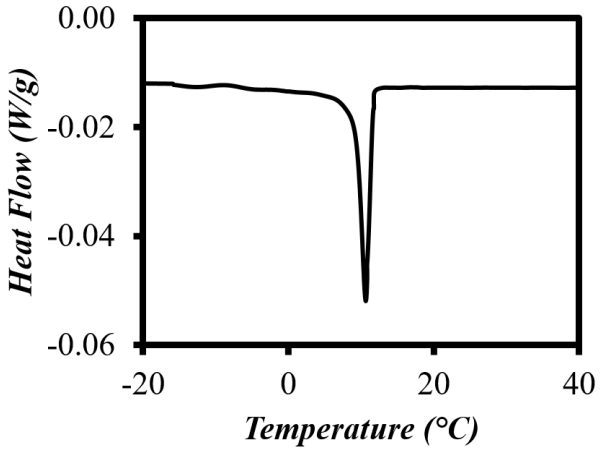

Figure S3.1. DSC trace $PC_{18}MA$ in the naked form in group II oil ([polymer] = 10 $g.L^{-1}$).

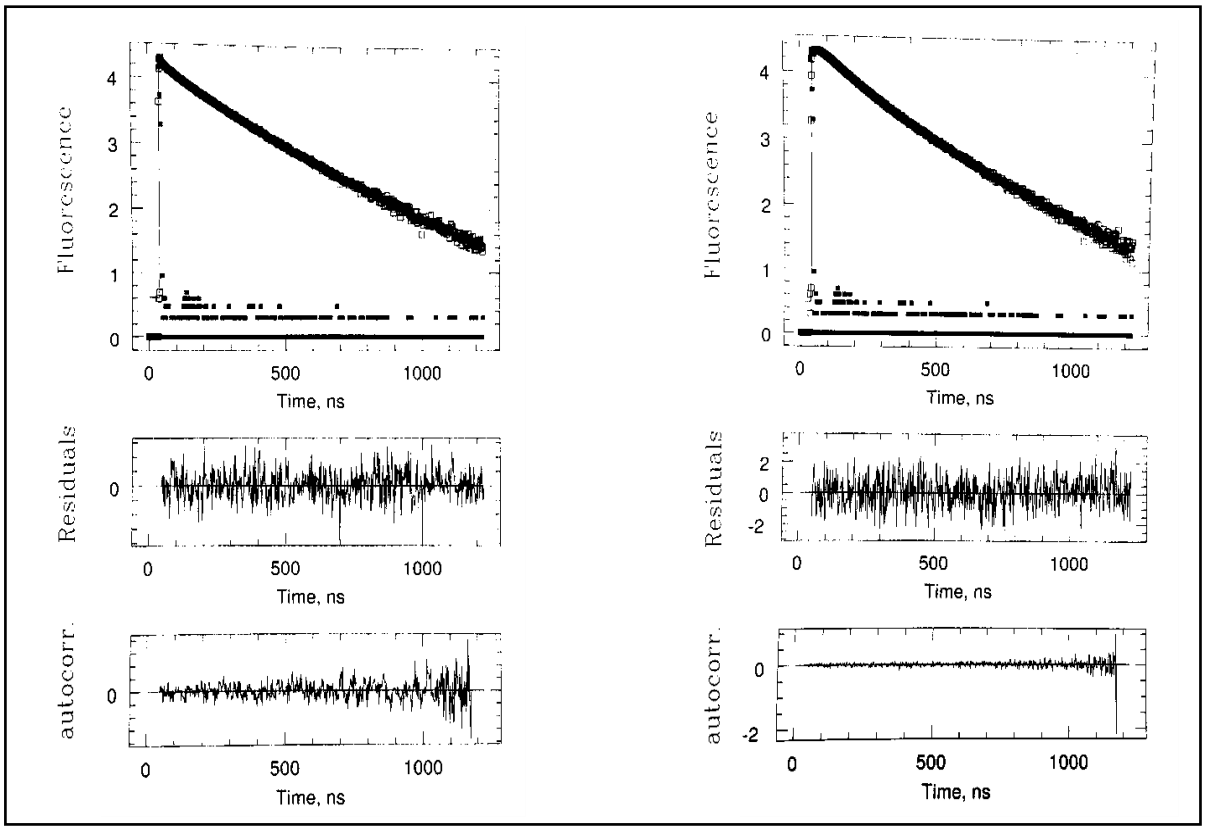

Figure S3.2. Monomer (left: λ_{ex} = 344 nm, λ_{em} = 375 nm; TPC = 2.04 ns/ch) and excimer (right; λ_{ex} = 344 nm, λ_{em} = 510 nm; TPC = 2.04 ns/ch) fluorescence decays of Py(6.7)-$PC_{18}MA$ at –30 °C in oil fitted according to the model free analysis (MFA).

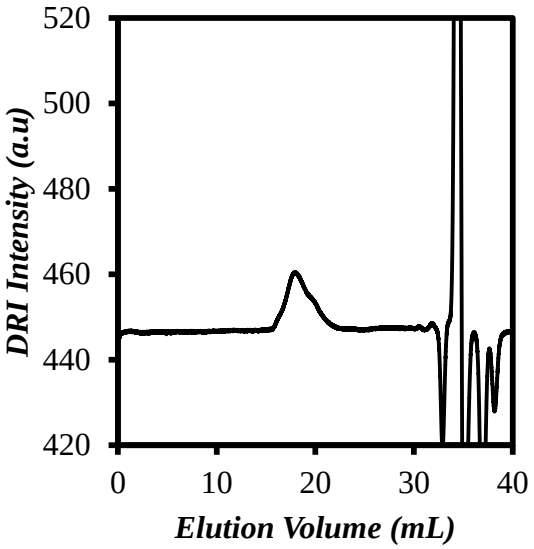

Figure S3.3. GPC trace of $PC_{18}MA$ (dn/dc = 0.071 ml/g^1)

Table S3.1. Pre-exponential factors and decay times retrieved from the MFA of the fluorescence decays acquired with the Py(6.7)-$PC_{18}MA$ in in oil. (λ_{ex} = 344 nm, λ_{em} = 375 νμ, and $C_{Py(6.7)\text{-}PC18MA}$ = 2 g/L)

T (°C)	a_{M1}	τ_1(ns)	a_{M2}	τ_2(ns)	a_{M3}	τ_3(ns)	a_M	τ_M(ns)	χ^2
25	0.100	13.214	0.275	68.484	0.512	172.896	0.113	220	1.16
-30	0.129	15.228	0.262	77.184	0.533	170.054	0.077	236	1.12
-25	0.118	11.462	0.275	68.285	0.536	168.257	0.072	236	1.04
-20	0.127	15.126	0.329	82.648	0.514	180.974	0.030	232	1.02
-15	0.114	11.933	0.266	66.770	0.545	164.334	0.075	230	1.07
-10	0.126	14.701	0.287	71.459	0.521	166.632	0.066	225	1.05
-5	0.146	13.852	0.257	69.593	0.483	151.647	0.114	216	1.03
0	0.136	12.410	0.289	67.184	0.519	155.197	0.056	227	1.12
5	0.129	11.187	0.327	65.372	0.502	153.05	0.043	223	1.01
10	0.140	12.355	0.278	62.711	0.500	143.140	0.082	222	1.03
15	0.125	13.147	0.240	70.333	0.452	173.751	0.183	221	1.06
20	0.123	12.066	0.219	62.948	0.441	158.375	0.216	221	1.05
25	0.123	11.790	0.257	64.089	0.472	161.508	0.147	220	1.026

Table S3.1. (Continued) Pre-exponential factors and decay times retrieved from the MFA of the fluorescence decays acquired with the Py(6.7)-PC_{18}MA in in oil. (λ_{ex} = 344 nm, λ_{em} = 375 νμ, and $C_{Py(6.7)\text{-}PC18MA}$ = 2 g/L)

T (°C)	f_{Ediff}	f_{EE0}	τ_{E0}	f_{ED}	τ_{D}
25	0.839	0.096	46.416	0.065	151.138
-30	0.798	0.108	51.014	0.094	182.290
-25	0.820	0.081	48.127	0.099	176.902
-20	0.817	0.093	50.140	0.090	178.512
-15	0.826	0.073	49.317	0.101	171.022
-10	0.823	0.072	49.387	0.105	168.203
-5	0.810	0.078	52.537	0.112	167.451
0	0.823	0.075	50.620	0.102	163.404
5	0.835	0.039	45.736	0.125	148.933
10	0.823	0.087	50.505	0.089	155.998
15	0.840	0.101	51.240	0.059	159.563
20	0.826	0.121	53.973	0.053	159.620
25	0.850	0.083	49.051	0.066	144.257

T (°C)	f_{diff}	f_{free}	f_{E0}	f_{D}	f_{agg}	<τ>	<k> (10^6 s^{-1})
25	0.748	0.063	0.101	0.088	0.189	122.2084	3.9
-30	0.771	0.060	0.077	0.093	0.169	118.8279	4.2
-25	0.797	0.025	0.091	0.088	0.178	125.9044	3.6
-20	0.774	0.063	0.068	0.095	0.163	117.5547	4.2
-15	0.778	0.055	0.068	0.099	0.168	116.8824	4.1
-10	0.734	0.094	0.070	0.102	0.172	105.1214	4.9
-5	0.784	0.047	0.072	0.097	0.169	107.6946	4.9
0	0.805	0.036	0.038	0.121	0.159	104.0167	5.1
5	0.767	0.068	0.081	0.083	0.164	98.86837	5.6
10	0.707	0.158	0.085	0.050	0.135	118.8433	3.9
15	0.673	0.186	0.099	0.043	0.141	108.7323	4.7
20	0.741	0.128	0.072	0.058	0.130	110.5125	4.5
25	0.758	0.096	0.086	0.059	0.145	122.5498	3.6

References

Chapter 1

1. Salino, P., Volpi, P. *Ann. Chim*. **1987**, *77*, 145-165.
2. Pawlak, Z. In *Tribochemistry of lubricating oils;* Elsevier: Warsaw, 2003; Vol. 45.
3. M. C. G. Fernandes, Power Loss in Rolling Bearings and Gears Lubricated with Wind Turbine Gear Oils. PhD thesis, **2015**, 217-218.
4. Pirouz, S.; Duhamel, J.; Jiang, S.; Duggal, A. Quantifying the Level of Intermacromolecular Interactions by Using Pyrene Excimer Formation, *Macromolecules* **2015**, *48*, 4620–4630.
5. Smeeth, M.; Spikes, H.; Gunsel, S. Boundary Film Formation by Viscosity Index Improvers. *Tribol. Trans.* **1996**, *39*, 726-734.
6. Ver Strate, G.; Wilchinsky, Z. W. Ethylene-Propylene Copolymers: Degree of Crystallinity and Composition. *J. Polym. Sci. A* **1971**, *9*, 127-141.
7. Nassar, A. M.; Ahmed, N. S.; Kamal, R. S.; Abdel Azim, A. A.; El-Nagdy, E. Preparation and Evaluation of Acrylate Polymers as Viscosity Index Improvers for Lube Oil. *Petrol. Sci. Tech.* **2005**, *23*, 537-546.
8. Tanveer, S.; Prasad, R. Enhancement of Viscosity Index of Mineral Base Oils. *Indian J. Chem. Technol.* **2006**, *13*, 398-403.
9. Simon, A. M.; Herbert, F. X-ray Fluorescence Detection of Waste Engine Oil Residue in Asphalt and its Effect on Cracking in Service. *Int. J. Pav. Eng.* **2010**, *11*, 541-553.
10. Castro, L. V.; Vazquez, F. Copolymers as Flow Improvers for Mexican Crude Oils. *Energy Fuel.* **2008**, *22*, 4006-4011.

11. Horne, W. V. Polymethacrylates as Viscosity Index Improvers and Pour Point Depressants. *Ind. Eng. Chem.* **1949**, *41*, 952-959.

12. Naga, H. H.; Azim, W. M.; Ahmed, M. M. Polymeric Additives for Pour Point Depression of Residual Fuel Oils. *J. Chem. Tech. Bio.* **1985**, *35*, 241-247.

13. Rudnick, L. R, *Lubricant Additives Chemistry and Applications* (2nd Ed.), 2009, pp 346-347.

14. Lakowicz, J. R. *Principles of Fluorescence Spectroscopy*. 3rd ed.; Springer: New York, 2006, 3-15.

15. Sippel, T. O. Microfluorometric Analysis of Protein Thiol Groups with a Coumarinylphenylmaleimide. *J. Histochem. Cytochem.* **1981**, *29*, 1377-1381.

16. Duhamel, J. Polymer Chain Dynamics in Solution Probed with a Fluorescence Blob Model. *Acc. Chem. Res.* **2006**, *39*, 953-960.

17. Zhang, M.; Duhamel, J. Study of the Microcrystallization of Ethylene-Propylene Random Copolymers in Solution by Fluorescence. *Macromolecules* **2007**, *40*, 661-669.

18. Farhangi, S.; Weiss, H.; Duhamel; J. Effect of Side-Chain Length on the Polymer Chain Dynamics of Poly(alkyl methacrylate)s in Solution. *Macromolecules* **2013**, *24*, 9738-9747.

19. Duhamel, J. New Insights in the Study of Pyrene Excimer Fluorescence to Characterize Macromolecules and their Supramolecular Assemblies in Solution. *Langmuir* **2012**, 28, 6527-6538.

20. Birks, J. B. *Photophysics of Aromatic Molecules*; Wiley: New York, 1970; p 301.

21. Siu, H.; Duhamel, J. Comparison of the Association Level of a Hydrophobically Modified Associative Polymer Obtained from an Analysis Based on Two Different Models. *J. Phys. Chem. B* **2005**, *109*, 1770−1780.

22. Pirouz, S.; Duhamel, J.; Jiang Sh.; Duggal, A. Using Pyrene Excimer Fluorescence To Probe the Interactions between Viscosity Index Improvers and Waxes Present in Automotive Oil. *Macromolecules* **2017**, *50*, 2467–2476.

Chapter 2

1. Pirouz, S.; Duhamel, J.; Jiang, S.; Duggal, A. Quantifying the Level of Intermacromolecular Between EP Copolymer Interactions by Using Pyrene Excimer Formation. *Macromolecules* **2015**, *48*, 4620-4630.
2. Pawlak, Z. *Tribochemistry of Lubricating Oils*; Elsevier: Warsaw, 2003; Vol. 45.
3. Pirouz, S.; Duhamel, J. New approaches to characterize polymeric oil additives in solution based on pyrene excimer fluorescence. *J. Polym. Sci. B: Polym. Phys.* **2017**, *55*, 7-18.
4. Horowitz, H. Predicting Effects of Temperature and Shear Rate on Viscosity of Viscosity Index–Improved Lubricants. *Ind. Eng. Chem*. **1958**, *50*, 1089-1094.
5. Fang, L.; Zhang, X.; Ma, J.; Zhang, B. Investigation into a Pour Point Depressant for Shengli Crude Oil. *Ind. Eng. Chem. Res*. **2012**, *51*, 11605-11612.
6. Sen, A.; Rubin, I. D. Molecular Structures and Solution Viscosities of Ethylene-Propylene Copolymers. *Macromolecules* **1990**, *23*, 2519-2524.
7. Mihaljuš S. V.; Podobnik, M.; Bambić, J. Engine Oil Viscosity Index Improver Behaviour at Extended Shear Stability. *Fuels Lubr.* **2008**, *47*, 118-128.
8. Port, W. S.; O'Brien, J. W.; Hansen, J. E.; Swern, D. Viscosity Index Improvers for Lubricating Oils. Polyvinyl Esters of Long-Chain Fatty Acids. *Ind. & Eng. Chem.* **1951**, *43*, 2105-2107.

9. Nassar, A. M.; Ahmed, N. S.; Kamal, R. S.; Abdel Azim, A. A.; El-Nagdy, E. Preparation and Evaluation of Acrylate Polymers as Viscosity Index Improvers for Lube Oil. *Petrol. Sci. Tech.* **2005**, *23*, 537-546.

10. Mortier, R. M.; Malcolm, F. F.; Orszulik, S. T. In *Chemistry and Technology of Lubricants;* Springer: London, 2009.

11. Zhang, M.; Duhamel, J.; Van Duin, M.; Meessen, P. Characterization by Fluorescence of the Distribution of Maleic Anhydride Grafted Onto Ethylene-Propylene Copolymers. *Macromolecules* **2004**, *37*, 1877-1890.

12. Zhang, M.; Duhamel, J. Effect of Solvent Quality toward the Association of Succinimide Pendants of a Modified Ethylene-Propylene Copolymer in Mixtures of Toluene and Hexane. *Macromolecules* **2005**, *38*, 4438-4446.

13. Nemeth, S.; Jao, T.-C.; Fendler, J. H. Excimer Formation in 1-Pyrenyl-Methane-Amine *Photochem. Photobiol. A: Chem.* **1994**, *78*, 22-235.

14. Zhang, M.; Duhamel, J. Study of Maleated Ethylene-Propylene Copolymers by Fluorescence: Evidence for Succinimide Induced Polar Associations in an Apolar Solvent. *Eur. Polym. J.* **2008**, *44*, 3005-3014.

15. Randall, J. C. A Review of High Resolution Liquid 13Carbon Nuclear Magnetic Resonance Characterizations of Ethylene-Based Polymers. *J. Macro. Sci. Rev. Macr. Chem. Phys.* **1989**, *C29*, 201-317.

16. Wanga, K.; Hua, Y.; Yang, W.; Shi, Y.; Li, Y., Solubilities of Succinimide in Different Pure Solvents and Binary Methanol + Ethyl Acetate Solvent Mixtures, *Thermochim. Acta* **2012**, *538*, 79–85.

17. Sen, A.; Rubin, I. D. Molecular Structures and Solution Viscosities of Ethylene-Propylene Copolymers. *Macromolecules* **1990**, *23*, 2519-2524.
18. Birks, J. B.; Dyson, D. J.; Munro, I. H. Excimer Fluorescence. II. Lifetime Studies of Pyrene Solutions. *Proc. Royal Soc. Series A, Math. Phys. Sci.* **1963**, *275*, 575-588.
19. Duhamel, J. Global Analysis of Fluorescence Decays to Probe the Internal Dynamics of Fluorescently Labeled Macromolecules. *Langmuir* **2014**, *30*, 2307-2324.
20. Nemeth, S.; Jao, T.-C.; Fendler, J. H. Concentration- and Solvent-Dependent Excimer Formation of 1-Pyrenemethylamine Covalently Attached to Maleic Anhydride-Grafted Ethylene-Propylene Copolymers. *Macromolecules* **1994**, *27*, 5449-5456.
21. Pirouz, S.; Duhamel, J.; Jiang Sh.; Duggal, A. Using Pyrene Excimer Fluorescence To Probe the Interactions between Viscosity Index Improvers and Waxes Present in Automotive Oil, *Macromolecules* **2017**, *50*, 2467–2476.
22. Nakajima, A. Fluorescence Spectra of Pyrene in Chlorinated Aromatic Solvents. *J. Lumin.* **1976**, *11*, 429-432.

Chapter 3

1. RohMax Publication RM-96 1202. *Pour Point Depressants, A Treatise on Performance and Selection*, Horsham, PA, 1996, pp 1-11.
2. M. C. G. Fernandes, Power Loss in Rolling Bearings and Gears Lubricated with Wind Turbine Gear Oils. PhD thesis, **2015**, 217-218.
3. Kinker, B.G. Polymethacrylate viscosity modifiers, in *Lubricant Additives Chemistry and Application*, (ed. Rudnick L.R), Marcel Dekker Inc., New York, **2003**, 329-353.
4. Sen, A.; Rubin, I. D. Molecular Structures and Solution Viscosities of Ethylene-Propylene Copolymers. *Macromolecules* **1990**, *23*, 2519-2524.

5. Mihaljuš S. V.; Podobnik, M.; Bambić, J. Engine Oil Viscosity Index Improver Behavior at Extended Shear Stability. *Fuels Lubr.* **2008**, *47*, 118-128.

6. Pirouz, S.; Duhamel, J.; Jiang, S.; Duggal, A. Quantifying the Level of Intermacromolecular Between EP Copolymer Interactions by Using Pyrene Excimer Formation. *Macromolecules* **2015**, *48*, 4620-4630.

7. Farhangi, S.; Weiss, H.; Duhamel; J. Effect of Side-Chain Length on the Polymer Chain Dynamics of Poly(alkyl methacrylate)s in Solution. *Macromolecules* **2013**, *24*, 9738-9747.

8. Alshaiban, A.; Soares, J. B. P. Effect of Hydrogen and External Donor on Propylene Polymerization Kinetics with a 4th Generation Ziegler-Natta Catalyst. *Macro. React. Eng.* **2012**, *6*, 265-274.

9. Conte, J. C., Oxygen quenching and energy transfer in pyrene solutions, Rev. Port. Quim, **1967**, *9*, 13-21.

10. Duhamel, J. New Insights in the Study of Pyrene Excimer Fluorescence to Characterize Macromolecules and their Supramolecular Assemblies in Solution. *Langmuir* **2012**, *28*, 6527-6538.

11. Duhamel, J. Global Analysis of Fluorescence Decays to Probe the Internal Dynamics of Fluorescently Labeled Macromolecules. *Langmuir* **2014**, *30*, 2307-2324.

12. Farhangi, S.; Duhamel, J. Probing Side Chain Dynamics of Branched Macromolecules by Pyrene Excimer Fluorescence. *Macromolecules* **2016**, *40*, 353-361.

13. Salino, P., Volpi, P. *Ann. Chim.* **1987**, *77*, 145-165.

14. Pirouz, S.; Duhamel, J.; Jiang Sh.; Duggal, A. Using Pyrene Excimer Fluorescence To Probe the Interactions between Viscosity Index Improvers and Waxes Present in Automotive Oil. *Macromolecules* **2017**, *50*, 2467–2476.

Chapter 4

1. Saxena, S. K. *Automobile engineering*, Laxmi publications Pvt Ltd, India, 2009, 70-76.
2. Collins, C. D. Implementing Phytoremediation of Petroleum Hydrocarbons in Phytoremediation Methods and Review. *Methods in Biotechnology* **2007**, *23*, 99 -108.
3. Farhangi, S.; Duhamel, J. Probing Side Chain Dynamics of Branched Macromolecules by Pyrene Excimer Fluorescence. *Macromolecules* **2016**, *40*, 353-361.
4. Pirouz, S.; Duhamel, J.; Jiang Sh.; Duggal, A. Using Pyrene Excimer Fluorescence To Probe the Interactions between Viscosity Index Improvers and Waxes Present in Automotive Oil. *Macromolecules* **2017**, *50*, 2467–2476.

Chapter 5

1. Kinker, B.G. Polymethacrylate viscosity modifiers, in *Lubricant Additives Chemistry and Application*, (ed. Rudnick L.R), Marcel Dekker Inc., New York, 2003, pp 329-353.
2. Pirouz, S.; Duhamel, J.; Jiang, S.; Duggal, A. Quantifying the Level of Intermacromolecular Between EP Copolymer Interactions by Using Pyrene Excimer Formation. *Macromolecules* **2015**, *48*, 4620-4630.
3. Mihaljuš S. V.; Podobnik, M.; Bambić, J. Engine Oil Viscosity Index Improver Behaviour at Extended Shear Stability. *Fuels Lubr.* **2008**, *47*, 118-128.
4. Pirouz, S.; Duhamel, J.; Jiang Sh.; Duggal, A. Using Pyrene Excimer Fluorescence To Probe the Interactions between Viscosity Index Improvers and Waxes Present in Automotive Oil. *Macromolecules* **2017**, *50*, 2467–2476.
5. Rudnick, L. R *Lubricant Additives Chemistry and Applications* (2nd Ed.), CRC, Florida, 2009, pp 346-347.